DESIGN AND APPLICATION OF THERMAL GRADIENT PROGRAMMING TECHNIQUES FOR USE IN MULTIDIMENSIONAL GAS CHROMATOGRAPHY-MASS SPECTROMETRY (MDGC-MS)

Thesis

Submitted to

The School of Engineering of the

UNIVERSITY OF DAYTON

in Partial Fulfillment of the Requirements for

The Degree

Master of Science in Chemical Engineering

by

Jesse Alberto Contreras

UNIVERSITY OF DAYTON

Dayton, Ohio

May, 2004

DESIGN AND APPLICATION OF THERMAL GRADIENT PROGRAMMING TECHNIQUES FOR USE IN MULTIDIMENSIONAL GAS CHROMATOGRAPHY-MASS SPECTROMETRY (MDGC-MS)

APPROVED BY:

Kevin J. Myers, D.Sc., P.E.
Advisory Committee Chairman
Professor, Chemical and Materials Engineering Department

Richard C. Striebich
Research Advisor
Research Scientist, UDRI
Environmental Engineering Department

Wayne A. Rubey
Research Advisor
UDRI Environmental Science and Engineering

Amy R. Ciric,
Committee Member
Associate Professor, Chemical and Materials

Phillip H. Taylor, Ph.D.
Committee Member
Group Leader, UDRI Environmental Science and Engineering

Donald L. Moon, Ph.D.
Associate Dean
Graduate Engineering Programs & Research
School of Engineering

Joseph E. Saliba, Ph.D.
Dean, School of Engineering

ABSTRACT

DESIGN AND APPLICATION OF THERMAL GRADIENT PROGRAMMING TECHNIQUES FOR USE IN MULTIDIMENSIONAL GAS CHROMATOGRAPHY-MASS SPECTROMETRY (MDGC-MS)

Name: Contreras, Jesse Alberto
University of Dayton, 2004

Research Advisor: Richard C. Striebich, Wayne A. Rubey
Academic Advisor: Dr. Kevin J. Myers

Multidimensional gas chromatography-mass spectrometry can provide significant improvements in the separation of complex organic mixtures. However, due to the extreme complexity of these organic samples, some zones in the chromatogram are often not adequately resolved.

An often-encountered difficulty experienced in the second-dimension separation represents a form of the general elution problem (GEP). Over the years, programmed temperature gas chromatography has been regarded as an acceptable solution to the GEP in gas chromatography (GC). Although, due to the fast separations required in the second-dimension, the application of rapid and quick turnaround temperature programming is very difficult to accomplish.

A potential solution for this operational situation can be the use of thermal gradient programmed gas chromatography (TGPGC). This technique is a novel mode of performing fast GC analyses, by applying three-dimensional thermal field programming. The application of thermal fields in TGPGC has been accomplished through the use of a column sheath assembly (CSA). The design, construction, and evaluation of CSA

capable of producing a variety of thermal contours with high-thermal compliance and uniformity was addressed in this thesis. A further goal was to employ the CSA concept in a MDGC-MS system to demonstrate its effectiveness to enhance the second-dimension separation, thereby improving analytical performance.

In order to test and tune the CSA, and the MDGC-MS system, only the secondary-column was used, and sample injections were performed to simulate the sample heartcuts coming from the first column. Results from the TGPGC experiments showed increased resolution improvements in the early eluting and clustered solutes, and a better spatial distribution for the analytes in the second-dimension.

We have successfully demonstrated TGPGC as an important technique for the second dimension of the complete MDGC-MS system. In contrast with conventional MDGC-MS, the application of TGPGC in MDGC-MS showed a more complete analysis of complex organic samples, in less time, while better addressing the GEP.

The application of the TGPGC mode in MDGC will be useful in the analysis of complex mixtures, e.g., petroleum products, combustion emissions, industrial effluents, etc., and in the detection of potentially toxic compounds found in the environment at trace level concentrations.

ACKNOWLEDGMENTS

I would like to express my sincere gratitude to my advisor Richard Striebich, for his willingness to share with me his knowledge and expertise, as well as his patience and guidance in this work. I thank him for his motivation and good humor at all times. Special thanks to Wayne Rubey for his knowledge, assistance and advice provided during this work. Without his ideas and innovations this work would not be possible. It has been a great honor for me to work with both of them.

I would like to acknowledge the organizations that have offered support through funding. The U.S.-Environmental Protection Agency's Science To Achieve Results (STAR) program has partially funded this effort through grant R-82819001-0. Dr. Paul Shapiro was the project officer. In addition I would like to acknowledge the support of the US EPA under grant 3C-R358-NAEX, Dr. Brian Gullett project officer. Also I acknowledge the Dayton Area Graduate Studies Institute (DAGSI), which has provided support through a full graduate tuition scholarship.

I would like to thank Dr. Kevin J. Myers for finding me the research opportunity at UDRI as well as his help and advice during these past few years, and to Dr. Amy Ciric, and Dr. Philip Taylor for helping with my thesis by serving on my committee.

I also wish to express my appreciation and thanks to a number of people for both their technical and moral support. Special thanks to Doug Wolf and Larry (Chuck) Sqrow for providing valuable assistance and advice in the automation of the system. I

owe my thanks to Andres Fullana for his many useful discussions, and to the Environmental Science Engineering Group members and my fellow graduate students for making a friendly and supportive atmosphere.

Finally I am really grateful to my family who supported and encouraged me on my decision to come to US. My caring parents Leticia Miranda and Carlos Contreras, their dedication to my education has made this thesis possible. Also my sisters Marites and Michelle cheered me over the course of this work. Evelyn Angel, my girlfriend, thanks for being by my side every moment supporting and motivating me.

I would like to dedicate this work to the loving memory of my Grand Mother Milagros Miranda, who was the reason for me coming to Dayton.

TABLE OF CONTENT

LIST OF ILLUSTRATIONS

LIST OF TABLES

LIST OF ABBREVIATIONS

$\|\Delta T\|$	Absolute Temperature Difference of a gradient profile
k'	Capacity Factor
CSA	Column Sheath Assembly
t_m	Elution time of a non-retained species or mobile phase
t_{rA}	Elution time of species A
FID	Flame Ionization Detector
F	Flow
GC	Gas Chromatography
GP	Gradient Profile
GEP	General Elution Problem
Q	Heat Flow Rate
H.E.T.P.	Height Equivalent to one Theoretical Plate
IHT	Initial Heating Time
MDGC	Multidimensional Gas Chromatography
MS	Mass Spectroscometry
TGP	Thermal Gradient Programming
TOFMS	Time-of-Flight Mass Spectroscometry
PTGC	Programmed Temperature Gas Chromatography
ID	Internal Diameter
ITGC	Isothermal Gas Chromatography

L	Length
u	Linear mobile phase velocity
LPM	Liters per minute
m	Mass Flow Rate
u_{opt}	Optimal Flow Veocity (cm/s)
OD	Outer Diameter
OPT	Open Tubular Column
U_o	Overall Heat Transfer Coeficient
K	Partition Coefficient
n_p	Peak Capacity
w_b	Peak Base Width
W	Peak Width
H	Plate Height
P	Pressure
SPE	Solid Phase Extraction
R	Resolution
k	Retention Factor
R_r	Retention Ratio
Cp	Specific Heat
STP	Standard Temperature and Pressure Conditions (21.1 ºC and 1 atm)
T	Temperature
$K_{polyimide}$	Thermal Conductivity of Polyimide
N	Theoretical Plates

CHAPTER I

INTRODUCTION

In nature, pure substances are rare to find; our world is mostly made of mixtures. For instance, the mineral water used for drinking contains more than 8 compounds[1], sea water contains more than 80 dissolved elements[2], petroleum may well contain over 100,000 components[3, 4], cigarette smoke contains more than 7,500 compounds[5] and even what we consider as clean rural air can contain at least 5,000 compounds with concentrations as low as parts-per-trillion[6].

Human nature has always been oriented upon seeking knowledge to understand and thereby characterize the physicochemical world. Knowing the exact composition of mixtures could lead us to identify compounds that can be useful, or harmful, for us and the environment. Such information allows us to understand physicochemical processes where mixtures are involved.

Among the separation sciences, gas chromatography (GC) occupies a rather unique position due to its sensitivity, separation efficiency, reasonable analysis time, and simplicity. It is the instrumental technique most widely used today for the analysis of volatile and semi-volatile organic compounds[4, 7, 8].

Many improvements have been made in GC over the years since its invention in the early 1950's. However, the complete separation of highly complex mixtures, e.g., petroleum products and environmental samples, requires extremely long analysis times or the use of more sophisticated systems, such as multidimensional systems[9-12].

Extensive peak co-elution presents a challenge for qualitative or quantitative analysis, even with the use of definitive confirmation technologies such as mass spectrometry[13] (MS). Different methods exist to reduce sample complexity by eliminating portions of the sample that contain compounds that are not of interest. Some of the preparative methods used are: single or multi-step solid phase extraction, size-exclusion chromatography, liquid chromatography (LC) or coupled-column techniques (LC-GC). Unfortunately, these methods can increase the chance of contamination and they are time-consuming.

With the introduction of the multidimensional GC (MDGC) technique in the 1969's, researchers started to separate complex samples without the need of difficult pre-separations techniques. Simplification of sample preparation was one of the advantages of MDGC that made the technique attractive. The MDGC technique consists of a sequential arrangement of two GC columns of different selectivity, where distinctive segments of eluant from the first column (first dimension) are transported into a second column (second dimension) to further separate any unresolved components. This technique combines the advantages of increased separation power with reduced analysis time[14-17].

Impressive results in MDGC have been obtained in terms of separation efficiency as a result of increased peak capacity, improved analysis speed, sensitivity, and moreover, an orderly separation based on chemical class[9, 10]. The further coupling of the MDGC technique with Mass Spectrometry (MDGC-MS) has shown remarkable gains in resolving power and compound identification i.e., beyond anything possible with one-dimensional systems such as single chromatographic columns[5, 16, 18].

In recent years, the use of MDGC-MS has not been restricted only to the analysis of complex samples, but also to less complex samples. With MDGC-MS, more

constituents are being revealed in complex samples than those found by conventional GC, showing how much more complex they are, than what we previously realized[13].

Even with the resolving power of MDGC-MS already an order of magnitude greater than one-dimensional techniques, complex mixtures, such as combustion effluents and petroleum-derived products, still require greater resolution than that achieved with MDGC-MS. Still some peaks or zones in the MDGC-MS chromatograms are not adequately resolved[6].

The typical MDGC-MS experiment involves slow-programming of a primary column and an isothermal secondary column separation. One difficulty confronted in the isothermal second-dimension separation represents a form of the general elution problem (GEP), where early eluting peaks are sharp and clustered together, while later peaks become broad and spread out, while exhibiting a wide range of migrations rates. The experimentally accessible peak capacity of the system is only a small portion of its potential.

Over the years, programmed temperature GC (PTGC) has been regarded as an acceptable solution to the general elution problem in GC. However, due to the fast GC separation in the second dimension, the application of rapid and quick turnaround temperature programming is very difficult to accomplish.

Several approaches have been considered to improve the chromatographic selectivity and separation, as well as minimize elution time in the second dimension within MDGC-MS operations. Some of the approaches considered were: to program the temperature of the secondary column independently from the first column[5, 10, 13, 19-21], modify the stationary phase selectivity, or use mixed stationary phases in the second dimension[10, 22, 23], use longer columns in the second dimension[24], employ narrower bore columns for the second dimension[25], change the flow in the second dimension[12, 26], apply fast temperature programming in the second dimension[22], use software to resolve

overlapped peaks directly from the signal data[27], and use of higher-order multidimensional separations or GCxGCxGC[6]. However, the gains in separation obtained through the application of these methods were relatively small and in some cases at a great expense in time or effort. Moreover, the enhancements were partial because only part of the chromatogram was improved[10].

A potential solution for this operational situation could be the use of thermal gradient programming gas chromatography (TGPGC). This operational mode can perform rapid analysis with complex mixtures in a short period of time; moreover, it permits rapid turnaround times and is a better solution to the general elution problem in high speed GC[28, 29]. All these attributes make the TGPGC method highly interesting to evaluate, as an alternative in optimizing the second dimension in MDGC-MS. This novel mode of conducting fast GC analysis is achieved by applying a three-dimensional (distance–temperature–time) thermal field programming. The TGPGC method creates a temperature gradient in the axial direction of the chromatographic column with the ability of modifying the gradient through time.

The application of thermal fields in TGPGC requires a special component known as column sheath assembly (CSA). In order to create a versatile range of thermal fields, the CSA needs to be thermally compliant and able to undergo rapid changes of temperature and pressure. Therefore, the design, construction, and evaluation of a CSA capable of producing a variety of thermal fields with high thermal compliance and uniformity were addressed in this thesis. Another goal was to employ the CSA within a MDGC-MS system to demonstrate its effectiveness in the enhancement of the second-dimension separation.

CHAPTER II

BACKGROUND AND LITERATURE SURVEY

History of Chromatography

One of the first works performed using chromatographic principles occurred during the middle of the nineteen-century, by F. F. Runge in 1843. He used unglazed paper and/or cloth to spot test dye mixtures and plant extracts[7]. The recognized introduction of chromatography is attributed to the botanist M. S. Tswett, who performed separations of plant pigments in 1903[30, 31]. Tswett presented the fundamentals of chromatography by scientifically describing the process. He discovered that plant dyes could be separated using calcium carbonate particles as the adsorbent and petroleum ether as the mobile phase. He called this process chromatography, literally from the Greek "color-writing". Tswett also mentioned that the principles of chromatography apply for both colored and colorless compounds[30, 31].

Chromatography is a physical method of separation in which the sample components to be separated (the analytes) are distributed between two phases, i.e., one is stationary with a large surface area (the stationary phase), while the other is a fluid and moves in a definite direction (the mobile phase). The separation is due to differences in the distribution of the analytes between the two phases[32, 33]. Currently the term chromatography is highly accepted, and is used for separation methods based upon established transport principles[31]. Since its conception, chromatography has undergone extensive development and has evolved into a wide variety of types and

techniques. The main four types of chromatography are liquid, gas, thin-layer and paper chromatography. Gas chromatography is a technique used for the analysis of volatile compounds, in which the mobile phase is a gas and the stationary phase is either a solid (GSL) or a liquid (GLC).

Evolution of Gas-Liquid Chromatography (GLC)

The initial work in GLC is generally attributed to A.T. James and A.J.P. Martin with the appearance of their 1952 paper, where they reported the separation of volatile fatty acids by partition-chromatography with nitrogen gas as the mobile phase, and oil/steric acid serving as the stationary phase. In fact, the origin of GLC lies in a sentence presented in an important publication in 1941 in which Martin, with R.L.M. Synge, first described liquid-phase partition chromatography[4]. They stated that partition chromatography could be also applied to volatile substances using a vapor as the mobile phase. This paper was the foundation of partition chromatography for which Synge and Martin would be given the Nobel Prize for Chemistry in 1952[4].

This new separation technique produced a rapid growth of interest among researchers, due to its simplicity, and its capability to be applied in several areas, e.g., the petrochemical industry, biochemistry, reaction kinetics, etc. However, the use of packed columns in the early GLC systems presented some difficulties, due to the fact that the resolution was limited by the column length, which was restricted somewhat by the pressure drop across the column. These restrictions were overcome by the invention of the open tubular column (OTC) or capillary column. First suggested by Marcel Golay in 1957 as a result of mathematical studies, and later in 1958, Golay demonstrated its theory and operation[4].

With the introduction of capillary columns, high GLC efficiencies were produced, where complete separation and faster analysis were possible for many types of samples. Even so, problems soon appeared with the use of glass capillary columns. The activity of the "common" glass towards polar analytes often gave severe peak tailing and due to the unstable liquid film and their fragility, the glass OTCs had a short life[4, 31].

The commercial introduction of fused-silica capillary columns in the early 1980s by Dandeneau and Zerenner, was an important answer to solving these problems. Fused-silica tubing externally coated with a protective layer of polyimide, were flexible, durable, and chemically inert, thereby making them especially suitable for gas chromatographic use. Nowadays fused-silica columns are the most used OTCs in GC analysis[4, 30, 31].

The development of fused-silica capillary columns greatly increased the application of high-resolution GC across the field of organic analysis and also the ability to separate complex mixtures. Furthermore, the access of a low-cost bench-top GC instrument made the technique widely available, becoming one of the most important and widely applied analytical techniques in modern chemistry.

History of Multidimensional Gas Chromatography

Contemporary analytical gas chromatography is an effective means for analyzing samples containing volatile to semivolatile organic compounds. High-efficiency capillary gas chromatography has progressed a long way to become the main method of analytical and physicochemical research[34, 35]. Despite the advances in column efficiency and instrumentation, conventional GC has some limitations that lessen or curtail its application in the analysis of complex mixtures.

For complex samples containing more than 150 to 250 randomly distributed relevant compounds, conventional GC can not completely separate all the individual analytes[21, 36]. The qualitative analysis task of recognizing an unknown as a specific compound out of a matrix of possible sample components is often constrained by the large number of solutes in the sample[37]. Even with the use of definitive confirmation technologies such as mass spectrometry (MS), the extensive peak coelution obtain, seriously restricts the qualitative analysis of many of the solutes[12, 13, 24]. Separation of complex mixtures using conventional GC can be achieved, but at the cost of prohibitively longer analysis times, due to the low peak capacity that a single GC column possesses[11, 12].

Peak capacity is a parameter used to describe the overall separation power of a single GC column[9, 38]. It is defined as the maximum number of peak profiles that can be placed, with complete separation, into the available separation space (chromatogram)[9, 39]. To alleviate the effects of peak crowding, column efficiency has to be increased by increasing peak capacity[10]. The limitations imposed by the use of a single column have been realized for many years. The search for improved or enhanced methods that address these deficiencies was undertaken shortly after the advent of the GC method itself.

An approach used to enlarge peak capacity was to increase column length, decrease column diameter, or a combination of both. However, the analysis times became unacceptably long to generate a reasonable separation[9] using longer columns. Another approach was to join together two different columns to obtain an improved selectivity in the separation i.e., multichromatography. However, a simple joining of two different columns was not satisfactory. This was merely a shifting of the peak relative retention due to the mixing of stationary phases. Although the selectivity of the separation was improved, still there was no increase in the peak capacity of the system[40].

J. Calvin Giddings described the fundamental aspects of multidimensional separations by defining it as a technique where the components of a mixture are subjected to two or more independent separation mechanisms in which their displacements depend on different factors[9, 18, 38] (volatility, polarity, etc.). Then multidimensional GC offered an attractive alternative to rapidly expand peak capacity. The overall peak capacity of a two-dimensional system could be estimated as the product of the individual peak capacities of the independent columns[41]. The experiment using two columns in series was further developed by D.R. Deans in 1968 by locating a pressurizing valve switching system between two columns, which had different selectivities. The switching system was able to isolate discrete fractions of effluent from the first column and then pass them to the second column. The experimental results showed that it was an effective way to increase the resolution for a separation analysis[4, 17, 40, 42]. The isolated zones from the first column received the name of "heart cuts" and therefore the "heart-cutting" two-dimensional GC, or multidimensional GC (MDGC) technique was born.

The invention of Deans switching system was an important early development for MDGC. Using Deans switching valve, Schomburg in 1972 reported that the resolution of

the selected heart-cuts could be further increased by using capillary columns[17, 42]. He also trapped the heart-cuts in a cold trap located between the columns, i.e., before the second separation. In this mode, the selectivity of the second-dimension separation was no longer influenced by the selectivity of the first separation. Furthermore, band-focusing (cryofocusing) permitted an increase in sensitivity to be achieved[12, 41, 42].

Using an SGE Dean's switching module and following the principles stated by Schomburg[43], Rubey and coworkers reported one of the first works on coupling a MS to a two-dimensional heart-cutting MDGC system[44]. Now a system was not only capable of separating complex mixtures, but also of identifying the unknown individual compounds using MDGC-MS.

The inherent drawback in heart-cutting techniques was that detailed GC and MS information was obtained only for the few fractions subjected to the two-dimensional operation. Krock and Wilkins addressed this problem to some extent by using multiple fraction traps where they could isolate contiguous heart cuts. However, they recognized that there was a clear physical and practical limitation to the number of traps that can be employed for this purpose[17, 40]. In both of the previously discussed techniques, the number of secondary chromatograms was quite limited.

Feasible technical solutions to this MDGC dilemma were not offered until the early 1990s, when Phillips and co-workers presented a new approach of applying two-dimensional GC[10]. The new method allowed doing a continuous two-dimensional separation to the entire first column effluent. The key to the procedure was the technical utilization of the interface between the two columns. A modulator that was able to continuously accumulate and focus small fractions of effluent from the primary column was used to inject solutes into the secondary column in a very fast and efficient manner.

Recent development work with MDGC systems has been directed to optimization and further enhancement. The incorporation of a MS detector for further accurate

identification of the unknown peaks is highly desirable. The first steps to interface a conventional quadrupole type mass spectrometer to comprehensive two-dimensional gas chromatography where done by Striebich and Klosterman[24, 28, 45]. However, the scan speed and mass range were somewhat limited. New generation of fast scanning TOF-based mass spectrometers (TOFMS) seems to be an ideal match for MDGC. Currently interfacing experiments using TOFMS and MDGC are underway[5, 10].

At present the most popular way of conducting comprehensive MDGC or "GCxGC" follows the technique established by Phillips and co-workers. Currently, many investigators are working with this powerful separation technique because of the remarkable results reported during the last decade. The MDGC technique is still in its evolving stage, and one can expect further improvements in the future.

Multidimensional Gas Chromatography Hardware Components and Principles

With the introduction of the new way of conducting MDGC by Phillips and co-workers, a technique has become available which is especially suited for the separation and identification of analytes in complex samples[16]. The system consists of two columns of different selectivity connected in series with a modulator between the columns. The modulator continually takes segments of the eluting peaks from the first dimension open tubular column and pulses them onto the second dimension column as refocused bands for further separation[37]. A general schematic of the MDGC system is shown in Figure 1.

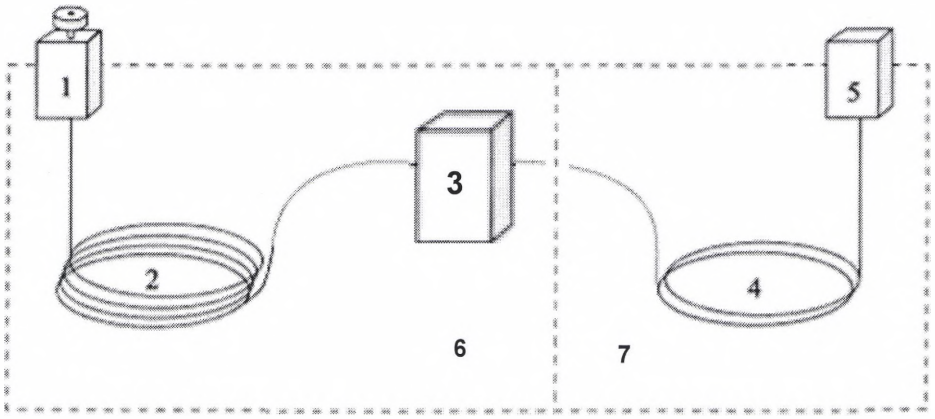

1=Injector, 2=First dimension column, 3=Modulator, 4=Second dimension column, 5=Detector, 6=First GC Oven, 7=Second GC oven.

Figure 1. Schematic of a MDGC system.

The column arrangement could be placed in a single oven[10, 22-24, 45] or each column could be placed in different ovens to allow more flexible and independent temperature programming[5, 6, 10, 13, 20, 22]. In the systems where two ovens are available, the second oven follows the heating rate of the first one, but at temperatures that were typically higher[13]. The primary (first dimension) column is usually longer and has a wider bore than the secondary (second dimension) column[10]. The primary column is typically a nonpolar type, where compounds are separated according to their volatility or pure-component vapor pressure[23]. Because the secondary column contains a more polar

stationary phase, compounds are separated based on their activity coefficient. The polar substances are more strongly retained than the less polar substances. The difference in the stationary phases of the columns allows compounds coeluting at the primary column exit to potentially be separated by the additional retention in the secondary column, whereas in one column, they may have co-elute[10, 23].

The migrations in the second column must be at much higher speed than the first column, so as to produce a series of analyses during the analysis time of the first dimension[36]. Also, it has to be fast enough to generate a complete chromatogram during the period of modulation to avoid "wrap around". Wrap-around occurs when fast moving compounds elute, before the last substance from the previous injection has left the secondary column[14]. Due to the high speed of the secondary column and the slow temperature-programming rate at which the first column operates, the separations in the second dimension are performed essentially with a constant temperature mode[10].

A flow-splitter is sometimes added between the columns to optimize column efficiency[45] in each dimension, although it is not a required component[10]. The most critical component of the MDGC system is the trap and release device. Its function is to periodically stop and turn on the movement of the effluent from the first column. The modulator separates the first column effluent into a very large number of adjacent small chemical fractions that are subsequently injected into the second column in the form of narrow and periodic spaced pulses of highly concentrated compounds. The focusing step in the modulator offers significant advantages. The most important is that the effect of peak dispersion from the first column can be reversed. In essence a wide peak can be sharpened into a narrow peak, resulting in lower detection limits and improved quantitation[10]. However, more than one peak can be contained in this zone, thereby undoing the separation work of the first column.

To preserve most of the first-column separation, the heartcuts should be no larger than a peak within the first dimension[16]. Larger heartcuts can adversely affect the resolution of the first dimension by partially recombining peaks again in the modulator. Consequently, for a peak eluted from the first-dimension, at least one to five heartcuts should be generated in the second-dimension[5, 25, 46, 47].

During the development of each secondary chromatogram the trap and release device accumulates the effluent fraction for the next injection. So every segment of the first dimension is thus subjected to both separative dimensions, which is the main requirement for achieving MDGC analysis. Figure 2 shows how two overlapping peaks emerging from the first-dimension are resolved in MDGC after passage to the second-dimension.

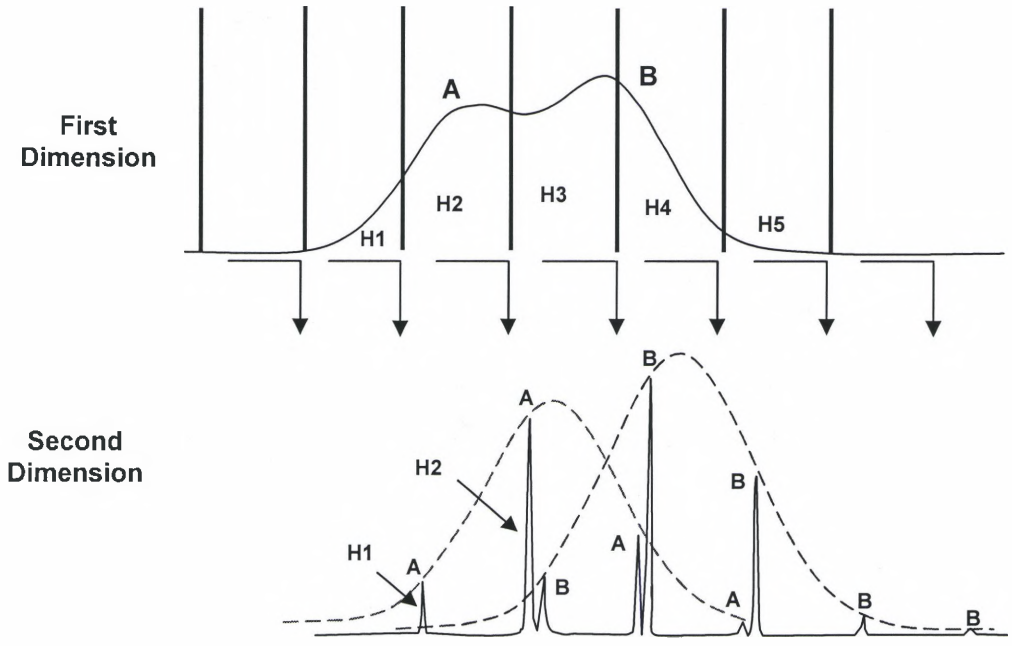

Figure 2. Illustration of how MDGC resolves two overlapping peaks.

The two components are labeled **A** and **B**. Thus heartcut **H1** contains only the **A** component, whereas heartcut **H2** has a larger amount of **A** and a small amount of **B**. The second-dimension can resolve **A** and **B** as shown, where the first dimension was unable to resolve them.

Modulator Types

The accumulation and periodic reinjection of effluent from the primary column into the secondary column presents a considerable technical challenge. Three major techniques are currently being applied for the implementation of this modulation step, each having particular advantages and disadvantages.

- Diaphragm Modulation:

A diaphragm valve diverts sections of the eluting zone from the first column onto the second dimension column, providing narrow pulses of effluent[12, 37] (see Figure 3). Diaphragm valves are particularly suitable because they can provide precisely defined cuts at a high frequency. However, the limitations of this technique are that it is molecular weight (MW) limited, part of the sample is vented in the process and does not reach the detector, and sensitivity is lost in this configuration. Moreover it has a limited working temperature range[10, 12].

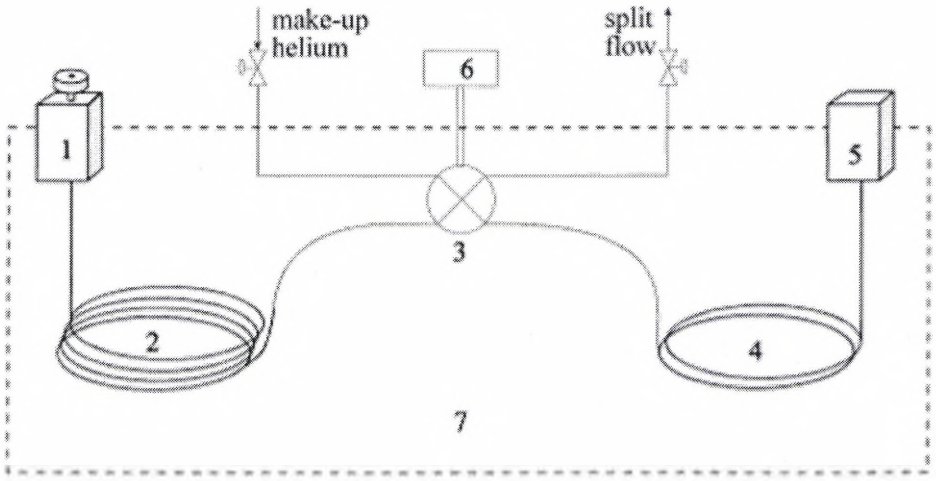

1=Injector, 2=First dimension column, 3=Diaphragm valve, 4=Second dimension column, 5=Detector, 6=Valve controller, 7=GC oven.

Figure 3. MDGC system with a valve modulator[36].

The principal used in the following modulators are based in the fact that almost all volatile substances can be physically retained onto and desorbed from a stationary phase film by manipulating the temperature. The approaches used are capable of producing very rapid changes in temperature to achieve and efficient trapping and release of the compounds.

- Thermal Desorption Modulator (TDM) or Sweeper:

Phillips and his group[14] developed a thermal desorption modulator (TDM). It consists of a mechanically actuated heater (Figure 4). A rotating slotted heater sweeps portions of the chromatographic band from a modulator capillary onto the second dimension column. The "chemical pulses" are produced by stationary phase focusing followed by volatilization from the mechanically actuated heater[10]. The system allows independent adjustment of desorption temperature. It must operate at 100 ºC higher than the oven temperature to achieve effective heart-cutting and refocusing of the solutes[10, 41]. So the maximum oven temperature, and therefore first dimension oven temperature, is thus lowered by 100 ºC.

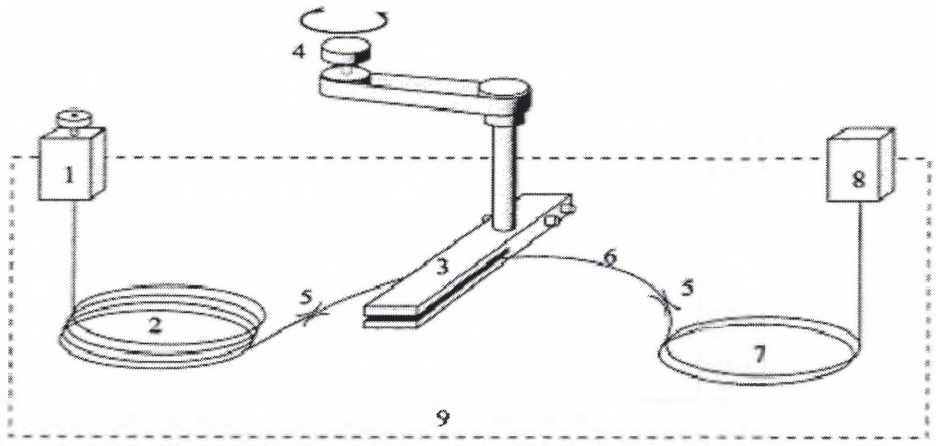

1=Injector, 2=First dimension column, 3=Slotted heater, 4=Stepper motor to turn the slotted heater, 5=Micro press fit column connections, 6=Thick film modulator capillary, 7=Second dimension column, 8=Detector, 9=GC oven.

Figure 4. MDGC system with a thermal modulator design[36].

- Cryogenic Modulator:

The mechanical modulator developed by Kinghorn and Marriott[48, 49] consists of a longitudinal modulating cryogenic system (LCMS). It is essentially a cryogenic trap which is moved by a motor or solenoid driven piston over a section of capillary column which acts as a modulator tube[10] (see Figure 5). The moving cryogenic trap cryo-focuses a portion of the eluting band and then releases or remobilizes the focused band segment into the second dimension column. By moving the cryogenic trap and allowing the cold capillary to heat up by the turbulent oven air, the trapped band is released[37]. This approach provides several key attributes; modulation speed is high, there is no need for an additional accumulator column, the column can be used until its maximum temperature limit, and narrow bands are achieved[37]. The drawback that this approach has is that it requires either liquid nitrogen or CO_2 in order to reach the low temperatures[36]. A similar trap and release method was applied in the MDGC-MS instrument used in our experiments, due to its advantages width respect to the other modulator systems.

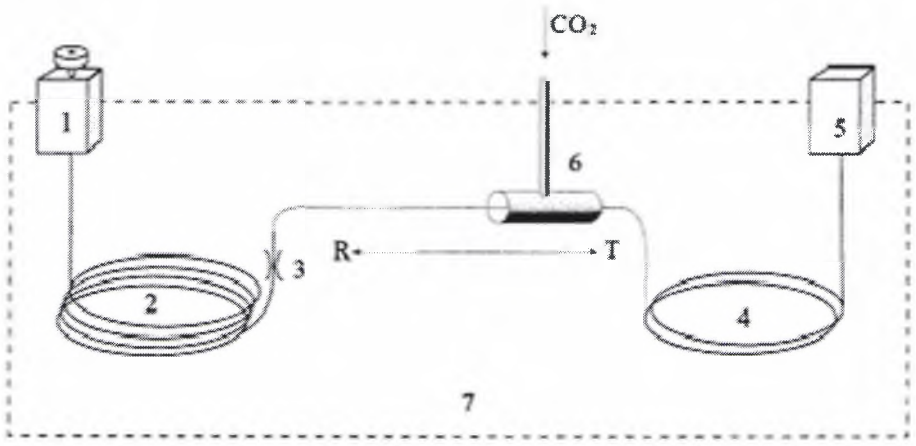

1=Injector, 2=First dimension column, 3=Column connection, 4=Second dimension column, 5=Detector, 6=Moving cryogenic trap, 7=GC oven.

Figure 5. MDGC system with a cryogenic modulator design[36].

Advantages of the MDGC:

MDGC is of use whenever a critical separation of an organic mixture cannot be achieved using conventional GC analyses. The very large peak capacity provided by the MDGC technique allows much more complete separation of not only complex mixtures, but also for mixtures of moderate complexity, providing remarkable gains in resolving power[13, 14, 18, 23]. Moreover, the refocusing step at the modulator increases the sensitivity of the system since peaks at the detector are sharper and therefore taller[14].

Remarkable results have been obtained in terms of compound classification. The peaks in the MDGC chromatogram display some order, based on the chemical or molecular functionality of the compounds. This is one of the strongest assets of MDGC[10, 21]. Furthermore, since a true baseline is often available, high match qualities and better identification of the peaks by using mass spectroscopy can be achieved[10, 13]. The MDGC system certainly combines the specificity for target analyses with the universality for unknowns and reasonable sensitivity for both[24, 45].

Optimization of the MDGC system:

In the past few years, MDGC has been shown to be a powerful technique for the analysis of complex samples. As can be seen in the MDGC chromatograms reported during the past decade[10, 14, 21, 23, 24, 44, 45], some peaks or zones in the second-dimension chromatograms are not adequately resolved. Mostly the nonpolar saturated and unsaturated hydrocarbons, which have very low activity coefficients in the second-dimension stationary phase, elute from the second-dimension as non-resolved peaks,[5]

while compounds with higher second-dimension retention times are seen to be much better separated.

This often encountered difficulty experienced in the second-dimension separation (or many isothermal separations), represents a form of the general elution problem (GEP): i.e., early eluting peaks are sharp and clustered together, while the later peaks become spatially broad[50] (See Figure 6). This uneven distribution of zones is seen when the separation is performed in an isothermal mode and the sample exhibits a wide range of migration rates, which is a measure of the time the analyte resides in the mobile phase relative to the total time it resides in the column.

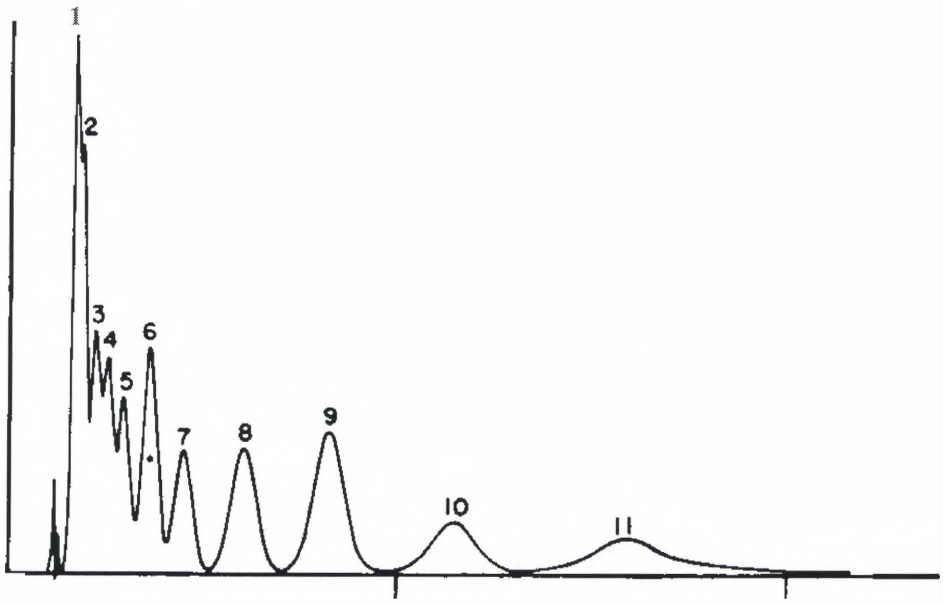

Figure 6. The General Elution Problem, each number represents a unique compound[50].

This is essentially the case in the second-dimension of MDGC chromatograms, where the separations are basically isothermal, and the segments eluting from the first dimension have solutes with widely differing migration rates, as can be seen in Figure 7.

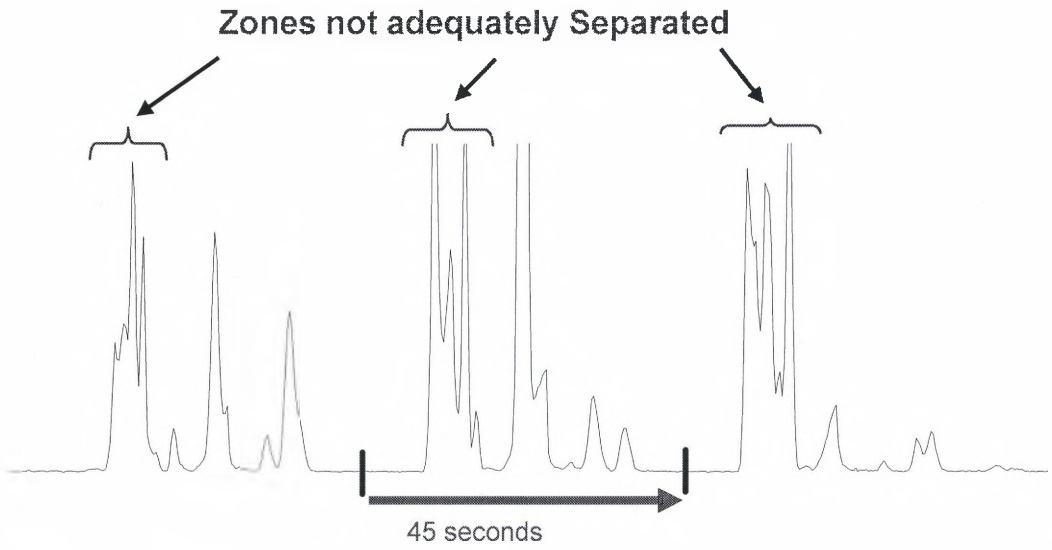

Figure 7. Heartcuts from MDGC-MS chromatograms of a Diesel Exhaust solution[45].

Programmed temperature gas chromatography (PTGC) has been regarded as an acceptable solution to the general elution problem in GC[29, 50]. Although, due to the high velocity flows and fast GC separations in the second dimension, the application of rapid and quick turnaround temperature programming is very difficult to accomplish.

Another important aspect to optimize in the MDGC system is the analysis time. The reduction of analysis time has remained one of the most important research subjects for chromatographers since the introduction of capillary columns by Golay in 1958[51]. Every reduction of analysis time, without significant loss of resolution, can be translated into a higher sample throughput and hence reduction in per sample analytical costs[52]. In MDGC the overall analysis time could be further reduced, due to the fact that the first-dimension column is usually operated at sub-optimum flow and at slow temperature programming rates, to enable the required number of heartcuts across a first-dimension peak[25]. Therefore, increases in the speed of analysis of the second-dimension without significant losses in resolution, would be desirable. Because then the

first-dimension column would be operated under optimum flow conditions, reducing the overall analysis time of the MDGC technique.

Several approaches have been considered to improve the chromatographic selectivity, analysis time, and separation in the secondary dimension within MDGC-MS operations. Some of the approaches considered were:

a) *To program the temperature of the secondary column independently from the first column.* To achieve this, the second-dimension column was installed in a separate oven. The separate oven provided a more flexible system since it allows fine-tuning of the retention in the second column. The temperature program in the second oven followed the temperature program rate of the first-dimension oven, but at a temperature that was typically higher[5, 10, 13, 22, 23, 25]. The hot second column served to reduce elution time and peak broadening of the more retained compounds. This configuration helped to speed up the second dimension separation, and to optimize peak broadening[5, 13, 20]. However, the separations of the compounds less retained in the second dimension where not improved. Although the use of lower second-dimension temperature improves separation, the increase in retention and analysis time is not acceptable[5, 22].

b) *Modify the stationary phase selectivity or use mixed stationary phases in the second dimension.* Increase in selectivity and separation in the second-dimension could be obtained by using appropriate phases with different polarities[10, 22, 23]. The aim is to maximize differences in activity coefficients (i.e. molecular interactions between different analytes and the stationary phase) on the secondary column to increase its resolution[10, 23]. That means that the second dimension has to be changed and adjusted for every type of sample, which is time consuming and not convenient.

c) *Use of a splitter and longer columns in the second dimension.* Increasing the length of the secondary-columns helps to increase the resolution of the second-dimension. Furthermore, employing a splitter between the columns of the MDGC system optimizes both columns efficiencies, by operating each column at its optimal carrier gas velocities for maximum resolution[24, 45]. The high resolution outcome that the system provides is obtained at the expense of both longer analysis times due to the longer secondary column, and lower sensitivity as a result of sample vented at the splitter.

d) *Use of shorter and narrower bore columns for the second dimension.* Reduction of the column diameter has proven to be a highly efficient tool to increase the speed of analysis while keeping GC resolution[52-55]. Therefore, the use of narrow bore columns for the second-dimension allows reduction of the analysis time without sacrificing resolution of the separation. The well-known disadvantages of small-diameter columns are the necessity of higher inlet pressures and their limited sample capacity that leads to column overloading and high demands on the detector[25, 52, 56].

e) *Fast temperature programming in the second dimension*. The use of this operational mode will help to minimize analysis time and increase the resolution of the separation. However, fast temperature programming gas chromatography (FTPGC) has been only performed in conventional GC[51-53, 57-61]. The incorporation of FTPGC technique into a MDGC system has not yet been performed due to the fast turnaround times required. Current FTPGC systems have turnaround times of 1 to 3.5 minutes[53], which are considerably long compared to the 4 to 45 seconds turn-around times of the secondary-dimension analysis[5, 10, 25, 45].

f) *Use software to resolve overlapped peaks directly from the signal data. The* Mass spectral deconvolution software is an effective and efficient tool to resolve co-eluting peaks and a way of enhancing the separation power and limits of detection in MDGC-MS. The software performs nearly perfect background subtraction of distinct MS spectra to identify individual components within a mixture that has been minimally separated by chromatography[27, 58]. This makes compound identification in GC-MS much better, faster, and easier than can be accomplished by a human operator. The technique uses the inherent MDGC-MS data structure to mathematically separate and quantify incompletely resolved signals, helping to save great amount of data processing and review time[27, 58]. The software requires fast data acquisition instruments to be efficient and the sacrifice of sensitivity to avoid false peak identifications from noise[58].

g) *Change the flow in the second dimension.* The selectivity of an ensemble of two capillary columns using different stationary phases can be modified by changing the carrier gas pressure at the junction point between the columns[34, 40, 62, 63]. The manipulation of the junction-point pressure can allow controlling the relative residence time of analytes in each of the columns, which can result in more efficient utilization of the available peak capacity of the system[40, 56, 62]. Moreover, selectivity tuning can be performed automatically instead of tedious column replacement[57, 63]. However, changes in flow rate represent a problem for mass spectrometer detectors where a signal loss occurs with an increase in flow rate[64].

h) *Use higher-order multidimensional separations or GCxGCxGC*[6]. This technique could undoubtedly have a huge peak capacity and thus separation power. However to make comprehensive three-dimensional gas chromatography (GC^3) practical, the use of a very fast tertiary column is required. Moreover, the visualization of

GC^3 chromatograms, integration of three-dimensional blob volumes, and computer aided identification of peaks and compound classes pose significant challenges to software development[6]. The technique is in its developing stage and the major drawback is that it is technically more demanding than MDGC-MS.

The gains in separation obtained through the application of these methods was partial because only part of the chromatogram was improved and in some cases at a great expense of time.

A potential solution for the operational situation on the second-dimension could be the use of thermal gradient programming gas chromatography (TGPGC). The operational aspects associated with TGPGC are such that rapid GC analyses can be achieved for complex samples and broad migration rate samples in a short period of time. Furthermore, it permits rapid turnaround times and it is a better solution to the general elution problem in high speed GC[3, 28, 29]. All these attributes make the TGPGC method highly interesting to evaluate as an alternative in optimizing the second dimension in MDGC-MS.

Thermal Gradient Programmed Gas Chromatography (TGPGC):

Fundamental Principles of TGPGC

The stationary phase and operating temperature of the column, the choice of carrier gas, and the carrier gas velocity are interrelated variables that can exercise profound effects on separation efficiencies and analysis times. However, the control of temperature is one of the easiest and most effective ways to influence the separation process. In GC the column is normally operated at temperatures where most compounds have a vapor pressure, it need not be in the gas state. However, the column temperature should be high enough so that sample components pass through it at a reasonable speed[33]. For this reason it is often required to maintain the column at a wide variety of temperatures, e.g. from cryogenic values[33] to 360 °C. Some degree of compromise is usually necessary, because for most of the samples, the lower the temperature, the better is the separation, and the longer the analysis time[30]. Currently the two major operational modes of conducting gas chromatography analysis are: isothermal GC (ITGC) and programmed temperature GC (PTGC). Temperature programming is very useful for the analysis of mixtures with a wide boiling range or migration rates, whereas the isothermal operation is limited to samples with a narrow boiling range; PTGC is normally the preferred analytical mode[30].

A novel operational mode of performing GC analysis is thermal gradient programmed gas chromatography (TGPGC)[3, 26, 28, 29, 65, 66]. This novel mode of conducting fast GC analysis is achieved by applying three-dimensional (distance–temperature–time) thermal fields to the column. The TGPGC method creates a negative temperature gradient in the axial direction of the chromatographic column with the ability

of modifying the gradient through time[26, 29, 65]. In TGPGC there is continually an axial negative temperature gradient applied to the column length[29]. An adequate characterization of the TGPGC technique can be achieved by showing the three-dimensional views (Figure 8) of the different operational modes applied in GC.

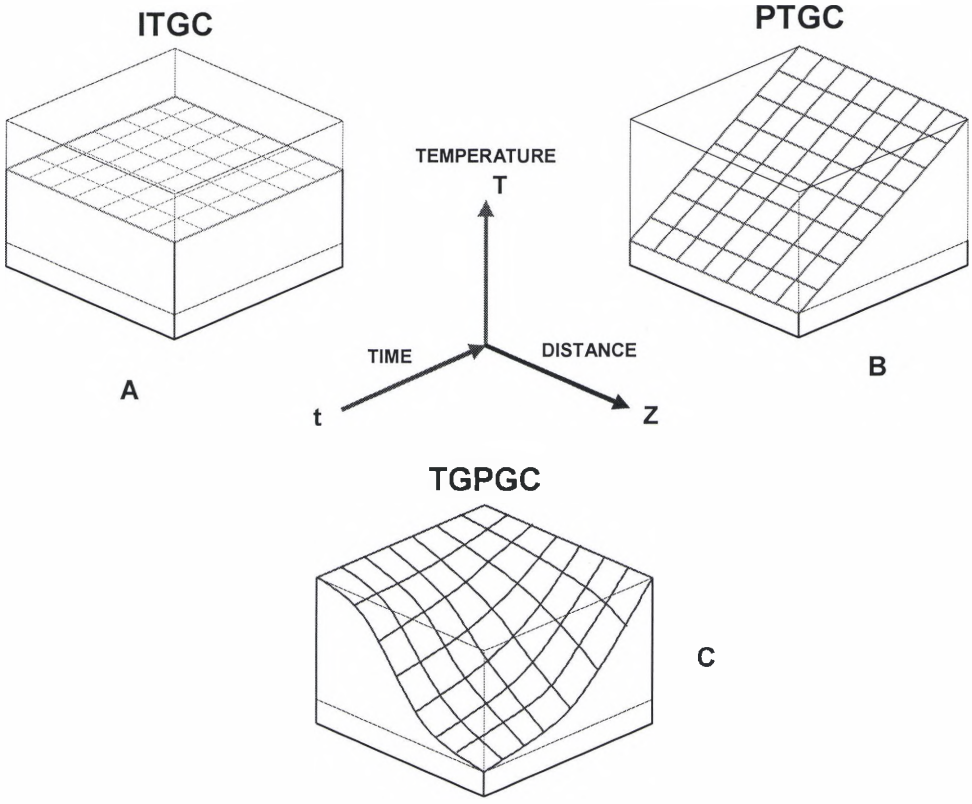

Figure 8. Three-dimensional views of the operational modes of GC[29].

Z is migration distance, T, temperature, and t, analysis time.

Figure 8 highlights the difference between the three existing methods. As is depicted in Figure 8-A, one dimension could be sufficient to describe the ITGC process and two dimensions are adequate for the PTGC technique, while three dimensions are needed to describe the thermal field (or "temperature surface") applied in the TGPGC technique. In TGPGC operations, (Figure 8-C) temperature continues to decline with distance at every axial location throughout the column. While in PTGC operations, the "whole column" temperature experiences a gradual increase as a function of time;

therefore, an inclined plane is observed in Figure 8-B. On the other hand ITGC operations can be viewed as a PTGC operation, but with a heating rate equal to zero. Once looking at the three-dimension views of these different operational modes, the TGPGC process becomes understandable[29].

An important operational aspect of TGPGC is that a solute zone continually encounters a negative thermal gradient throughout its chromatographic axial migration[26, 66]. Therefore, a solute zone will continually be migrating into regions of lower temperature, greater retention, and, therefore, lower axial velocity, "v" (see Figure 9). The negative thermal gradient provides a mechanism for solute zone axial compression of a nature somewhat similar to that produced by cryofocusing[29].

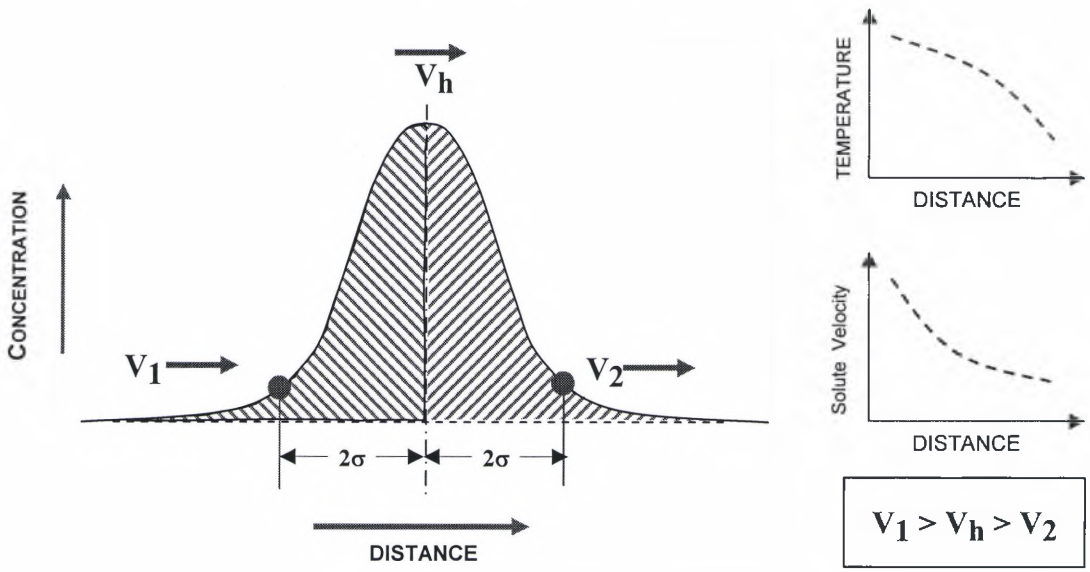

Figure 9. Migrating zones velocity aspects[29, 66-68].

This behavior is markedly different from that which is experienced in other GC modes, e.g. ITGC and PTGC, where the axial length of a migrating solute zone continually increases with migration distance. With the axial compression provided by TGPGC operation, a migrating solute zone's longitudinal spread can actually diminish as depicted in Figure 10. Although the axial length of migrating zones in TGPGC is smaller,

the axial distance between the centroids of adjacent migrating zones is also usually less than in ITGC and PTGC, and this must be taken into consideration with regard to the peak capacity and chromatographic resolution[29].

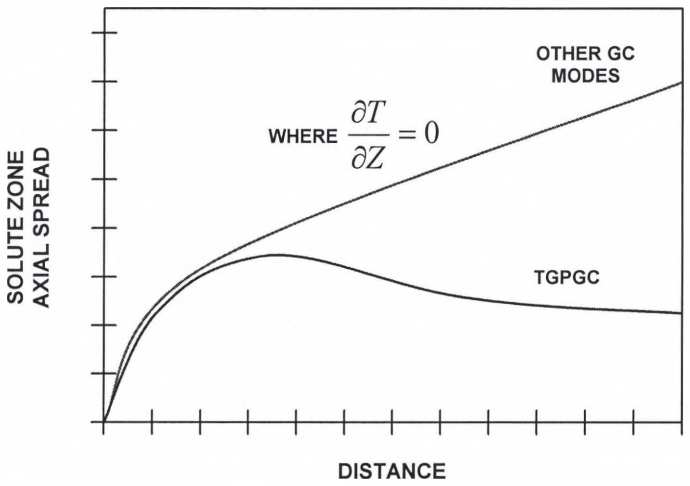

Figure 10. Migration behavior relative to axial length of solute zone for different modes of gas chromatography[26, 66].

The resolution is a measurement that describes how well resolved or separated two adjacent peaks are[33]. Figure 11 shows how a resolution of 1.5 provides an adequate separation between two adjacent peaks.

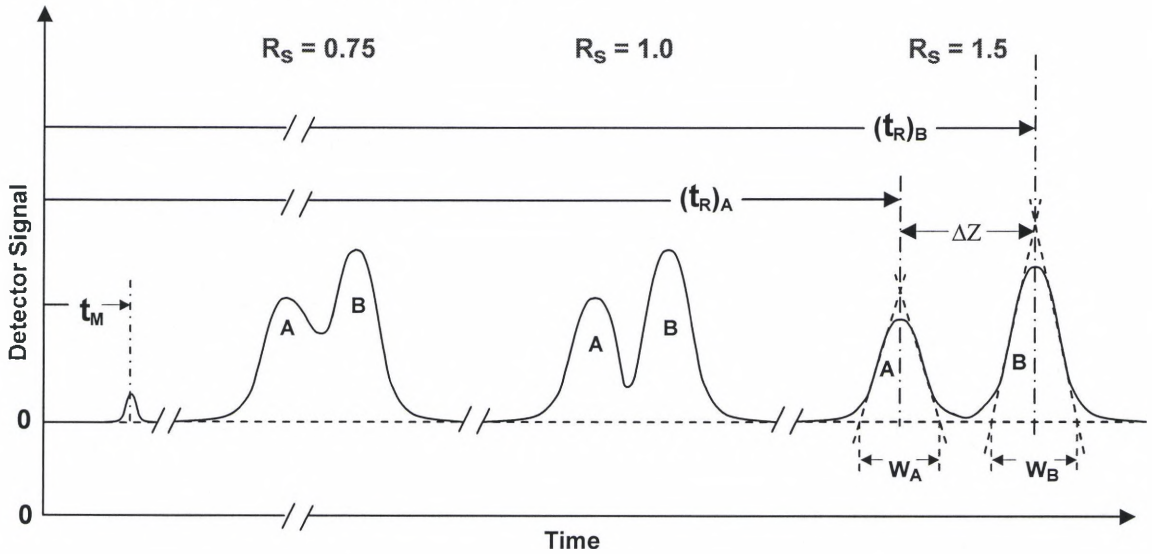

Figure 11. Separation of peaks A and B for three resolutions.

Where, (t_R) are the retention times of each peak, t_M, retention time of an unretained compound, and w is the with of each peak.

The resolution of two adjacent peaks takes into account the individual average widths of each peak (W) and the distance between the two peak maxima (ΔZ). And it is expressed by the Equation 1[33].

$$R_S = \frac{2 \cdot \Delta Z}{(W_A + W_B)} = \frac{2 \cdot ((t_R)_B - (t_R)_A)}{(W_A + W_B)} \quad (1)$$

By rearranging Equation 1, the resolution can be then written as Equation 2[3, 39].

$$R_S = \underbrace{\frac{\sqrt{N}}{4}}_{\text{Dispersion Effect}} \cdot \underbrace{\frac{(\alpha - 1)}{\alpha}}_{\text{Selectivity Effect}} \cdot \underbrace{\left(\frac{k}{k+1}\right)}_{\text{Partitioning Effect}} \quad (2)$$

where N is the observed plate number of the column, α is the relative retention, which describes the relative behavior of two analytes, and k is the capacity factor, which is a measure of the time the analyte resides in the stationary phase relative to the time it spends in the mobile phase. The expression 2 can be further subdivided by different chromatographic influences[3]. The dispersion effect is a function of the column length, diameter, film thickness, mobile phase velocity, and it has almost insignificant influence upon resolution at different column temperatures[3, 69]. The selectivity effect depends on the choice of the mobile and stationary phases, and it was found to decrease by a factor of 1.5-2 over an operational range of approximately 100 °C. Consequently, it does have a significant impact upon the loss of resolution with increasing temperature[3, 69]. The partition effect is a function of the temperature and it is the one that causes the greatest loss of chromatographic resolution at extremely high temperatures[3, 69].

In ITGC operation, the k value of a migrating solute zone is constant, whereas in normal PTGC operation the "whole column" temperature is changed in a linear manner

as a function of time. Thus a migrating solute zone's localized k value will diminish in an approximately exponential manner with distance or time[3, 65]. While by selecting a suitable TGPGC temperature surface, chromatographic migration can theoretically be accomplished in which solutes experience a nearly constant relative retention behavior and practically optimum operational k values for their entire chromatographic transport.

The retention ratio R_r (Equation 3)[39], which is related to the partitioning ratio can be plotted for the various chromatographic operation modes.

$$R_r = \frac{1}{1+k} \qquad (3)$$

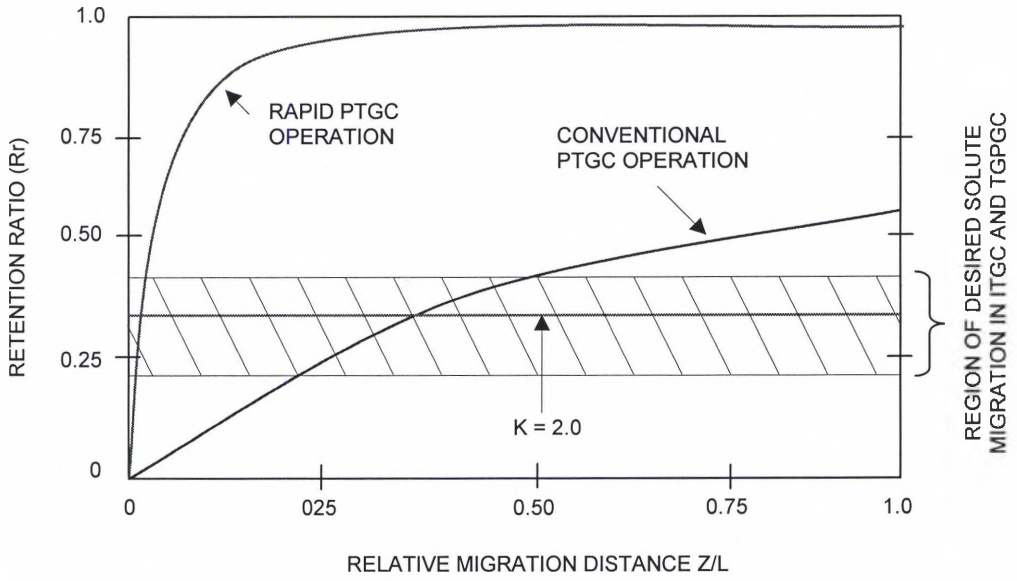

Figure 12. Plot of retention ratio against migration distance for different modes of chromatographic operation[3].

It is apparent form Figure 12 that in conventional PTGC a solute initially migrates at a rate below desired, and that a considerable amount of analytical time is consumed during this early slow migration. After this period, approximately 1/3 of the column length experiences solute zone migration within the desired region. In the last portion of the migration, the solutes experience essentially gas-phase transport[3]. When the PTGC is operated rapidly the effective chromatographic migration is further reduced. The ITGC

mode could operate within the region of desired chromatographic migration but for a narrow range of compounds. By selecting a suitable TGPGC temperature surface, chromatographic migrations of a wide range of compounds can, theoretically, be accomplished with optimalpartitioning[65].

Another behavioral aspect of TGPGC is associated with inherent chromatographic selectivity. Specifically, with the larger number of variables or parameters associated with TGPGC, there are correspondingly more operational variables available for obtaining increased selectivity for closely spaced solute zones. Figure 13 shows a variety of thermal fields that could be achieved for their use in TGPGC technique.

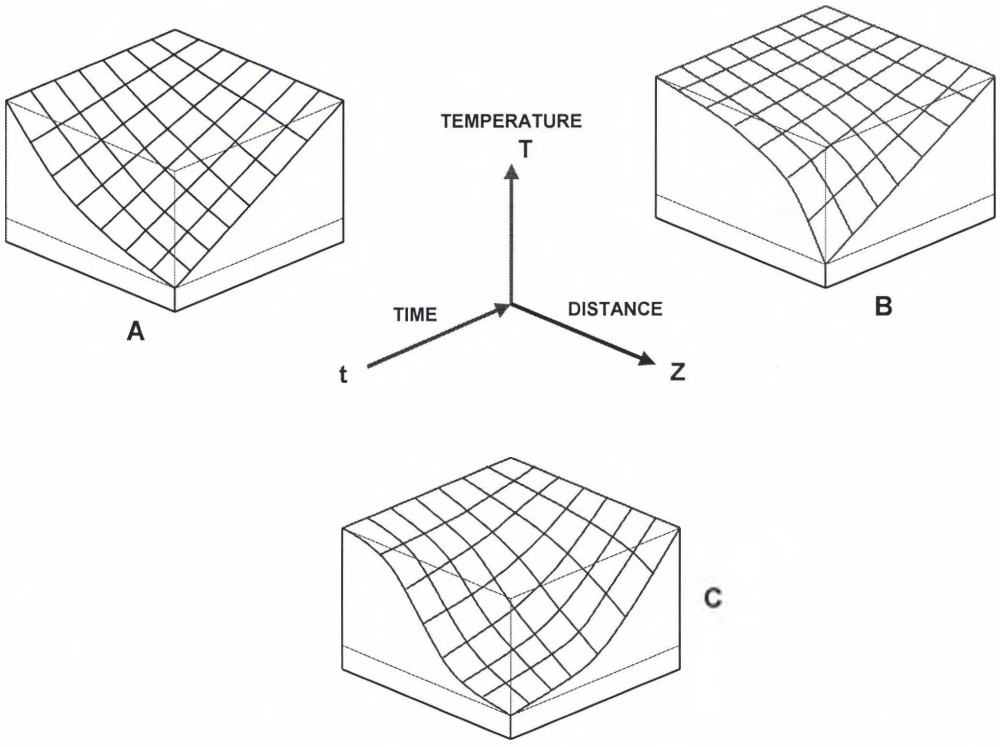

Figure 13. The three basic forms of TGPGC temperature surfaces[29, 67, 68].

An inherent advantage of the TGPGC operational mode is that it can be performed very rapidly. It requires less energy to heat the column in TGPGC operations

than in PTGC mode. Since in TGPGC the column experiences a temperature gradient, the column temperature can effectively be much more rapidly increased than in PTGC operations where the "whole column" is at a uniform temperature. The fast TGPGC analysis translates into shorter turnaround times, which is an important factor in MDGC instrumentation[69]. TGPGC mode is also very beneficial because it allows us to modify the axial temperature decline (temperature surface), during the chromatographic analysis. This temperature surface is very important to achieve complete separations, since there are regions in the chromatogram where one wants a significant negative temperature gradient and others where only gradual negative gradients are preferred. For all these reasons GC analyses of the general elution problem type can, therefore, be solved and conducted more rapidly using the TGPGC mode[3, 29].

Column Sheath Assembly (CSA)

The application of rapid analysis using the TGPGC technique requires special components to achieve the axial temperature gradient and the fast changes in temperature, needed for its implementation. An important requirement is that the chromatographic column must exhibit a high degree of thermal compliance. In that sense, fused silica columns are a good choice. Even though they are manufactured from materials which can be classified as thermal insulators, the extremely thin walls enable them to follow rapid thermal changes with fidelity[26, 29, 67, 68]. In addition to a thermally compliant column, the TGPGC technique requires a special component called a column sheath assembly (CSA) to produce the temperature contour and three-dimensional thermal fields. The CSA also needs to be thermally compliant to facilitate rapid localized

thermal changes, and also be able to undergo rapid and broad changes of temperature and pressure, in order to create a versatile range of thermal fields and have long-term durability.

The early CSA designs used a counter-current heat exchanger principle for invoking the axial thermal gradient along the column axis. Here, cold nitrogen gas was the coolant and preheated in-line nitrogen gas was used to change the temperature over distance and time within the CSA. Also a controlled flow of nitrogen gas was needed for producing the convective heating, and alternatively, the cooling within the CSA[66]. A sketch of a basic CSA design, which was used for developing the method, is shown in Figure 14.

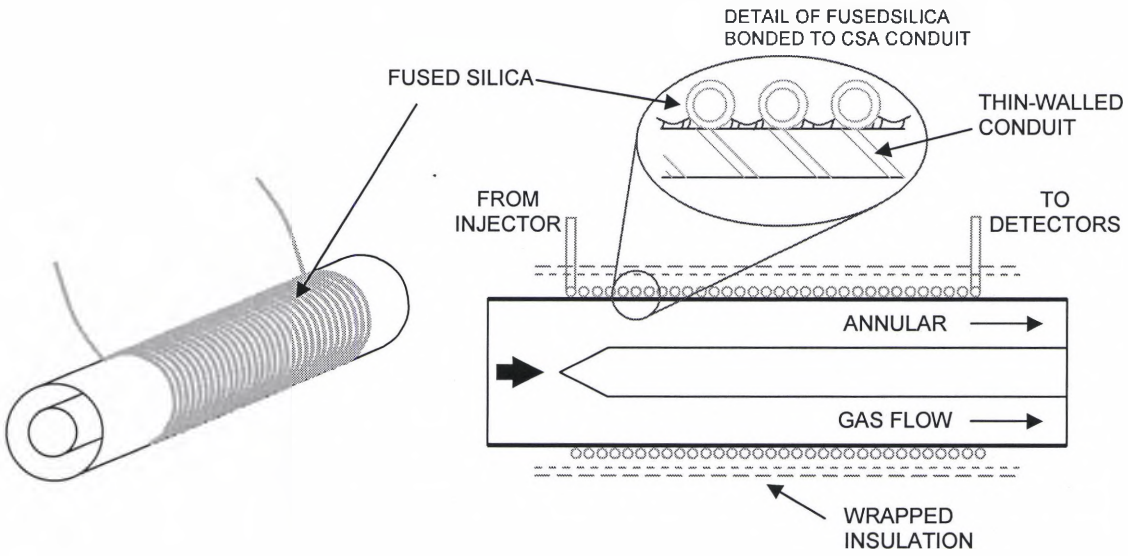

Figure 14. A column Sheath Assembly, for performing TGPGC thermal fields[3].

After reviewing the theoretical and technical aspects of the TGPGC technique, it becomes evident that its implementation in the MDGC system will definitely be a promising approach for the optimization of the separation in the second dimension.

Capillary Column Heating Techniques (GC Ovens)

The various means to heat gas chromatography columns and the latest innovations are: forced-air convective heating, resistive conductive heating and recently developed microwave heating technology.

Forced Convection GC Ovens

Most laboratory bench-top GC systems today, use resistive heated air-bath ovens to heat the entire column and its contents[63]. Actual GC ovens are large in volume, and most of the thermal energy generated by these ovens is needed to heat the oven itself. The large thermal mass of the conventional GC oven dramatically retards the rate at which the column can be heated and cooled[71]. The maximum heating rate of most conventional GC ovens is approximately 1 to 2 °C/s[58, 61, 63, 72], and the cool down times from 300 to 30 °C is around 5-7 min (0.6 °C/s)[51, 53, 56, 72]. In this type of oven the cool-down time is a limiting factor for fast chromatography[51].

The thermal mass is the capacity of storing thermal energy and it is related to the specific heat capacity of the substance and its amount of mass, High thermal mass systems implies that it takes large amounts of energy to change its temperature. Such systems react slowly to temperature variations, which is the case of the bulky GC ovens. Materials with low thermal mass such as fused-silica columns, can rapidly follow the temperature variations readily.

Therefore the heating and cooling rate of a system is strongly dependent on its thermal mass. It is for this reason that conventional GC ovens are just not well suited for high speed heating and cooling cycles[51].

Solid-State Resistive Heating

In the pursuit of fast column heating techniques, a number of alternatives have been developed. One of the alternatives is the use of resistive heating, where the column can be heated by a conductive coating, a metal sheath around the GC column, or a wire closely adjacent to the column. The operating principle is essentially the same in all cases: when a voltage is applied to the conductive material, the passage of electrical current increases the temperature of the metallic heating element and heat is transferred to the column mostly via conduction[53, 63].

Commercially systems have recently become available (EZ-Flash GC system, ThermoOrion and Flash GC, Thermedics) in which a fused silica capillary column runs coaxially inside a coiled resistively heated metal tube. These devices can achieve heating rates up to 20 °C/s[58, 60, 72] and cool-down times of 1 min from 325 to 35 °C (5 °C/s)[60, 73]. However it is very important in these systems to carefully insulate each column coil, thermally and electrically, from adjacent coils as well as from the column supports. Any contact between the coils creates uneven thermal gradients (cold spots) and electrical shorting[63, 73]. Even small cold spots can drastically decrease the column resolution in fast chromatography[59].

Microwave GC Ovens

An innovative alternative for heating the GC column is the use of microwave technology. A microwave GC oven has been engineered to generate a uniform microwave field around the column, eliminating cold spots, and furthermore heating only the capillary column. The columns used in microwave ovens need to be coated with a

microwave-absorbent material that converts microwave energy to thermal energy, which heats the column and stationary phase.

Heating rates in excess of 10 °C/s, and 1-min cool-down times from 350-35 °C (5 °C/s) can be achieved[71], yet the oven is cool to the touch and small enough to be held in the palm of one's hand.

CHAPTER III

EXPERIMENTAL

The application of the three dimensional thermal fields in TGPGC requires the use of a column sheath assembly (CSA). Therefore, the design, construction, and evaluation of a CSA capable of producing a variety of thermal contours with high-thermal compliance and uniformity were necessary.

An instrument was designed and built to evaluate the different CSA designs by measuring the temperature inside the CSA along the length, as a function of time. This instrument allowed the 3D mapping of the thermal fields created in the CSA, and also the application of a wide range of thermal and pneumatic conditions to study the operational limits of the CSA designs. These parameters were used in choosing the best performing CSA design for its application in rapid TGPGC analysis.

The further use of the TGPGC technique in the second-dimension of the MDGC-MS system required the tuning and adjustment of the CSA. In these experiments only the trap-and-release device and the second-dimension column of the MDGC-MS system were used, and the sample injections were performed simulating the heartcuts coming from the first column. The sample used for the tuning of the CSA consisted of five selected compounds that possessed similar boiling points and demonstrated different chromatographic polarities. The sample simulated a narrow collected fraction from the first dimension.

After tuning the CSA with the second-dimension column, the primary column was incorporated into the MDGC-MS system. A low dead-volume tee was used to connect the two columns together. Finally, after carefully adjusting the optimal flow in both columns the experiments of the TGPGC mode with more complex mixtures and heartcuts were performed.

The Column Sheath Assembly Testing Instrument

The initial experiments were performed to evaluate the different designs of the CSA. The experimental set up used is shown in Figure 15. The axial cooling and heating of the CSA designs were achieved within a modified gas chromatography oven (Carlo Erba HRGC 5300) and by using nitrogen gas (Air Products) as the heat exchanger fluid. The CSAs were placed inside the GC oven and connected to the system by ¼ inch Swagelock fittings. The connections between the Swagelok fittings and the polyimide tubing where performed by placing a ¼" outer diameter (OD) PTFE tubing (Cole-Parmer A-06407-44) inside the polyimide tubing (see Figure 16). The PTFE tube worked as an intermediate between the polyimide tube and the Swagelock fitting. The polyimide was attached to the PTFE tubing with the help of polyimide tape (Airtech Airkap 477349), while the PTFE tubing was directly used with the Swagelock fittings.

A heat exchanger made of a ¼" OD copper tubing (Cole-Parmer A-34671-10) was designed and built to heat the nitrogen gas from room temperature to oven temperature, thereby providing the heating fluid. The cooling fluid used was room temperature nitrogen gas.

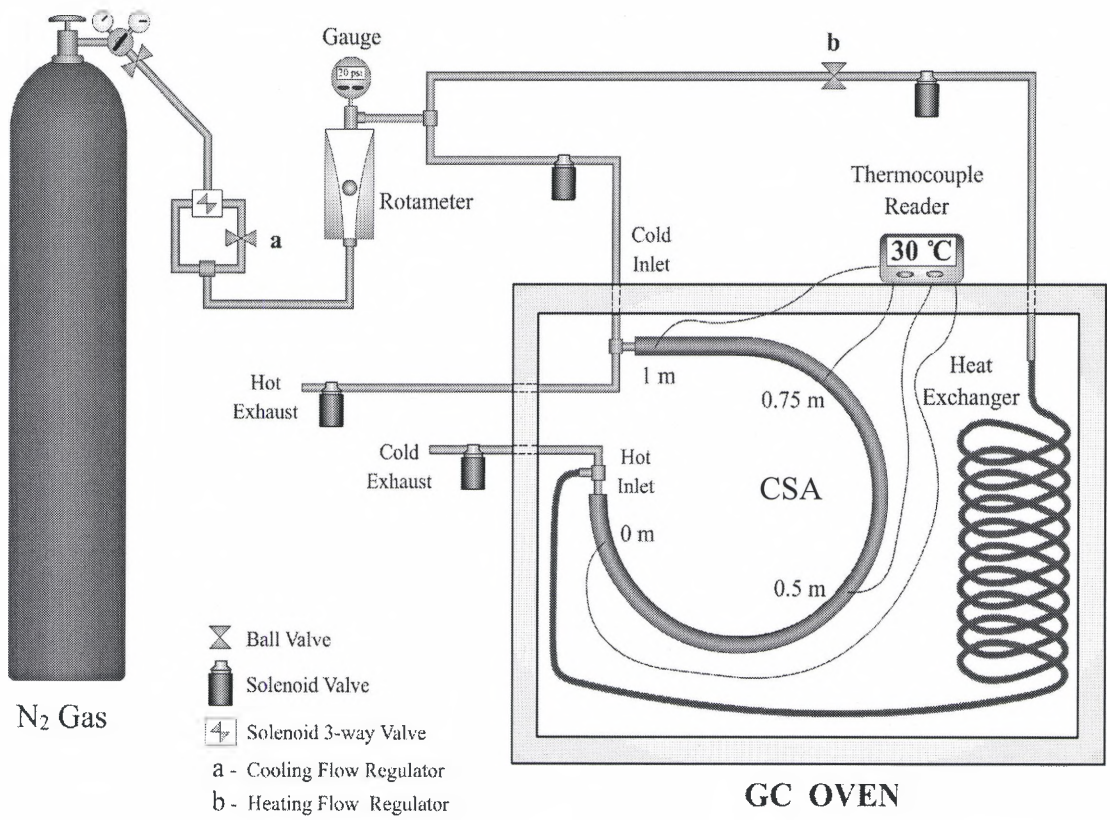

Figure 15. Scheme of the apparatus used for testing the different CSA designs.

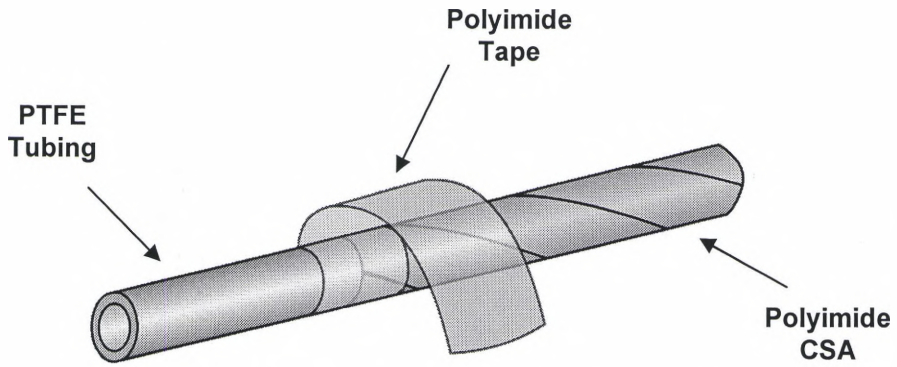

Figure 16. PTFE-Polyimide tubing connections.

The nitrogen gas flow rate was measured with a rotameter (Cole-Parmer A-32461-56) positioned at the beginning of the CSA testing apparatus. Since the

operational conditions of the experiments differed from the calibration conditions of the rotameter, the rotameter scale could not be used directly. Adjustments were done by using Equation 4, allowing the use of the rotameter scale to obtain the corrected flow rate at the experimental conditions. The pressure at the outlet of the rotameter was measured by a digital pressure gauge (Cole-Parmer A-68110-20)[74].

$$F' = F^{\circ}\sqrt{\frac{P'}{P^{\circ}} \times \frac{T^{\circ}}{T'}}$$

F = Flow rate; P = Pressure; T = Temperature
° = Conditions of calibration of the rotameter
' = Conditions of the rotameter at the experiment (4)

Computer-controlled solenoid valves (Nema-4 SV-127 and Skinner 3-way C series) were used to accurately and instantly change the heating and cooling process in the system, allowing a precise control of the flows. The cooling process or temperature gradient formation in the CSA was achieved when the solenoid valves 2 and 4 where opened and 3 and 5 where closed (see Figure 15), while the opposite was true for the heating process. The 3-way solenoid valve was used to rapidly switch between a high flow and a low (or restricted) flow that was needed to generate a wide range of thermal fields. The ball valves "a" and "b" worked as flow restrictors, allowing more experimental flow flexibility.

The temperature inside the CSA was measured at 4 different axial positions, to provide an adequate profile of the temperature gradient through the CSA. Furthermore, the use of unsheathed fine diameter type K thermocouples (wire diameter 0.005" OMEGA Chromel/Alumel) ensured a fast response time using the thermocouples to precisely follow the temperature variations inside the CSA. The thermocouples were positioned inside the CSA through small holes across the CSA and kept in place with polyimide tape; see Figure 17 for details.

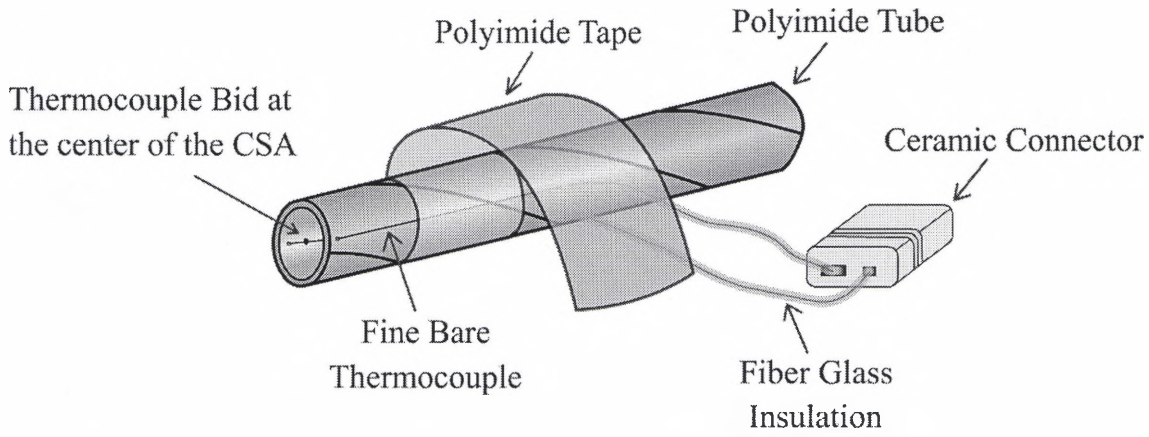

Figure 17. Thermocouple Positioning.

The thermocouple bare wires were insulated with fiberglass sleeve (ALPHA wire Company PIF-240-20). The wires were then coupled to ceramic connectors (OMEGA high temperature connectors SHX-K-(F)) that were attached to thermocouple wires that transmitted the temperature signal outside the GC oven.

The temperature readings were gathered by the use of an acquisition device (LabJack U12) and stored in a PC workstation. First, the analog signal output of the thermocouples were amplified, (Electronic Innovations EI-1040) and then input into the acquisition device that allowed the monitoring of the temperatures at a sampling rate of up to 300 Hz. This fast data acquisition system permitted the collection of an accurate profile of the temperature changes within the CSA device as well as the 3D plotting of the thermal fields.

The experiments performed in this system consisted of determining the speed of heating and cooling that could be achieved with the different CSA configurations. For these experiments a cyclic cooling and heating mode was performed. First, the oven was kept at a constant temperature between 100 and 200 ºC, so the temperatures inside the CSA were axially constant. Then, the solenoid valve 1 was positioned in high flow and the cooling flow path was opened. Fast cooling was achieved by intensely sweeping

nitrogen gas through the CSA by using inlet pressures of approximately 30 psig. After 1 or 2 seconds the solenoid valve 1 was switched to low flow to keep a desired constant temperature gradient along the CSA. Valve "a" was previously regulated to achieve the particular temperature gradient. Then, after a period of 10 seconds the heating path was opened and either high or low flow was used for heating the CSA again (valve 1 in high or low flow position). After 10 seconds the cycle was repeated and measurements were taken when the temperature profiles cycles showed a steady state. The heating flow was performed in the opposite direction of the cooling flow, in order to keep the negative gradient during the heating processes.

To study the limits of operation, each CSA design was submitted to a wide range of temperature and pressure conditions while applying the cyclic mode explained above. The oven temperatures used for these experiments were between room temperature and 300 °C, while employing pressure between 5 and 35 psig.

The MDGC-MS System Specifications

The multidimensional system assembly was housed in a modified Hewlett-Packard 5890 gas chromatograph. The GC was equipped with a split/split-less injector, constant pressure flow control, and a flame ionization detector (FID). The secondary column effluent was directed to a mass selective detector where the qualitative identifications of products were done. The MSD was a Hewlett Packard 5969B that incorporated a quadrupole design. The raw data was recorded on a PC workstation. The general schematic of the MDGC-MS system is shown in Figure 18.

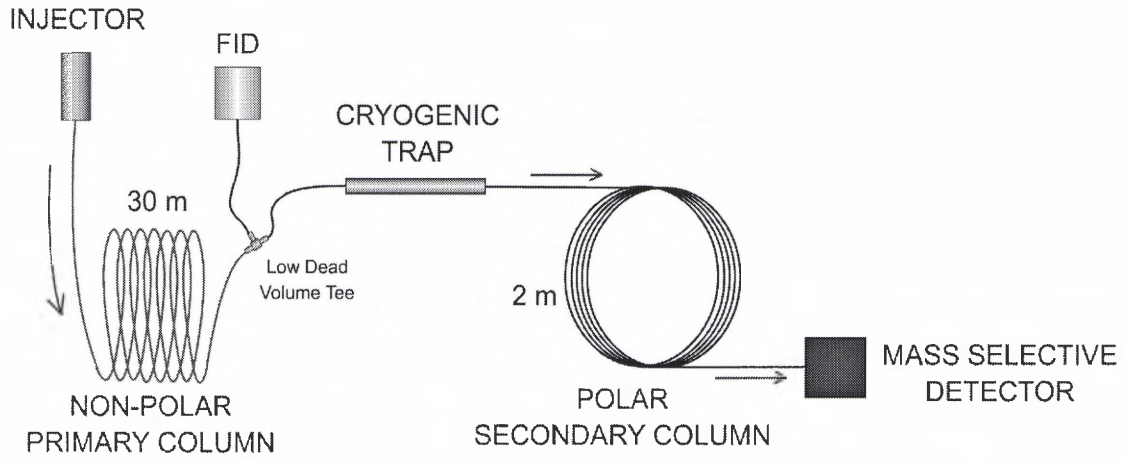

Figure 18. General Schematic of the MDGC-MS system.

The primary separation was performed using a megabore stainless steel column, approximately 30-m in length. This megabore column had a 0.53-mm internal diameter, and a 1.0-μm film thickness. The stationary phase was non-polar ((5%-Phenyl)-methylpolysiloxane (MXT-5 Restek)), an excellent general-purpose substrate with low bleed over a wide temperature range (-60°C to 310°C)[75]. The secondary column was of microbore design necessary for fast chromatography. Two secondary columns where used, the length of the columns were 4-m and 2.3-m, the internal diameter and film thickness for both columns were 0.1-mm, and 0.1-μm respectively. The secondary columns' bonded stationary phases were trifluoropropylmethyl polysiloxanes (RTX-200) and polyethylene glycol (BP20 SGE)[76]. These phases were chosen because of their high selectivity for polar molecules and their high thermal stability (up to 320°C for the RTX-200 and 280°C for the BP20).

Since the carrier gas used in the system was high purity helium (purchased from Air Products), the optimal carrier gas velocity for the primary column was around 25-cm/sec according to the Van Deemter curves. However since the second dimension is a fast GC analysis, higher carrier velocities around 100-cm/sec were desired. An example

of the van Deemeter curves is shown in Figure 19 where the H.E.T.P is the height equivalent to one theoretical plate. The smaller the HETP the more efficient the column.

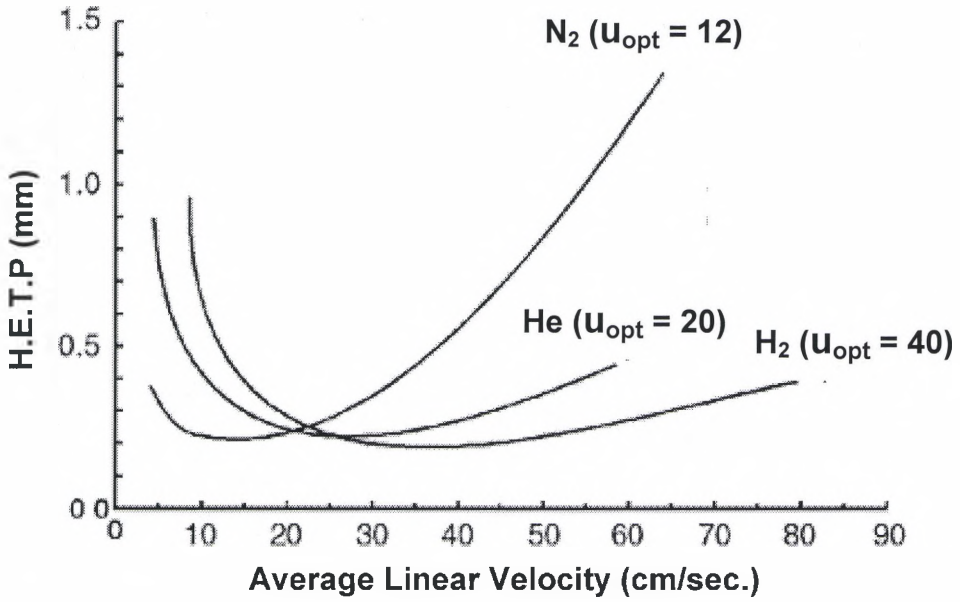

Figure 19. The van Deemter curves for nitrogen, helium and hydrogen, showing their optimal flow velocities[69].

To maintain the optimal flow in both columns, a low dead-volume tee (J&W Scientific) was used to connect the two columns. At the tee, the flow was divided and part of it was vented thereby maintaining the required flow in both columns. The vent flow at the tee was adjusted by modifying the dimensions (length and diameter) of the venting restrictor. The pressure within the tee connection was experimentally measured. Due to the complexity of the MDGC-MS system, the average velocity in each column was estimated by Flow Calculator Software from the Hewlett-Packard Company[77]. The software required only the characteristics and pressure gradient of the column to determine the average velocity, making it very convenient to use. The optimal flows in both columns were then obtained by modifying the primary column inlet pressure and the vent at the tee connection. These parameters where adequate to generate the optimal flow through the primary and secondary column.

The Modulator

The MDGC-MS instrument used a cryogenic trap system that followed the same principles as the one presented by Marriott and Kinghorn[41, 49]. Instead of moving the cryogenic trap along a section of a fixed column, the column was moved through a stationary cryogenic zone.

During the accumulation phase, solutes moving towards the cryogenically cooled zone essentially stop moving through the column and become refocused in a narrow band, thus removing the effects of zone dispersion within the first column. After a pre-set and constant period of time, the column was quickly moved to a new upstream position. There, the previously focused zone was exposed to the thermal environment of forced flow convection provided by the GC oven. Quickly the trapped components were released. On average, it was estimated that the component release time was 30 milliseconds[45].

The movement of the column through the trap was created through the use of a linear actuating device manufactured by a Swiss company (Sulzer Electronics AG). The linear actuator had an extendable arm that could be computer-programmed to move at various speeds. A brass bar attached to the end of the actuator arm extended into the right side of the GC oven. This bar was attached to the capillary column by two high-temperature silicon septa, which prevented the capillary column from slipping. When the actuator was extended, the system was in "trap" mode and the chemical components within the cold section of the column were no longer migrating. As the arm retracted, the trapped section of column was pulled into the heated oven, where the components were released and transported through the secondary column[45]. This trap and release motion is further described in Figure 20. It was determined that the most effective motion of the actuator was a slow extension followed by a rapid retraction. The slow trapping motion

created a continual refocusing of the components at the beginning of the trap, preventing the potential breakthrough or migration of the solutes through the cryogenic trap, and lessened the risk of breaking the column[45].

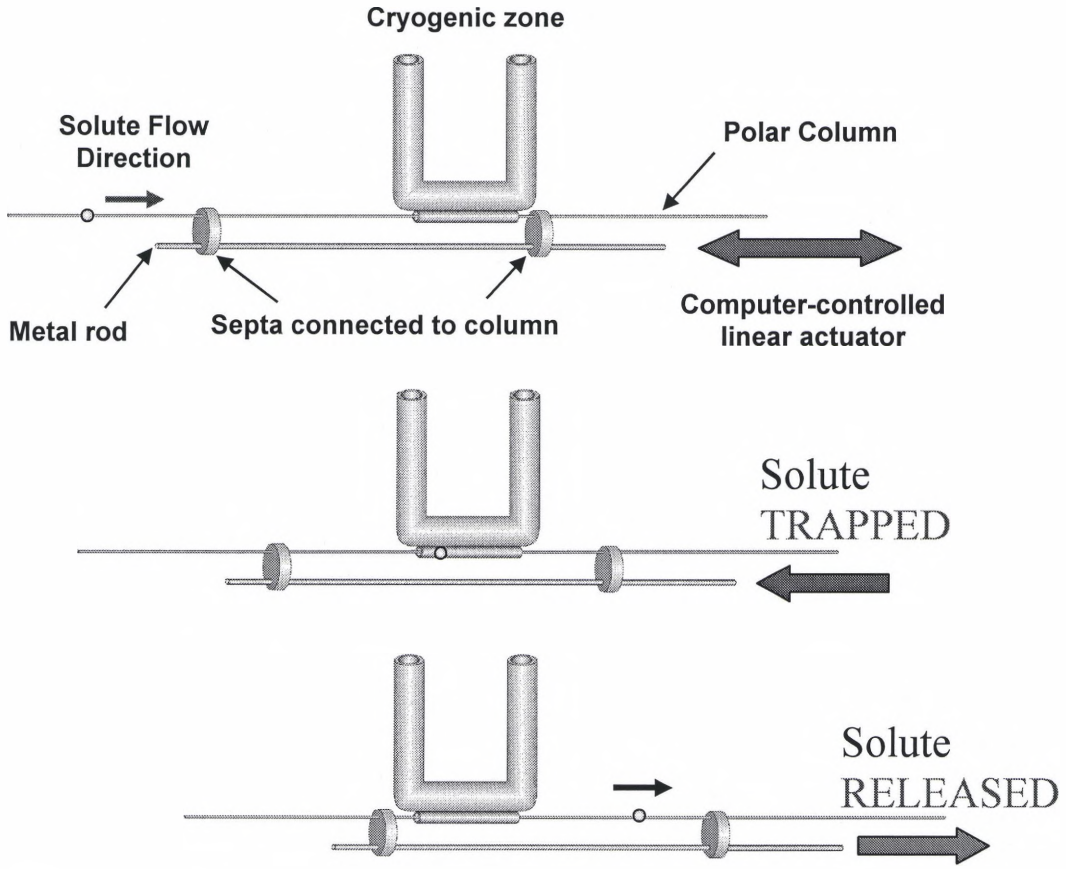

Figure 20. A diagram describing the trap and release processes using a stationary cryogenic zone and moving capillary column.

The trap operated at approximately -30 ºC and it was achieved by using a low-pressure (22-psi) reservoir of liquid nitrogen (Air Products). After flowing through the trap, the cold nitrogen was warmed to room temperature and released back into the heated oven (see Figure 20). This nitrogen flow helped to remove excess water vapor from inside the oven and prevented ice formation on the trap.

Integration of the CSA in the MDGC-MS Equipment

For the tuning of the TGPGC apparatus, the coupling of the CSA with the multidimensional system was necessary. The CSA testing system was modified and rebuilt to fit in the remaining free space inside the GC oven of the MDGC-MS instrument. In this experimental set up only the second column and the modulator where used. Figure 21 shows the final configuration of the CSA in the multidimensional system.

The CSA was suspended down into the GC oven through the top plate, while keeping the same flow and valve configuration as in the CSA testing instrument. Thus the operation of the CSA in the MDGC-MS system followed the same steps previously explained. The temperature flexibility of the CSA system was further improved when the metal tee at the cooling inlet (see Figure 21) was changed for a thin walled ¼" polyimide tee. The low thermal mass of the polyimide tee, allowed not only rapid changes of temperature at the tee connection, but also lower temperatures during the cooling stage. The polyimide tee was hand-made from the ¼" polyimide tape tube and polyimide resin.

The secondary open tubular column (OTC) was placed inside the CSA through small perforations in the polyimide sheath. Radial temperature uniformity associated with the fused silica column positioning was achieved by keeping the column in the middle of the CSA without touching the conduit walls. A fine wire coiled design was used to keep the OTC in the middle of the CSA. Tungsten wire of 0.005" diameter was used for the coiling system, due to its low thermal mass and excellent strength (U-TW-005 Small Parts).

Figure 22 shows the coiling arrangement, where an alternating sequence of two coils diameters ¼" and 1/16" were used to keep the fused silica column in the middle of the CSA.

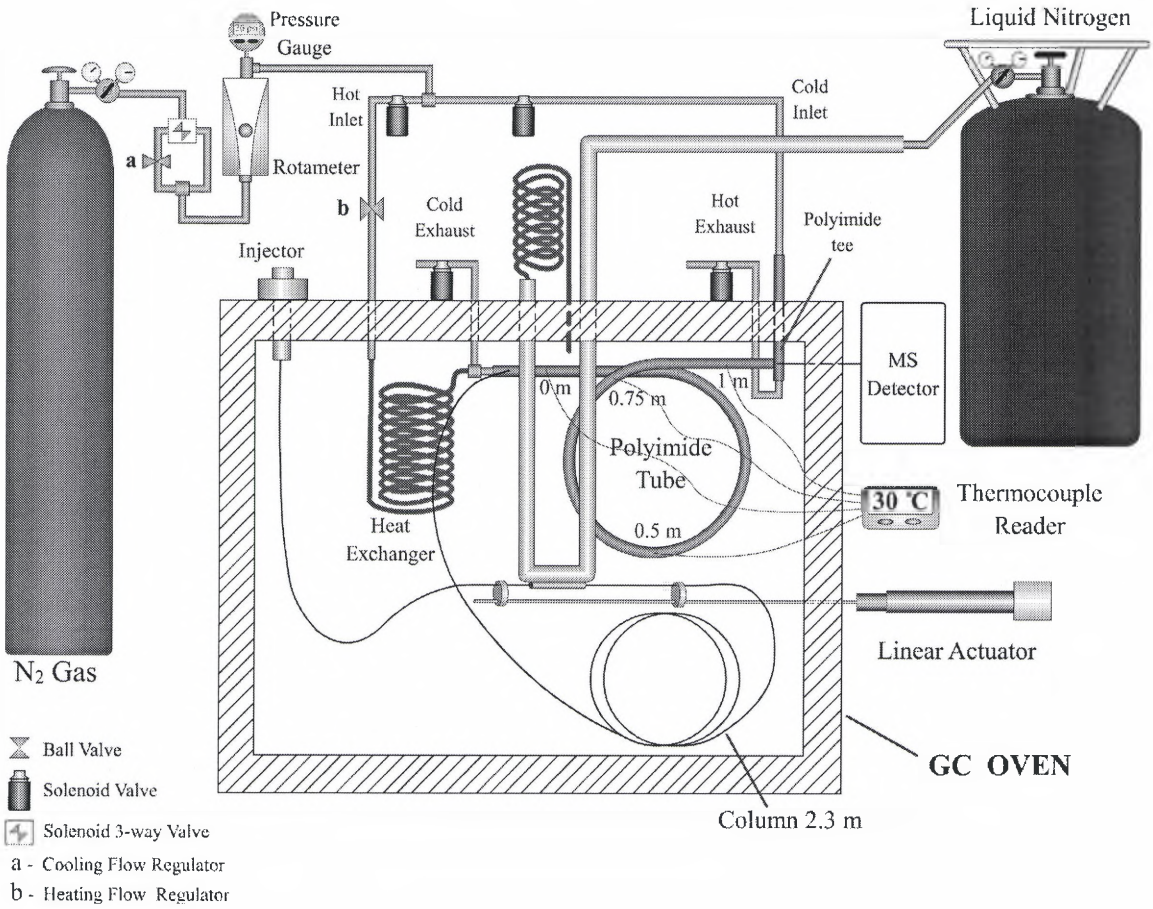

Figure 21. Apparatus assembly of the CSA in the MDGC-MS system.

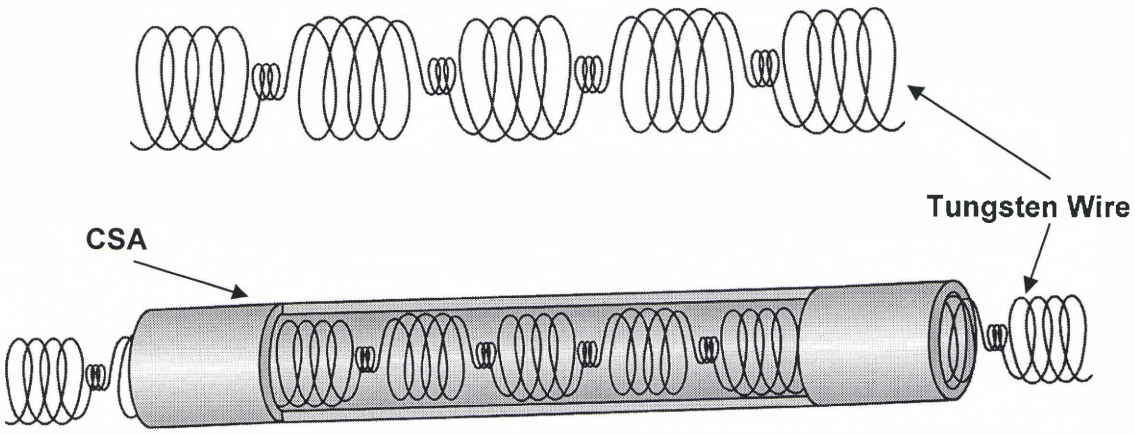

Figure 22. Coiling arrangement that keeps the OTC in the middle of the CSA.

After tuning the second dimension separation using the TGPGC mode, the remaining first dimension column was incorporated. The configuration of the complete multidimensional system with the application of the TGPGC technique in the second dimension is shown in Figure 23. Figure 24 and 25 show the entire system.

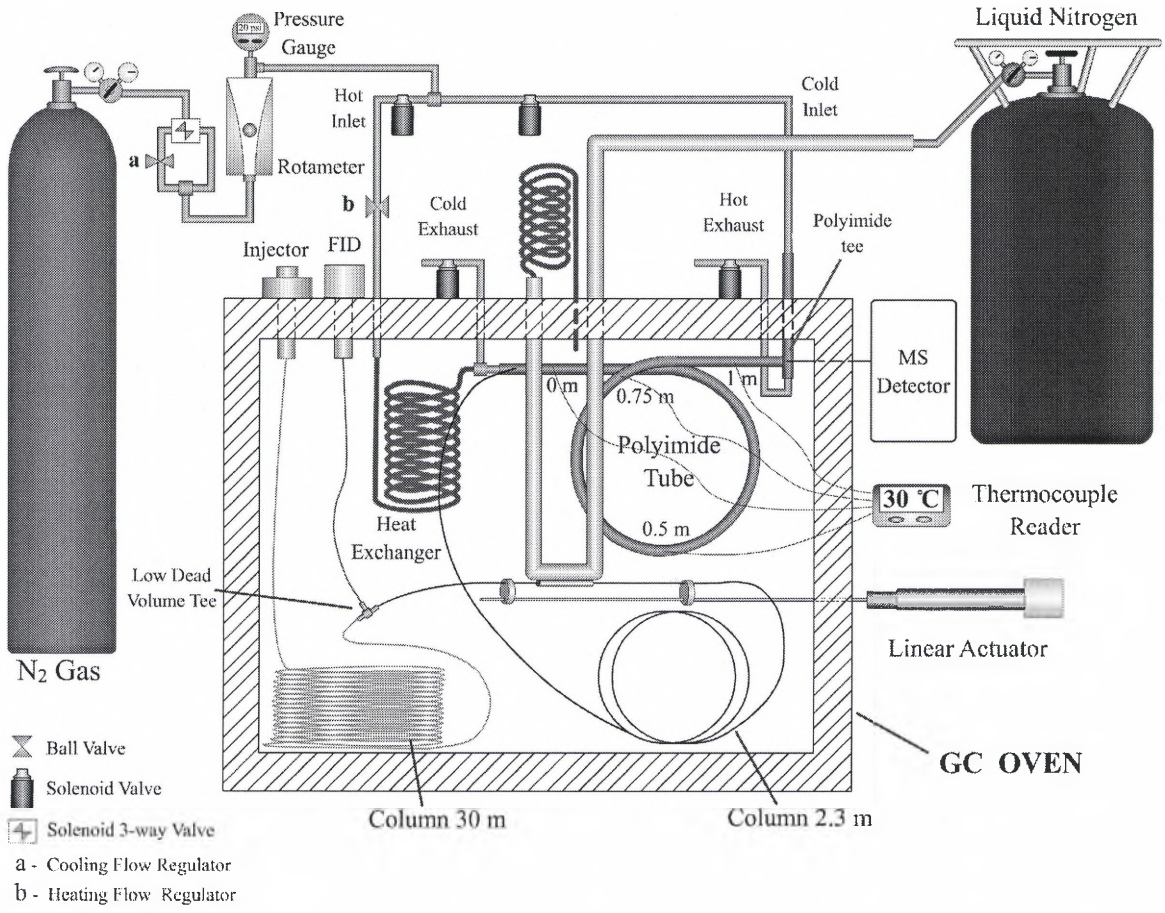

Figure 23. System configuration of the MDGC-MS system with a TGPGC mode in the second dimension.

The general flow path of a sample injected into the MDGC-MS (with TGPGC) system was as follows. After volatilization in the hot split/split-less injector, the sample was transported into the non-polar primary column by the carrier gas. From this column, the separated sample flowed into a low dead-volume tee connection, where it was split

between the secondary column and the vent column. Sample that passed into the secondary column immediately reached the cryogenic trap. In the trap it was subambiently refocused into a narrow band of solute and then released into the polar secondary column. In the secondary column the sample was submitted to a negative temperature gradient where it was constantly refocused. After a certain period of time the negative gradient was eliminated and the secondary column was heated to oven temperature where the rest of the sample was eluted. At the completion of the secondary separation, the components of the sample were detected using a mass selective detector (MSD).

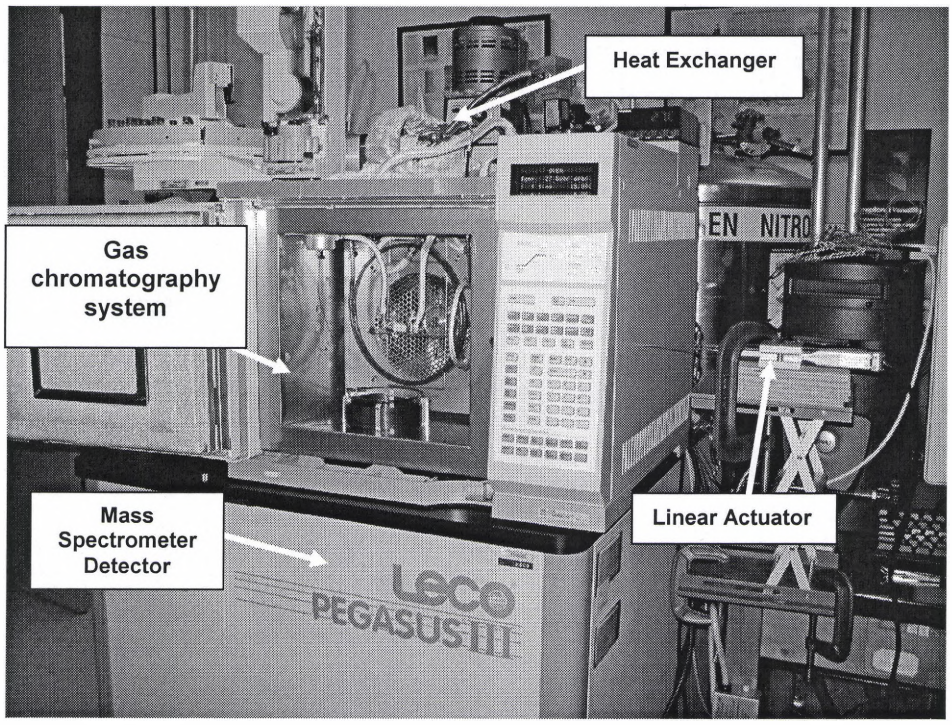

Figure 24. Picture of the MDGC-TOFMS with TGPGC system incorporated.

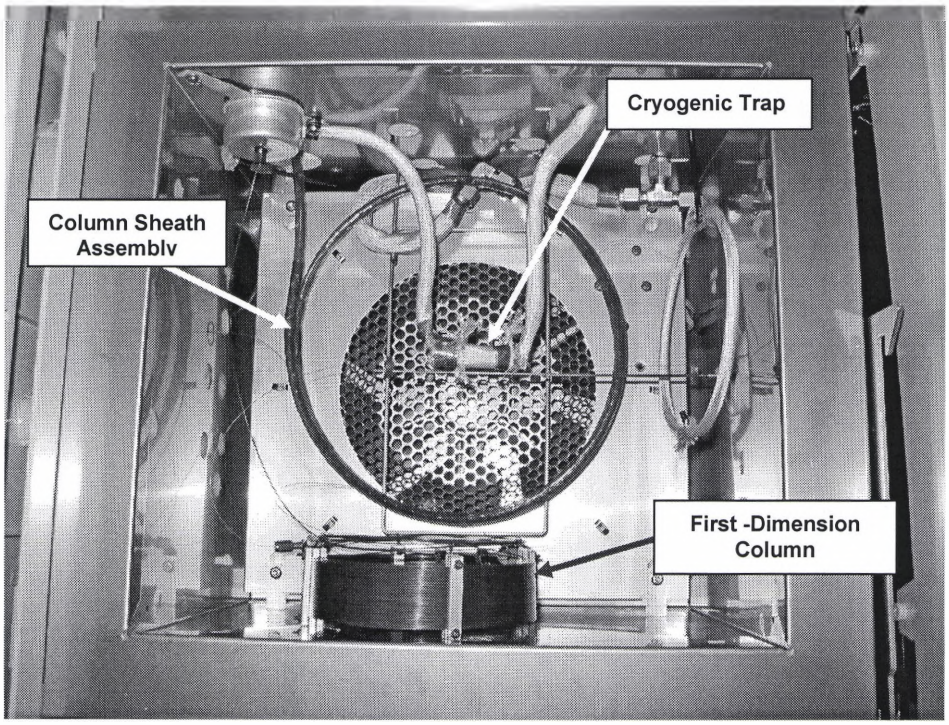

Figure 25. Picture of the MDGC-TOFMS GC oven arrangement.

Sample Preparation

For the tuning of the TGPGC technique in the MDGC-MS second dimension, five pure selected compounds that had similar boiling points, and offered different chromatographic polarities, were used to constitute samples that simulated a heart cut. The components chosen needed to include a wide range of chromatography polarities in order to distribute the compounds through the second dimension separation. The components chosen are shown in Table 1.

Table 1. Selected pure compounds for the simulation of a heartcut.

Compound Name	MW	Density	Boiling Point (°C)	Company
n-C12 (normal dodecane)	170	0.75	215	Aldrich
n-C16 (normal hexadecane)	226	0.77	287	Aldrich
n-C16 (normal hexadecene)	224	0.78	273	Aldrich
2-methyl naphthol	148.2		264	Aldrich
1-decyl benzene	218	0.85	293	Aldrich
1-tetradecanol	214	0.82	289	Aldrich

The compounds where dissolved in dichloro methane and the solutes that were used were added approximately in the same proportion (V/V) to the mixture. The dichloro-methane used was 99% pure purchased from Aldrich.

The GC injections were performed using only needle dead-volume injection technique, due to the high concentration of the sample. In the sample, the n-C12 functioned as the unretained compound, and was used to determine the average carrier velocity in the second dimension column. The sample was injected (Hamilton 691 syringes) in the split injection mode at 280 °C with a split flow of 120 ml/min. The temperatures of the GC oven for the tuning experiments were held at 180°C and 200 °C isothermal temperatures. The pressure inlet at the column entrance was 30 psig, since an average carrier velocity of 100 cm/sec was desired for the second dimension.

The quadrupole mass selective detector was operated in full scan mode, at a spectrum storage rate of 14 Hz, using a mass range of 50-110 m/z. All instrumental parameters and data acquisition was controlled through the Hewlett Packard ChemStation software (version D.01.00.). The qualitative identification of each compounds, mass spectra was searched against the NIST (National Institute of Standards Technology) mass spectral library.

The calculations of the peak capacity resolution were calculated with the data retrieved from the ChemStation, e.g. retention time, area height and peak with. The calculations of the raw data were performed using Microsoft Excel software.

With the tuning and complete assembly of the MDGC-MS TGPGC system accomplished, experiments with real and challenging heartcuts were required. Complex samples were selected to provide complicated heartcuts and test the functionality and separating power of the TGPGC mode against the isothermal GC mode, which is commonly used for the second dimension separation. Most of the complex sample

preparation (extraction, blow-down, etc.) were performed by the combustion researchers who generated the samples.

Polyimide Tape Tubing Assembly

The ¼" OD coiled polyimide tubing needed to be hand-made and manufactured since it could not be found commercially. The construction of the polyimide tube was essentially performed by wrapping a stainless steel tube with polyimide tape. The straight polyimide tube obtained (after removing the metal tube) was then coiled and strengthened; thereby obtaining the required polyimide tube. The polyimide tape used for the construction of the finished tube was ½" wide and 2 mil thick (AirKap, purchased from AirTech). The stainless steel tube that was used as a mold was 1.3 m long and ¼" OD (obtained form Cole-Parmer (A-06407-44)).

First, a portion (1.1m) of the stainless steel tube was wrapped with polyimide tape. In this step, the non-adhesive part of the tape was fixed facing the metal tube. It is important to previously cover the metal tube with a thin layer of mineral oil, to allow the removal of the polyimide tubing once prepared. To achieve the wrapping, the polyimide tape needed to be held to an end of the metal tube with adhesive tape. And when the metal tube was wrapped, adhesive tape was also needed to keep it wrapped. For the wrapping, the tape was either superimposed with itself or carefully placed right next to each other. Figure 26 shows these two ways of wrapping the metal tube.

After wrapping the metal tube with the polyimide tape, another layer of polyimide was placed on top, covering the gaps of the first wrapping. In this case, the tape was placed with the adhesive part facing the covered tube. As before the wrapping was made by either superimposing the second tape or by placing it carefully near each other.

Moreover, the tape could be wrapped in the opposite direction. Figure 27, shows how the second polyimide layer was applied. Once the polyimide tube was completed and the metal tube was taken out, the coiling process was performed.

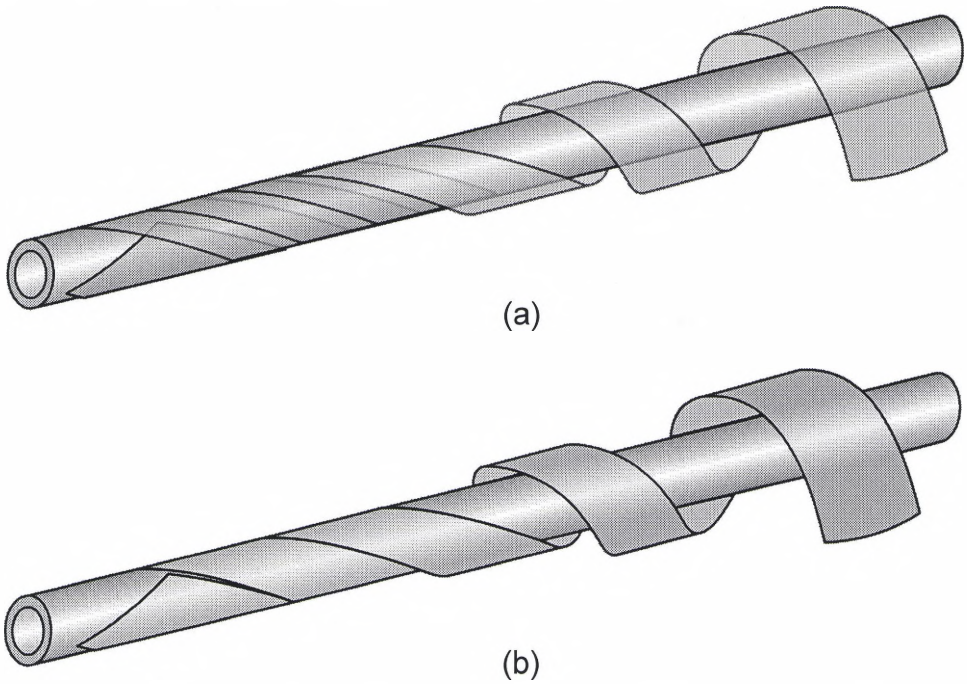

Figure 26. a) Wrapping the metal tube superposing the tape; b) Wrapping the metal tube locating the tape right next to each other.

Initially a ¼" OD PTFE tube (Cole-Parmer A-34671-00) was placed inside the polyimide tube to avoid buckling the tube during the coiling process. To keep the PTFE tube in a coiled position, a 1/8" copper tube (Cole-Parmer A-34671-10) was placed inside the PTFE tube. A coil diameter of less than 30 cm was used, due to the dimensions of the GC oven.

To strengthen and make leak proof the polyimide tube, polyimide resin was used (purchased from RESTEK (Cat.# 20445)). The polyimide resin was placed at the junctions of the polyimide tape and thermally treated to cure it. The temperature profile of the curing process is shown in Figure 28[75].

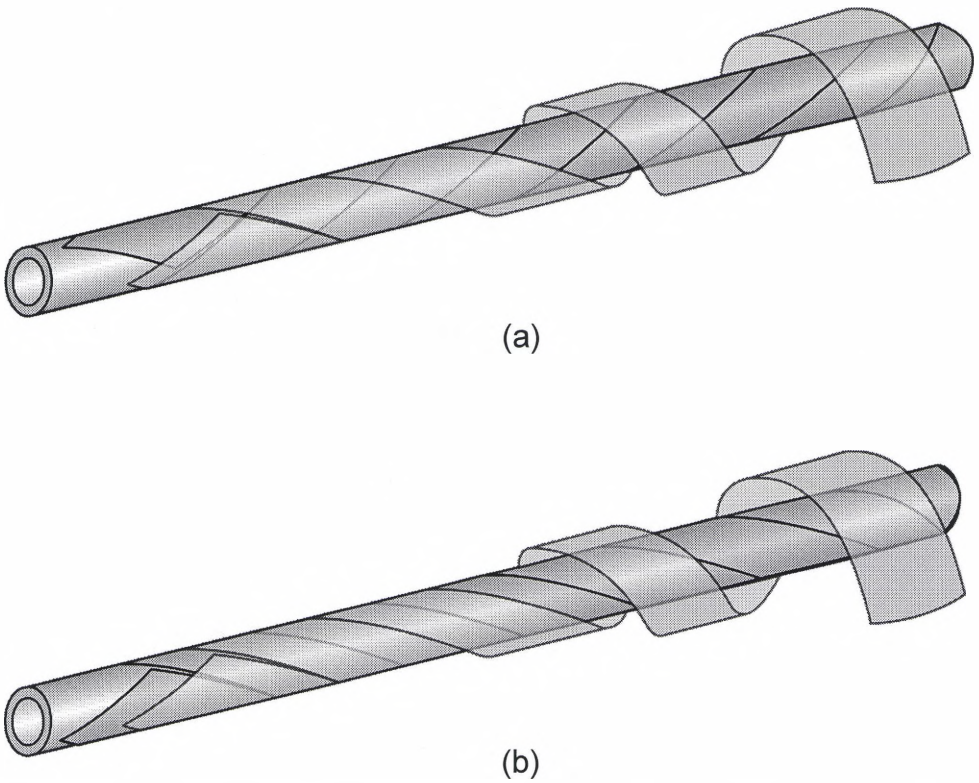

Figure 27. a) Applying the second polyimide layer in the opposite direction; b) Second polyimide layer wrapping placing the tape right next to each other.

The coil arrangement of tubes was then thermally treated to cure the resin and coil the polyimide tube. The coiling of the polyimide tube was accomplished due to the thermal expansion characteristics of the PTFE. When the coiled arrangement of the PTFE and polyimide tube was heated, it made the PTFE tube expand. The expansion of the PTFE tube inside the polyimide tube forces the tapes of the polyimide tube to move into new positions to relieve the stress that the coil arrangement places on them. The relocation of the tapes was what kept the polyimide tube coiled after being thermally treated.

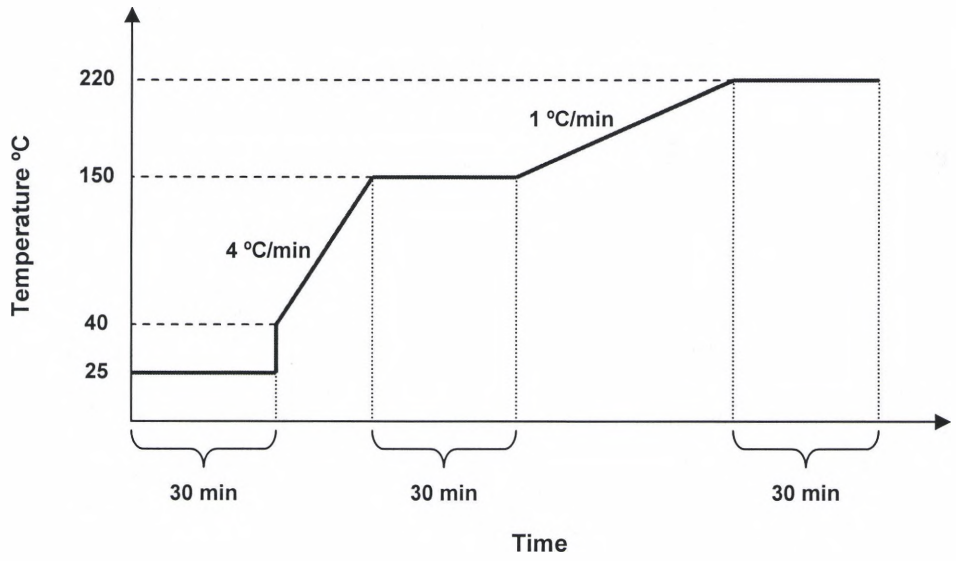

Figure 28. Temperature profile of the thermal treating of the polyimide tube for curing the resin and coiling the tube.

After thermally treating the arrangement of tubes, the already coiled polyimide tube was separated. Even though the polyimide tube was already coiled, the application of wide temperatures, fast thermal and pressure changes during the experiments could collapse and buckle the tube. To keep the structural circular form of the polyimide tube, additional polyimide tapes were placed in three different positions around the coil. Figure 29 shows how the additional tapes were placed in the coiled polyimide tube. The positioning of the 3 tapes allowed using the same forces that try to collapse the circular tube to keep its integrity by balancing the forces around the coil, when it is subject of high temperatures and fluctuating pressures.

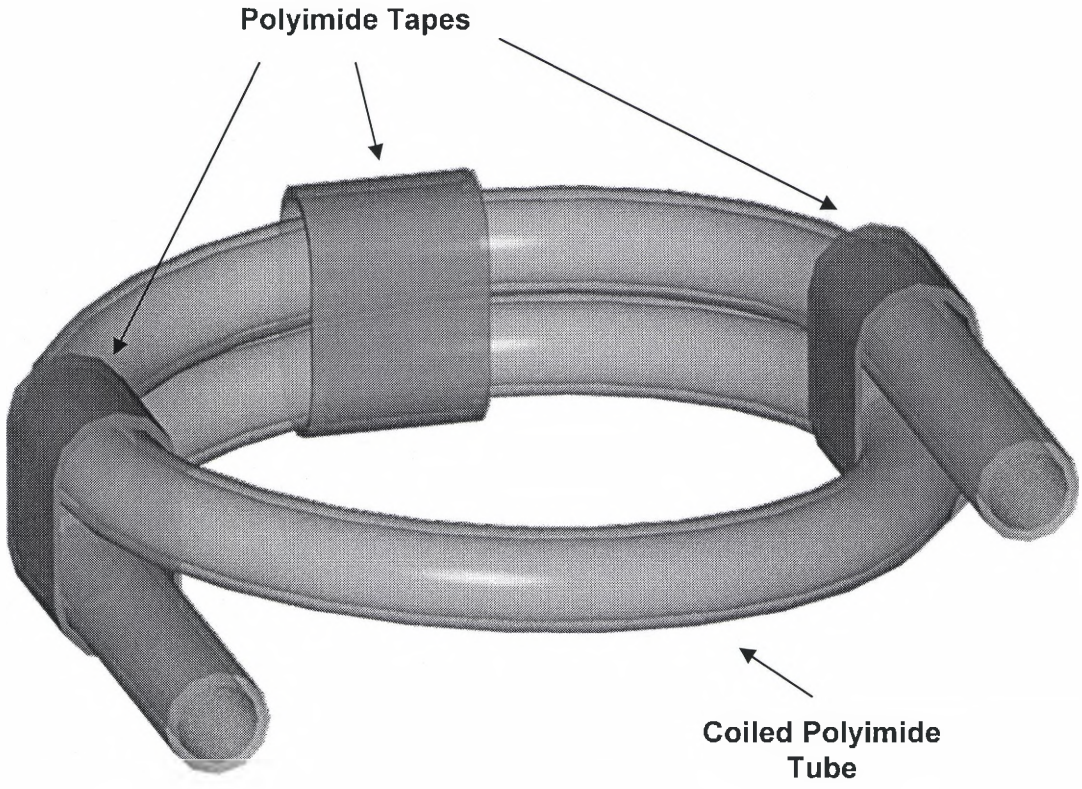

Figure 29. Polyimide tape position that keeps the polyimide tube from buckling.

Solenoid Valves Control

The solenoid valves were controlled with a custom-made controller that contained a Basic Stamp, a microcontroller (develop by Parallax Inc.) that is easily programmed using a form of the BASIC programming language. The PBASIC (Parallax BASIC) is the language used to program the BASIC Stamp, which is a hybrid form of the BASIC programming language.

A BASIC Stamp Windows Editor downloadable from the Internet[78] is used to write the PBASIC program. The editor consists of one main window that can be used to view and modify the source code files (see Figure 30).

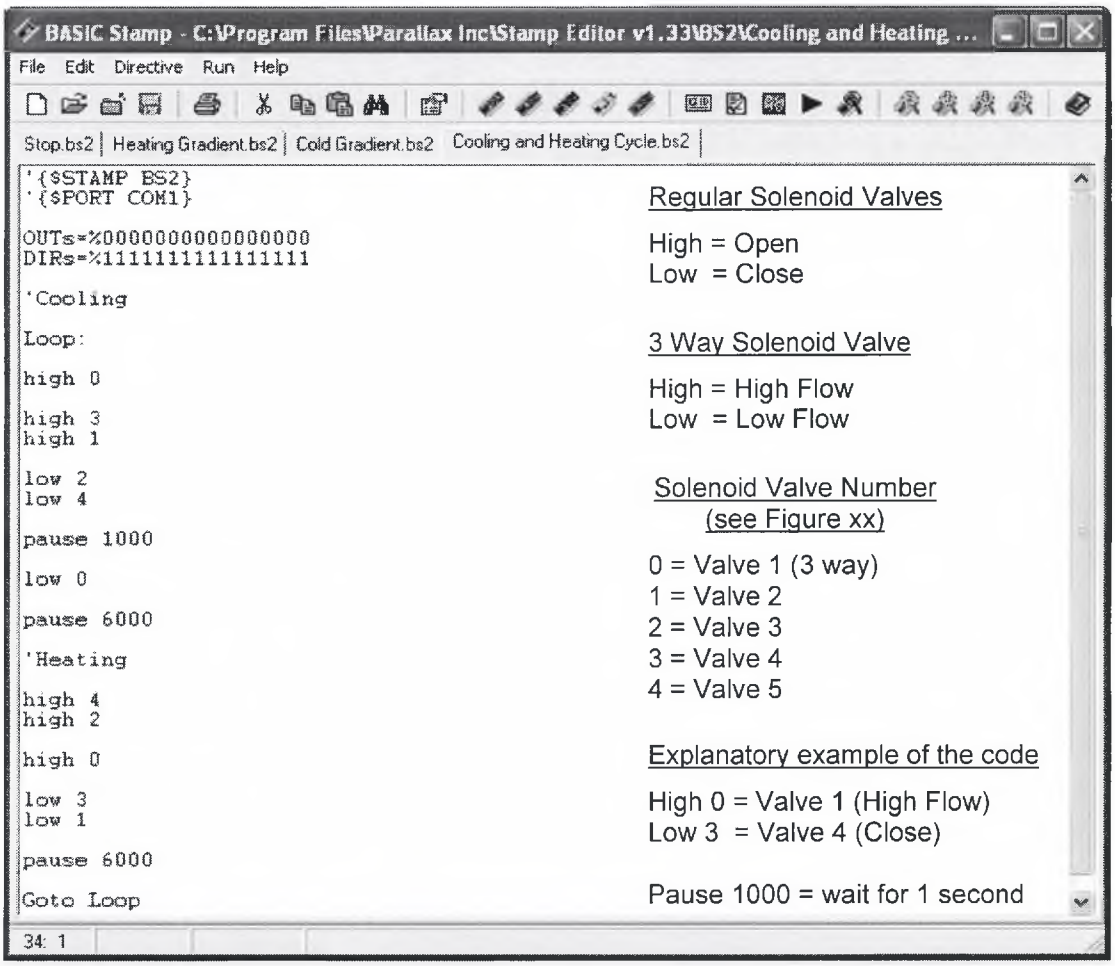

Figure 30. BASIC Stamp Windows Editor, showing a Heating and Cooling Cycle code.

After opening a new source file and entering the desired code in the editor window, the program is downloaded by connecting the computer to the Stamp through the computer's serial port. Selecting RUN (or pressing Ctrl-R) will download the code to the BASIC Stamp. As soon as the program is successfully downloaded, it begins executing the new program from the first line of code. The BASIC Stamp must be powered in order to receive the new program.

To make the program continue endlessly, a label (loop:) at the start of the code and a GOTO statement at the end of the code directing logical execution back to the label need to be added (see Figure 30). Without this, the BASIC Stamp will run the program only once and then will remain unresponsive until the power is cycled or a reset condition is created.

Thermocouples Data Acquisition

The temperature readings were gathered with a data acquisition system, a LabJack U12 (see Figure 31). This system provides an easy to use interface between computers and the physical world. It is a USB based measurement and automation device that provides analog and digital inputs and outputs.

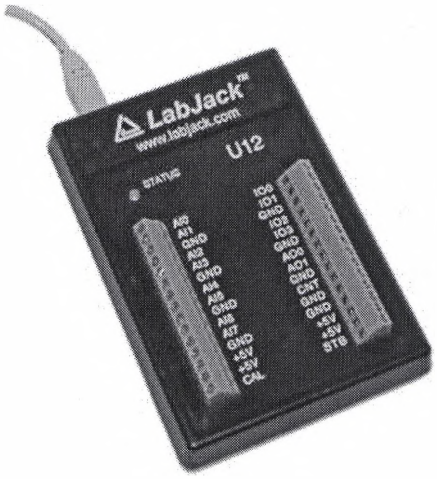

Figure 31. The LabJack U12 the temperature data acquisition system.

The data is stored in a personal computer using software that comes with the LabJack. The LJstream is a sample application of the DAQLab software (AzeoTech Inc.)

that allows acquiring data continuously and graphing four analog input channels at a rate of 300 Hz. This application program has a single screen shown in Figure 32.

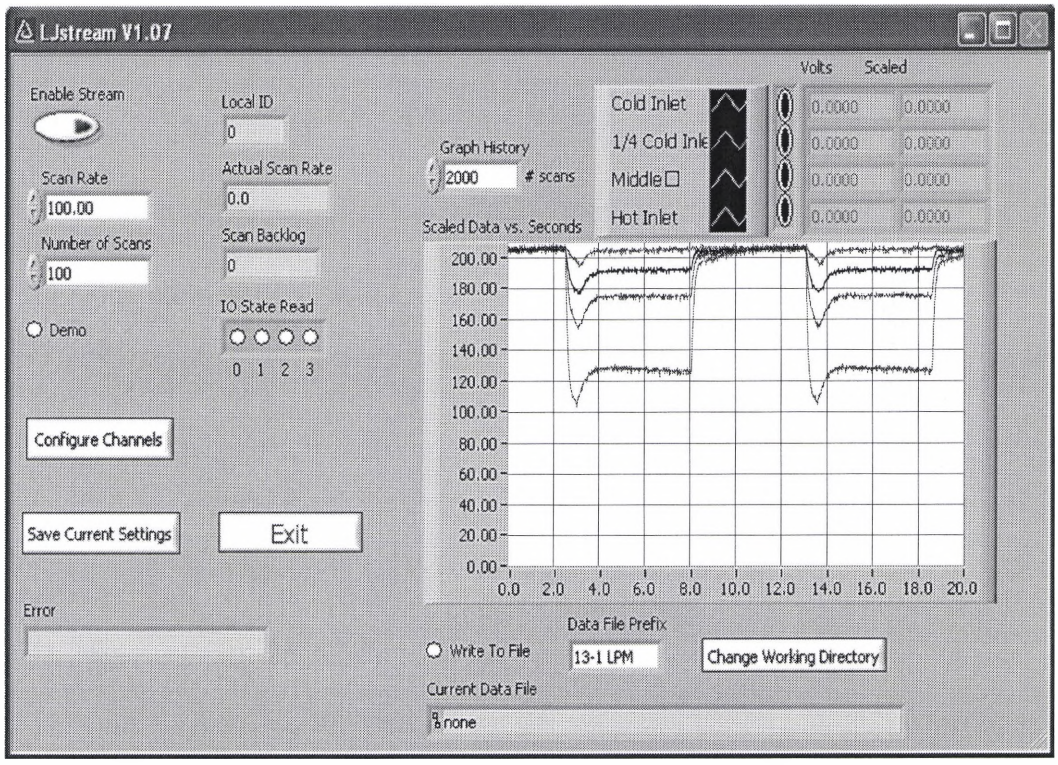

Figure 32. Windows of the LJstream showing a graphic of a heating and cooling cycle of the CSA.

At the top left of the window is the on/off button (ENABLE STREAM) to start or stop the acquisition. The data can be stored at anytime during the acquisition. The file name and store path is set at the lower right of the window and the store operation starts and ends by selecting the WRITE TO FILE option.

Along the top right of the window is displayed the color coding for the four channels, along with the average voltage and scale for the last second's data. One can set the scale for either channel by entering a scaling equation in the Channel Configuration Windows (see Figure 33). The "v" is the measured voltage and the "y" is the output of the scaling equations.

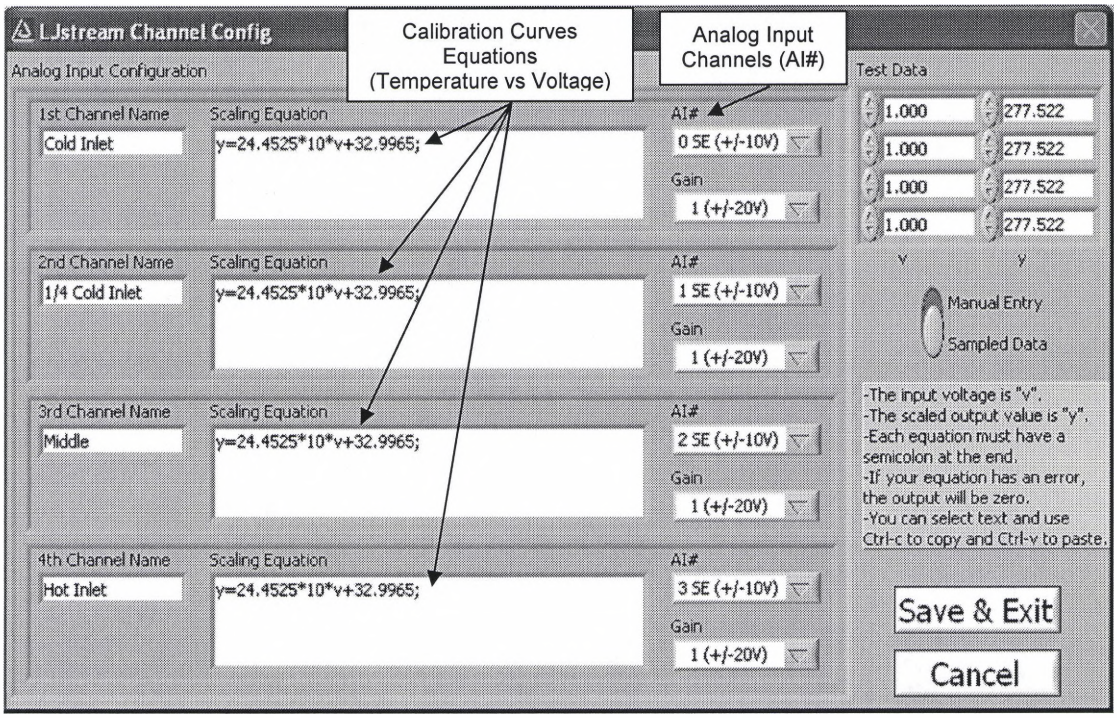

Figure 33. LJstream Channel Configuration Window.

The graph shown at the main window of the LJstream program shows the incoming data at the scale chosen versus time. The data could be monitored at a rate up to 300 Hz by changing the SCAN RATE at the main LJstream window. A rate of a 100 scans/second was used in the experiments, because it was enough to precisely follow the temperature variations in the CSA.

This fast data acquisition system permitted obtaining an accurate profile of the temperature changes within the CSA device. The data was further processed with Microsoft Excel and MATLAB software for 2D and 3D plotting of the thermal fields.

CHAPTER IV

RESULTS AND DISCUSION

Design of the Column Sheath Assembly (CSA)

The challenge in applying the TGPGC technology in the second-dimension of the MDGC-MS system was the development of a CSA. This CSA needed to be capable of creating an axial temperature gradient in the column, have a fast heating and cooling cycle, while keeping radial temperature uniform within the column.

Of the various qualities that the CSA must have, the fast heating and cooling characteristic is most challenging. Many approaches have been used for achieving fast column heating and cooling instruments. None of the systems have reached cooling and heating cycles of the order of 4-45 seconds[5, 10, 25, 45], which is the analysis time of the second dimension separation in most MDGC systems. The minimum analysis times reported (including cooling) were between 1 and 3.5 min[53].

Heating is usually not a problem using the new low thermal mass resistive heating systems (EZ Flash and Flash GC), which have reached heating rates of 20 °C/s, though rapid cooling is not easily achievable[63]. Conventional GC ovens have cooling-down times of approximately 5-7 min, from 300 to 30 °C (0.6 °C/s)[51, 53, 56, 72]; and even with the low thermal mass resistive heating systems[51, 53, 56, 59, 60, 69] and the recently introduced microwave oven, the minimum cooling times are about 1 min (5 °C/s)[71].

Among the column heating methods, the resistive heating approach is currently being use to achieve fast heating rates. However, this method is technically more difficult to accomplish and still requires the use of forced convection methods to achieve fast cooling rates and uniform column temperatures[60, 73]. It is for these reasons that forced convection was the technique chosen for the heating and cooling of the CSA.

A heat exchanger design was used for the CSA system, where the fused silica capillary column runs coaxially inside of the CSA, and not outside the heating and cooling sheath as in previous designs (see Figure 14), thus achieving radial temperature uniformity in the column. The CSA consisted of coiled tube placed inside of an air-bath GC oven, which provided a constant temperature on the external side of the CSA. We are assuming that any amount of energy removed by the CSA will not affect the oven temperature since the energy would be replaced by the controlled electrical heaters of the GC oven. Furthermore, the oven itself can act as a thermal reservoir to keep temperature constant. Nitrogen gas was used as the heat exchanger fluid inside the CSA (see Figure 15).

The temperature gradient along the column axis was generated when cold nitrogen gas was increasingly heated as it flowed through the CSA. Heating of the temperature gradient to oven temperature was achieved when preheated (oven temperature) nitrogen gas flowed through the CSA. To maintain a constant negative gradient through the CSA during the cooling and heating process, the cooling and heating inlets were placed in separate entrances of the CSA. Figure 15 shows the arrangement used to achieve the heating and cooling of the CSA.

Different experiments using various tubes and materials were performed to decide on the construction, tube diameter, and tube length of the CSA design.

Length of the CSA

The application of the TGPGC mode was performed in the last part of the second dimension column to take advantage of its separation improvements and to avoid any further isothermal broadening effect. While previous work used lengths of 4m for moderate polarity columns (RTX-200), 2.3m was chosen for using more polar Carbowax OTC columns. Since an isothermal pre-separation of the mixture was desired, prior to TGPGC, one meter of the Carbowax would be inside the CSA and 1 meter at the isothermal oven temperature for polarity separation with 0.3 meters of transfer line in the MS.

Diameter of the CSA

To determine which diameter to use for the CSA design, experiments using PTFE tubes of 1/8", 1/4" and 3/8" OD (COLE-PARMER A-06407-42, -44 and A-06605-04) were performed, where the temperature gradient measured along the tubes was for a constant mass flow rate. The measurements were performed after 20-s of cooling from oven temperature using thermocouples of 0.01" sheath diameter (Omega KMQss-010(U)-12). The instrumentation used for this experiment is depicted in Figure 15, and the conditions of the experiment are given in the Table 2. PTFE tubes were used since it was one of the material options for the construction of the CSA that was available in different diameters.

In Figure 34, the temperature gradient of the 1/8" and 1/4" outer diameter (OD) PTFE tubing are similar, however the conditions of each experiment are quite different. Table 2 shows that the inlet pressure of the 1/8" OD CSA needed to be 10 times higher

than the one required in the ¼" PTFE CSA to achieve similar mass flow rates. This implies that the use of 1/8" OD tubing will require the need for a more robust CSA, which translates to either stronger materials or the use of thick wall tubing to support the high pressures. The use of tubing with higher thermal mass to support the high pressures will negatively influence the heating and cooling rates of the system.

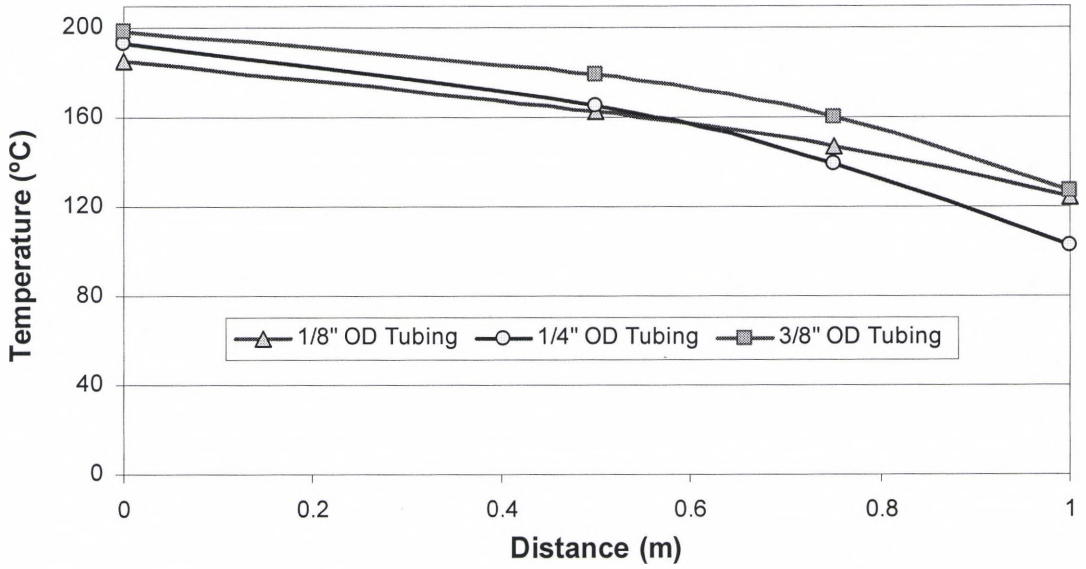

Figure 34. Temperature profiles of three different tubing diameters at a similar mass flow rate.

Table 2. Experimental conditions of the different diameter PTFE tubes.

	OD Tube	1/8"	1/4"	3/8"
	Wall thickness (mm)	0.8	1.2	1
Rotameter	P (psig)	50.5	5.4	3.6
Rotameter	T (°C)	24	24	24
Rotameter	Level (LPM)	13	25	25
	Actual Volume Rate at STC (LPM)	27.7	29.6	28.2
	Mass Flow (g/s)	0.535	0.570	0.545
	Reynolds Number	8,870	4,740	3,000
	ΔT (°C)	75	98	72
	Oven Temperature °C	200	200	200

On the other hand, the 3/8" OD PTFE CSA showed that due to the increase in heat transfer area, residence time and thermal mass due to the larger fitting

connections, the temperature gradient profile was higher than the one obtained for the 1/8" and 1/4" OD tubing. This implies that to generate a temperature gradient profile similar to that gradient generated with the 1/8" or 1/4" diameter tube will require an increase of the mass flow rate. The disadvantage that the 3/8" tubing is the bulky connections as compared to smaller diameter tubes. The ¼" tubing was determined to be a good compromise between 3/8" and 1/8" tubing.

The temperature profiles shown in Figure 35 were created by varying the nitrogen mass flow rate through the 1/4" OD CSA. With higher nitrogen mass flows, lower temperatures can be achieved, cooling down the CSA. Thus temperature profiles become lower when the mass flow rate increases. Higher mass flow implies the need for higher inlet pressure, and an operating pressure range between 1.5 and 17 psig, which was easily obtained.

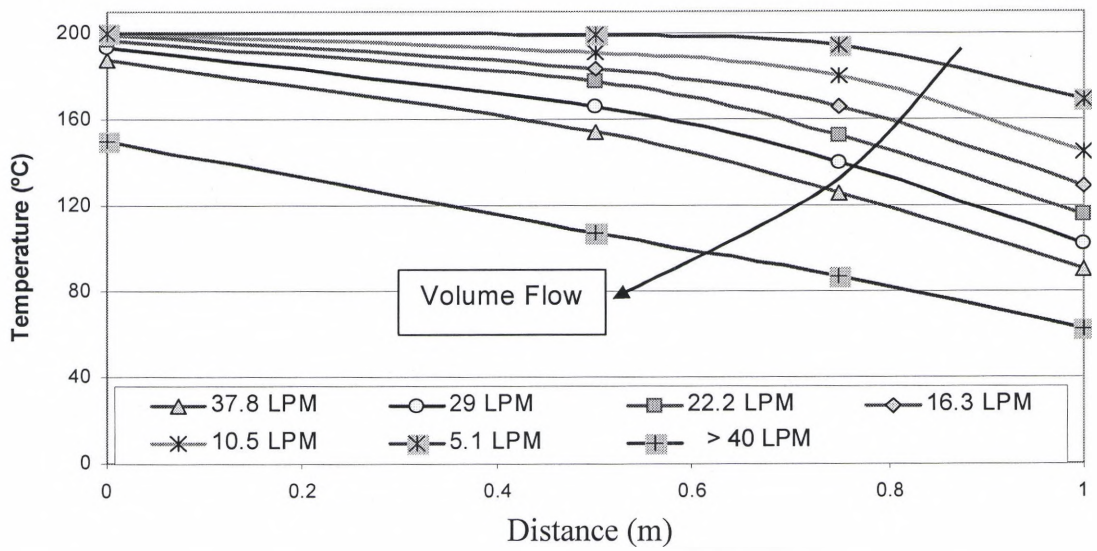

Figure 35. Temperature gradient profiles of the PTFE tube ¼" OD at different volume flow rates of N_2 at 25 °C. The LPM units are at standard conditions (21.1°C and 1 atm).

The 1/4" diameter tubing was determined to be the best option for the CSA design due to its low operational pressure and wide range of temperature gradients that can be achieved. The low operational pressures of the 1/4" OD tube, implies that tubes

with thinner walls (lower thermal mass) can be used for the construction of the CSA, so that fast heating and cooling rates can be achieved.

Selection of the material for the construction of the CSA

The CSA needed to be constructed with a low thermal mass, such that small changes in thermal energy would result in major temperature variations. And at the same time it needed to be structurally strong to support wide and rapid changes in temperature and pressure.

Metal was not considered as a possible material, since even thin walled tubes will have more thermal mass than polymeric materials. Among polymers, PTFE , Polyimide, and PEEK, are promising materials for the construction of the CSA, due to their high thermal properties and mechanical stability, and their capability to be extruded into tubes with extremely thin walls. Table 3 lists the physical and thermal properties of these polymeric materials, as well as copper to serve as a metal reference[79-81].

Table 3. Thermal and physical properties of the polymer materials and copper.

	Units	PTFE	Polyimide	PEEK	Copper
Specific Gravity	g/cc	2.2	1.42	1.32	8.9
Temperature Working Range	°C	-260 to 260	-270 to 400	-260 to 260	-198 to 540
Melting Point	°C	335	not applicable	343	1083
Thermal Conductivity	W/m/K	0.25	0.33	0.17	394
Specific Heat @ 25 °C	Cal/g/°C	0.23	0.24	0.76	0.092
Maximum Continuous Operating Temperature	°C	260	288	250	540
Heat Deflection Temperature 0.45 MPa (66 psi) 1.8 MPA (264 psi)	°C	 122 55	 - 238	 - 140	not applicable
Tensile Strength 23 °C 200 °C	MPa	 21 4	 92 41	 91 10	221

To achieve a low thermal mass CSA, a tube with a very thin wall was required. However, the wall thickness of a tube is a function of its operational pressure and its material tensile strength. This implied that the material that should be used must exhibit a high tensile strength even at high temperatures, qualities that only the polyimide polymer offered, as can be seen in Table 3. PTFE and PEEK lack rigidity when the temperature is relatively high. Polyimide is one of the highest performing engineering plastics currently available. It will not melt, so it does not soften at high temperatures keeping its rigidity, and it can operate continuously from cryogenic temperatures to 288 °C, with occasional excursions to 400 °C[80]. The ability of polyimide to maintain its excellent physical and mechanical properties over a wide temperature range makes it the best material option for the construction of the CSA.

However, polyimide is difficult to manufacture because of its high working temperatures, no thin wall polyimide tubing is commercially available in the sizes required. Therefore, polyimide tubing needed to be hand-made. Polyimide Tape was used for the construction of the tubing; the tape consisted of Kapton® polyimide film and silicon adhesive. The construction of the polyimide tube was essentially performed by wrapping polyimide tape on a ¼" OD stainless steel tube. The spiraled tube was set with the adhesive and strengthened with polyimide resin. A polyimide tube of ¼" ID and 5 mils wall thickness was then obtained by removing the stainless steel tube; the construction is further explained in the experimental section.

In wrapping and constructing the polyimide tube, the arrangement where the polyimide tape layers were placed right next to each other was the strongest, according to experiments performed at 250 °C and 30psig. Regardless of the superior strength and resistance of polyimide, the mechanical strength of the tubing was now restricted to that of the adhesive and the polyimide resin. Further experiments were then required to test

the structural and thermal stability of the hand-made polyimide tube at high pressures and temperatures.

The results of the experiments showed that the hand-made polyimide tube supported up to 30 psig at 260 °C. At higher temperatures the silicon adhesive decomposed and caused the seam of the tubing to fail, buckling or bursting the tube.

The maximum temperature of the hand-made polyimide tube imposed some restriction on the analysis of complex mixtures, since complex mixtures usually require a temperature of 300 °C to completely analyze the sample. The sacrifice of the maximum temperature was necessary to apply the TGPGC method in the MDGC-MS.

Transient Temperature and Heating and Cooling Rates

First, we needed to demonstrate the efficiency of the new polyimide CSA in obtaining fast temperature changes, and to show how the thermal mass of the CSA plays a roll in the heating and cooling rates. Experiments with 3 different tube materials were performed: PTFE , Polyimide, and copper. A cooling and heating cycle was performed with each CSA material at an oven temperature of 200 °C. Figure 36 shows the temperature gradient profiles that were obtained for each ¼" OD CSA material. Table 4 shows the conditions at which each experiment was performed.

As was expected, the temperature profile for the copper tubing shows higher temperatures I the cooling cycle, due to the high thermal mass of the tube. While for the PTFE and the polyimide tubing, the temperature profiles reached lower temperatures than that reached by the copper tube. Also the temperature rapidly increased to oven temperature, due to the lower thermal mass of the polyimide and PTFE CSA compared to the copper CSA.

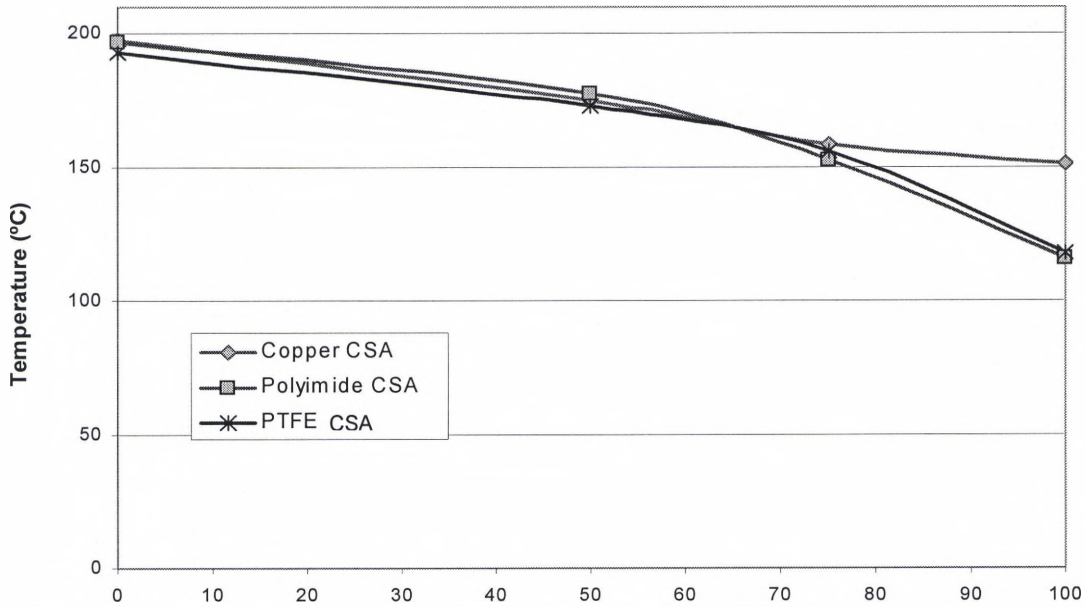

Figure 36. Temperature profile obtained in different CSA materials of ¼" OD at a constant mass flow rate.

Figure 37 and Figure 38 show the transient temperature cooling and heating of the different materials, where we can appreciate that even though PTFE and the Polyimide have similar temperature gradients, the PTFE has a lower cooling and heating rate than the Polyimide CSA. This was expected since the hand-made polyimide tubing has thinner walls and lower thermal mass compared to the PTFE CSA.

Table 4. Experimental conditions of the heating and cooling test for the different CSA materials.

		Copper	PTFE	Polyimide
	OD Tube	**1/4"**	**1/4"**	**1/4"**
	Wall Tubing Thickness (mm)	0.8	1.2	0.1
Rotameter	P (psig)	2.8	3.1	2.6
Rotameter	T (°C)	24	24	24
Rotameter	Level (LPM)	20.5	20	20
	Volume Rate (LPM) STC	22.63	22.26	21.95
	Mass Flow (g/s)	0.4377	0.43	0.424
	Reynolds Number	3,620	3,560	2,345

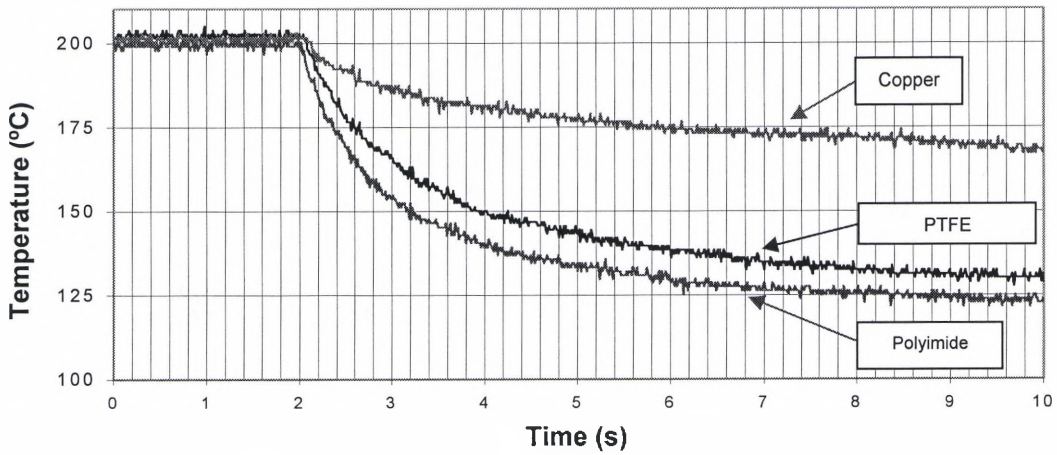

Figure 37. Formation of the temperature gradient (Cooling cycle) in the CSA.

In this plot only the temperature of the cold flow inlet for each CSA is shown. Thermocouple diameter is of 0.01"

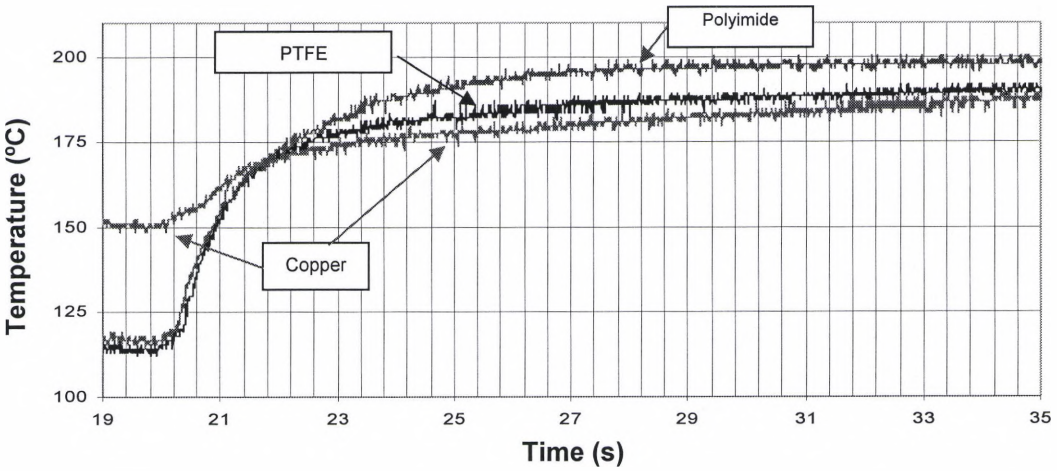

Figure 38. Heating the CSA to oven temperature (heating cycle) in the CSA.

In this plot only the temperature of the cold flow inlet for each CSA is shown. Thermocouple diameter is of 0.01"

The heating rates obtained in the experiment are shown in Table 5, and it is clear that the Polyimide CSA can heat and cool more efficiently than the other CSA materials. We obtained a cooling rate of 9.5 °C/s, which is faster than the 5 °C/s obtained with the current column heating technology[60, 73]. However, the heating rate of 8.4 °C/s achieved with the polyimide tube is still not as fast as the heating rates obtained with the resistive heating devices (20 °C/s) described earlier.

Table 5. Heating and cooling rate for the different materials of CSA.

Rates measured as the slope from the beginning of the temperature cycle to the end.

					Rate °C/s	
	T1 (°C)	T2 (°C)	t1 (s)	t2 (s)	Cooling	Heating
Polyimide	200	124	2	10	9.5	
	116	200	19.4	29.4		8.4
PTFE	200	132	2	10	8.5	
	116	190	19.4	29.4		7.4
Copper	200	169	2	10	3.9	
	150	183	19.4	29.4		3.3

Further improvements needed to be made in order to reach higher heating and cooling rates. One of the improvements was the replacement of a ¼" OD metal tee at the cooling inlet with a hand-made ¼" polyimide tee. The previous metal tee that was used contributed a high thermal mass. As a result, part of the cooling time of the CSA was consumed in cooling the metal tee, and the same was true during the heating stage, where part of the time required to heat the CSA was consumed in heating this tee. The system with the new hand-made polyimide tee is shown in Figure 21. The polyimide tee was made using the same procedure as the hand-made polyimide tube using polyimide resin.

The expected improvement in reducing the thermal mass of the tee connection at the beginning of the CSA was observed in the heating and cooling rates obtained (Figure 39). Using the 0.01" thermocouple diameter used in the previous experiments, heating and cooling rates of 25 and 66 °C/s, respectively, were obtained with the new low thermal mass polyimide tee design. Cooling rates are much higher than resistive heating devices, and heating rates are slightly higher as well.

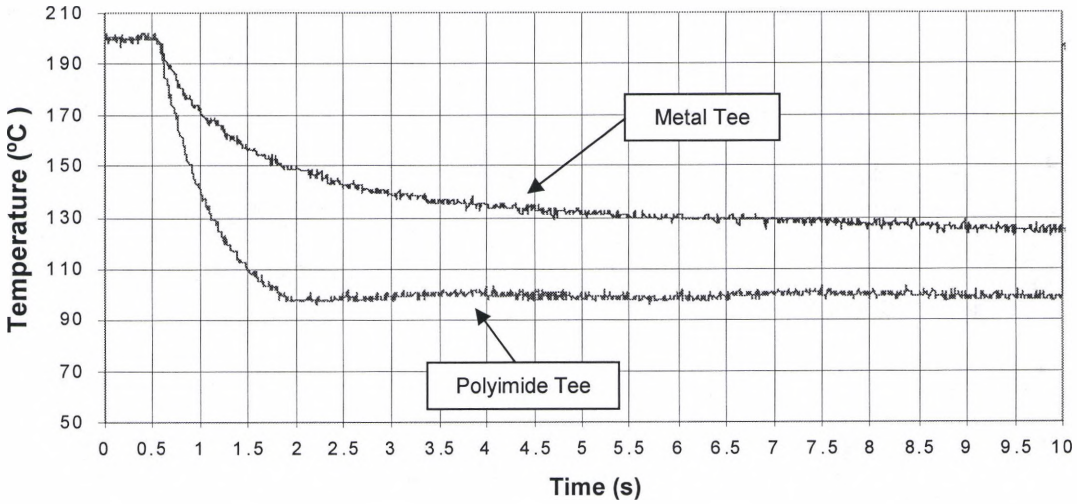

Figure 39. Transient temperature comparison between the metal and polyimide tee connection.

Rates measured from 0.5s to 2s for the polyimide tee and from 0.5s to 10s for the metal tee.

Thermocouple size reduction to track gradients

Another improvement was the use of smaller thermocouples to track the fast thermal changes occurring inside the CSA. Figure 40 shows the difference in measuring the temperature of a cooling and a heating cycle using different thermocouple diameters. The smaller diameter thermocouples have a faster response, thus they can follow the temperature change in the CSA more accurately.

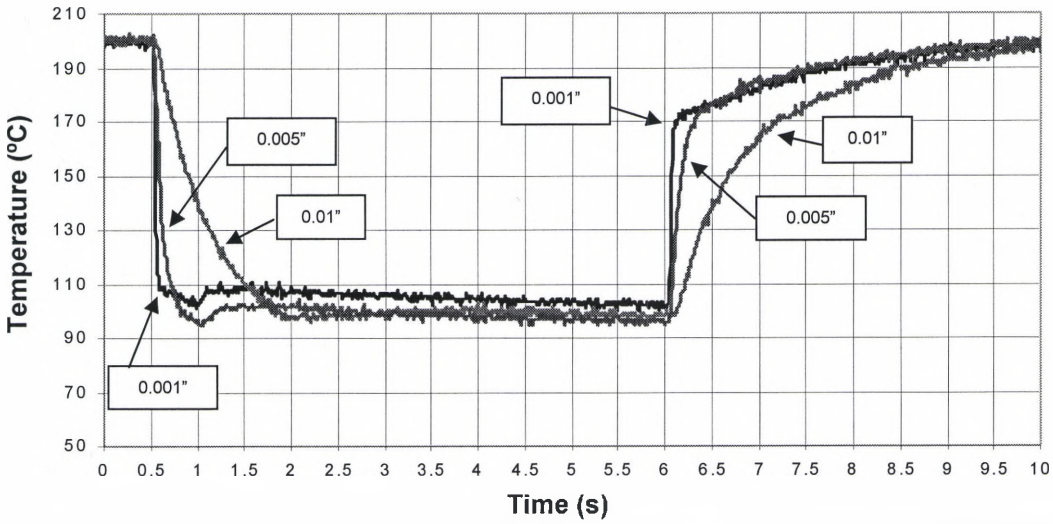

Figure 40. Temperature measured using different thermocouple diameters in the heating and cooling cycle of the polyimide CSA.

Rates determined from 0.5s to 1s for the cooling cycle and from 6s to 10s for the heating cycle.

Using the data obtained with the smaller diameter thermocouples, we can obtain a more accurate heating and cooling rate. Table 6 shows the new heating and cooling rates obtained.

Table 6. Heating and cooling rates obtained with the new polyimide tee and the new thermocouples.

Thermocouple Diamter					Rate °C/s	
	T1 (°C)	T2 (°C)	t1 (s)	t2 (s)	Cooling	Heating
0.01"	200	100	0.5	2	66.7	
	100	200	6	10		25.0
0.005" & 0.001"	200	100	0.5	1	200.0	
	100	200	6	9		33.3

The heating and cooling rates achieved were of 33.3 and 200 °C/s for each case, rates that were definitely higher than any other heating column device, and fast enough to apply the TGPGC method in the second dimension of the MDGC-MS system. The high heating and cooling rates were achieved by exposing the CSA to high flow rate of nitrogen gas (higher than 40 LPM STP). The high cooling rate of 200 °C/s obtained shows how efficient the CSA is on changing its temperature, due to its low thermal

mass. This means that heating rates of the same order of magnitude as the cooling rate can be achieved. The difference between the heating and cooling rates observed was due to the temperature of the heating and cooling fluid. The cooling fluid was nitrogen at 25 ºC, which provides a big driving force being able to cool down from 200 to 100 ºC very quickly. On the other hand the heating fluid was at 200 ºC or oven temperature, making possible high heating rates of 240 ºC/s up to 160 ºC as it is observed in Figure 41. However, once the gradient temperature is closer to the heating fluid temperature and the temperature difference is smaller, the heating driving force is reduced, thus the heating rate starts to decrease, in this case after 160 ºC (see Figure 41). To obtain high heating rate one needs to heat the heating fluid higher than the oven temperature (e.g. 50 ºC), so the heating driving force will be high enough to keep a high heat rate up to oven temperature, avoiding the zone where the heating rate starts to decrease.

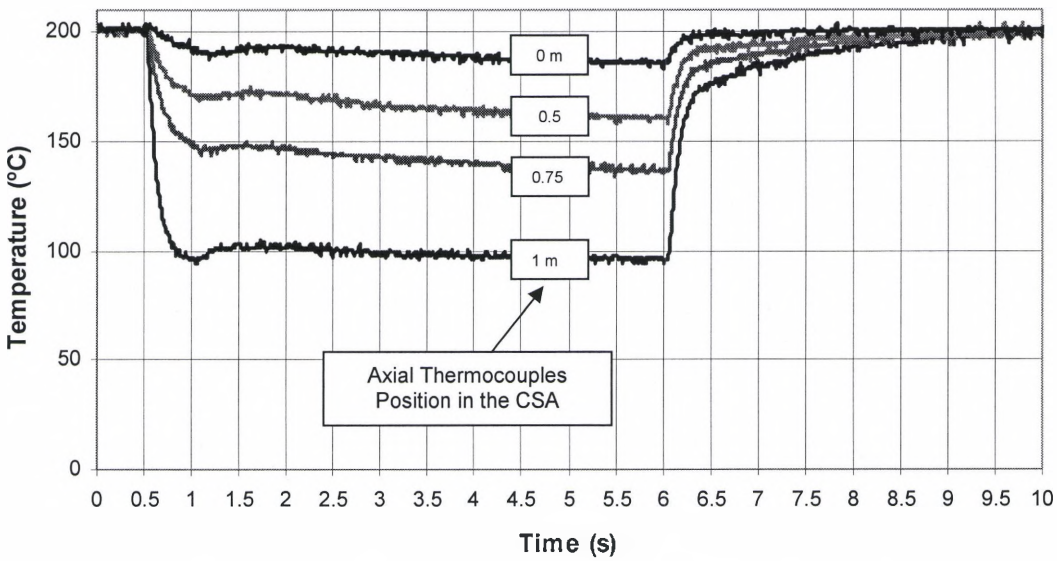

Figure 41. Cooling and heating cycle of the CSA design.

The thermocouple diameter chosen for the experiments was the 0.005", since it was easier to handle than the 0.001" diameter and had a response time that was good enough to monitor the temperature changes inside the CSA, as can be seen in Figure 40. An example of a heating and cooling cycle obtained with the polyimide CSA design

used for the tuning of the CSA in the MDGC-MS system is shown in Figure 41 and its temperature gradient is shown in Figure 42.

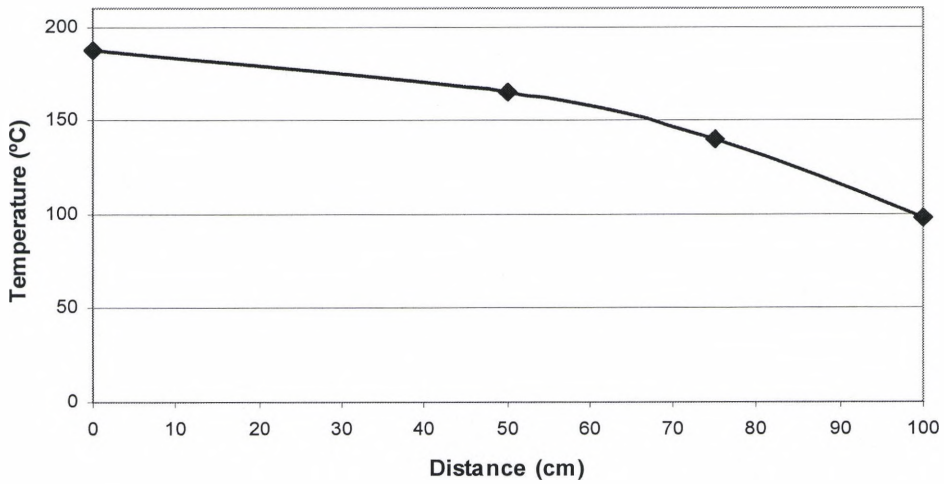

Figure 42. Temperature gradient of the ¼" Polyimide CSA design.

To generate the square response plot of the heating and cooling of the temperature gradient (TG), initially high flow of nitrogen gas at room temperature was used to quickly form the TG desired. Then, the high flow of nitrogen was reduce to a flow that would maintain the desired TG constant. Heating the TG was achieved by using high flow of nitrogen gas preheated at oven temperature. The operational conditions of the heating and cooling cycle are shown in Table 7.

Table 7. Operating conditions of the CSA for the heating and cooling cycle.

		Constant Temperature	Cooling & Heating
	ID Tube	**1/4"**	**1/4"**
Rotameter	P (psig)	7.5	23
	T (°C)	24	24
	Level (LPM)	21	-
	Volume Rate (LPM) STC	26.11	-
	Mass Flow (g/s)	0.505	-
	Reynolds Number	4,180	Turbulent

Thermal field mapping and determination of best gradient

Taking advantage of the data obtained in Figure 41 and by using MATLAB, the thermal field of the heating part of Figure 41 was plotted. The temperature surface obtained when slower heating rates are used is shown in Figure 43 and 44.

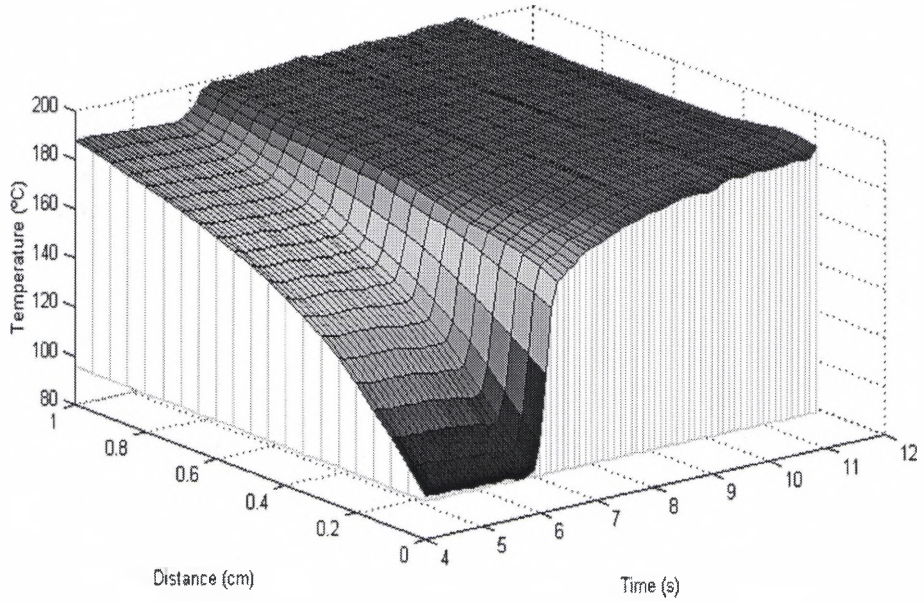

Figure 43. Temperature surface for a heating rate of 33 °C/min.

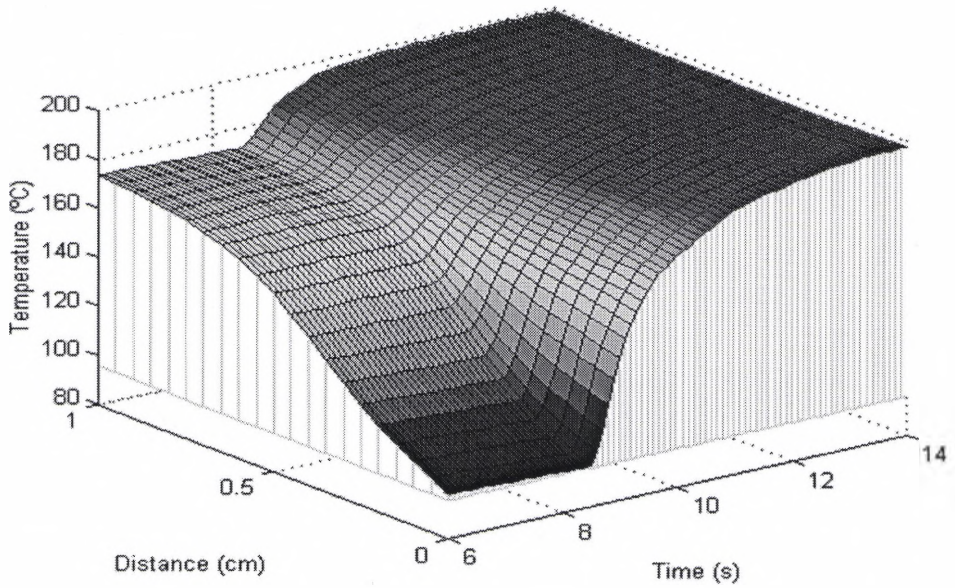

Figure 44. Temperature surface for a heating rate of 20 °C/min.

Further experiments where performed to establish the flexibility in producing different temperature gradient profiles. The temperature gradient profiles shown in Figure 45 correspond to the ¼" polyimide CSA with the polyimide tee. Steeper temperature gradients were achieved compared to Figure 35, where the connection was a metal tee. The polyimide tee allows colder fluid to reach the inlet of the CSA creating the steeper gradients.

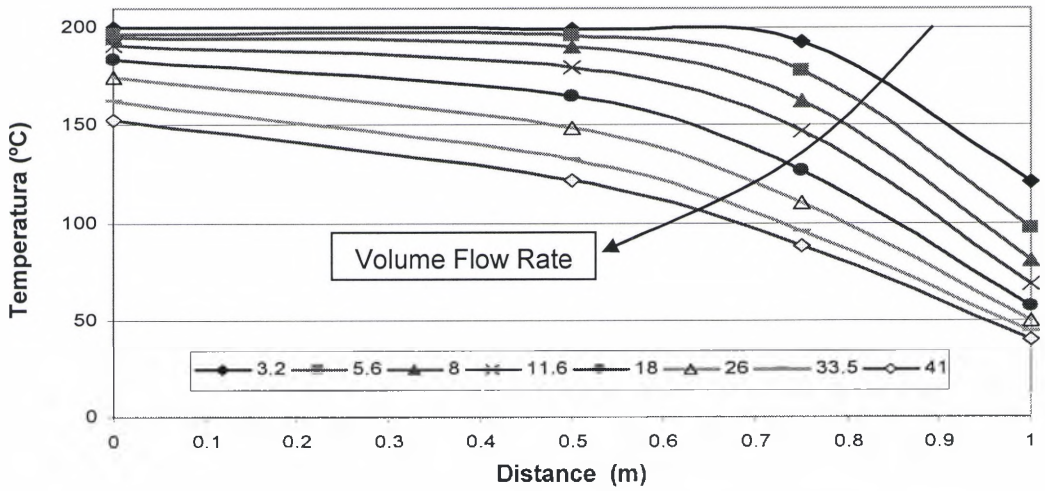

The LPM units are at standard conditions (21.1°C and 1 atm)

Figure 45. Temperature gradient profiles of the ¼" OD polyimide tube at different volume flow rates of N_2 at 25 °C.

Tuning of the TGPGC Mode in the Second Dimension Column

The thermal gradient programmed gas chromatography method is performed by the application of adjustable three-dimensional thermal fields as shown in Figure 43 and 44. The thermal fields are formed by generating in the axial direction of a chromatographic column a negative temperature gradient that can be modified through time (Figure 43).

An advantage that the TGPGC method has, compared to the ITGC and PTGC methods, is that the thermal field can be modified during the chromatographic analysis. This feature is very important in achieving complex separations, since there are regions in the entire GC analysis where one wants a significant negative temperature gradient and others where only gradual negative gradients are preferred.

The flexibility of the thermal field implies that the TGPGC method has more operational variables available for the separation process than the ITGC and PTGC methods. The main operational variables that are encountered in the TGPGC method are:

a) The negative gradient shape or profile

b) The gradient temperature difference (inlet-outlet)

c) The heating rate of the column within the gradient

d) The initial heating time of the gradient

The large number of operational variables that the TGPGC mode offers[3, 66] makes the technique more powerful for the separation of a wide variety of samples, though it also makes it more difficult to apply. Table 8 shows a comparison of the main operational variables encountered in the different thermal application modes for performing chromatographic analysis.

Table 8. Operational variables encountered in different chromatographic separation modes.

ITGC	PTGC	TGPGC
Carrier gas flow rate (velocity)	Carrier gas flow rate (velocity)	Carrier gas flow rate (velocity)
Oven temperature	—	Temperature gradient shape or profile
—	—	Temperature gradient difference
—	—	Time to initiate the heating
—	Heating rate	Heating Rate

The tuning of the TGPGC technique consisted of finding the correct values of operational variables that enhanced the separation of a heartcut in the second dimension column of the MDGC-MS system. Experiments were performed to understand their influence in the separation process, and to achieve the tuning of the TGPGC method. However, it should immediately be made clear that the study of the effect of the main variables of TGPGC in the separation process has an exploratory nature.

In these experiments only the cryogenic trap and the second-dimension column of the MDGC-MS system were used. The sample injections into the secondary column were performed with the cryogenic trap simulating a narrow collected fraction (heartcut) coming from the first column. The sample mixture used for the tuning of the CSA was based on five selected compounds that possessed similar boiling points and demonstrated different chromatographic polarities. The components chosen are shown in Table 1.

Influence of the negative gradient profile and its temperature difference $|\Delta T|$ in TGPGC

Due to the CSA design, the gradient profiles studied were restricted only to negative convex curves. The CSA was housed in a GC oven where the oven temperature was kept higher than the CSA flow inlet temperature and as a result, the gradient generated by the heating of the cold inlet flow produced convex curve profiles.

There was no independent control between the gradient temperature difference and the gradient profile since the CSA inlet flow temperature was kept constant. Increasing the cooling flow inlet rate produced higher temperature differences, as well as a less pronounced convex curve profile (see Figure 45). Therefore, the temperature gradient profile was then specified by the absolute temperature gradient ($|\Delta T|$) only. For these reasons, a study of the influence of different gradient profiles in the TGPGC separation mode could not be made. However, the influence of the temperature gradient difference in TGPGC separations was studied.

The compounds used in these experiments were n-hexadecane, 1-decyl-benzene and 1-tetradecanol, which were chosen because they characterize a nonpolar, a semi-polar and a polar compound, comprising the whole chromatographic separation range of the second column. The GC conditions used were isothermal at 200 °C, 3.5 psig head column pressure, split mode with 100 ml/min of helium carrier gas. The first chromatographic column used was a polar 4 m RTX-200, 0.1 mm ID, employed in previous MDGC-MS studies[45].

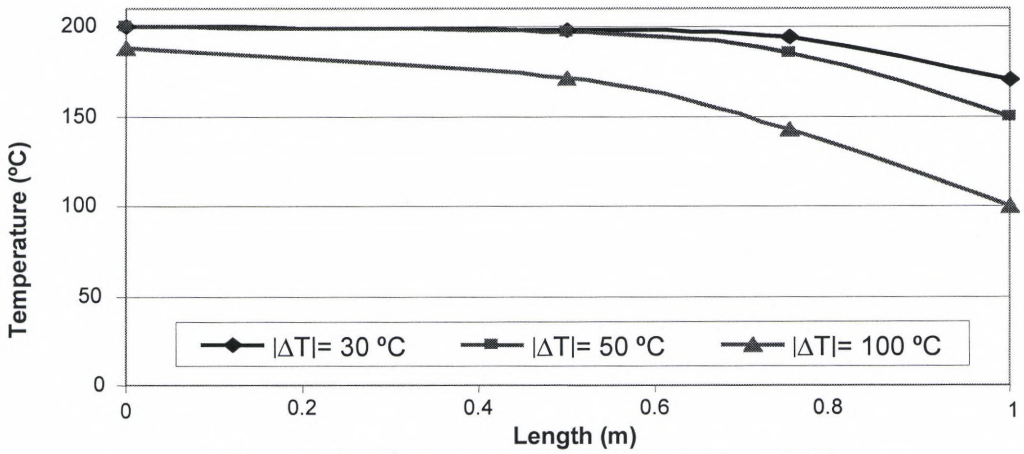

Figure 46. Gradient profiles for the different $|\Delta T|$.

The influence of the absolute temperature gradient difference ($|\Delta T|$) on the TGPGC separation process was studied by comparing an isothermal separation with

separations done using three gradient profiles with different $|\Delta T|$. The temperature profiles used in the experiments are shown in Figure 46.

The second-dimension separation in MDGC-MS is always assumed to be under isothermal conditions; therefore, an isothermal separation of the heartcut sample was performed to compare the application of the TGPGC mode with an isothermal separation. However, two situations can take place when the TGPGC separation technique is applied:

1) *Allowing the compounds to breakthrough the negative temperature gradient.*
2) *Releasing the compounds before they get through the gradient, by heating the negative gradient to the isothermal oven temperature.*

These situations were studied using the different $|\Delta T|$ profiles shown in Figure 46. The heating rate used for releasing the compounds was 33 °C/s, the fastest achievable for the CSA design. The isothermal separation chromatogram and the chromatograms obtained from the separation performed by using the TGPGC mode are shown in Figure 47. All the chromatograms in Figure 47 were plotted using the same scale, except Figure 47-D, which had a larger scale x-axis. The sample amount was equal for all the experiments performed.

The isothermal separation chromatogram of the compounds is shown in Figure 47-A where coelution is observed between the two last compounds, the 1-decyl-benzene and 1-tetradecanol, showing that the isothermal separation does not provide a complete separation of the heartcut. Figure 47-B to G shows the remarkable influence of the application of the TGPGC mode in the chromatographic separation of the compounds. To quantify the separation of the compounds and analyze the chromatograms of Figure 47, bar plots are presented in Figure 48 to 50.

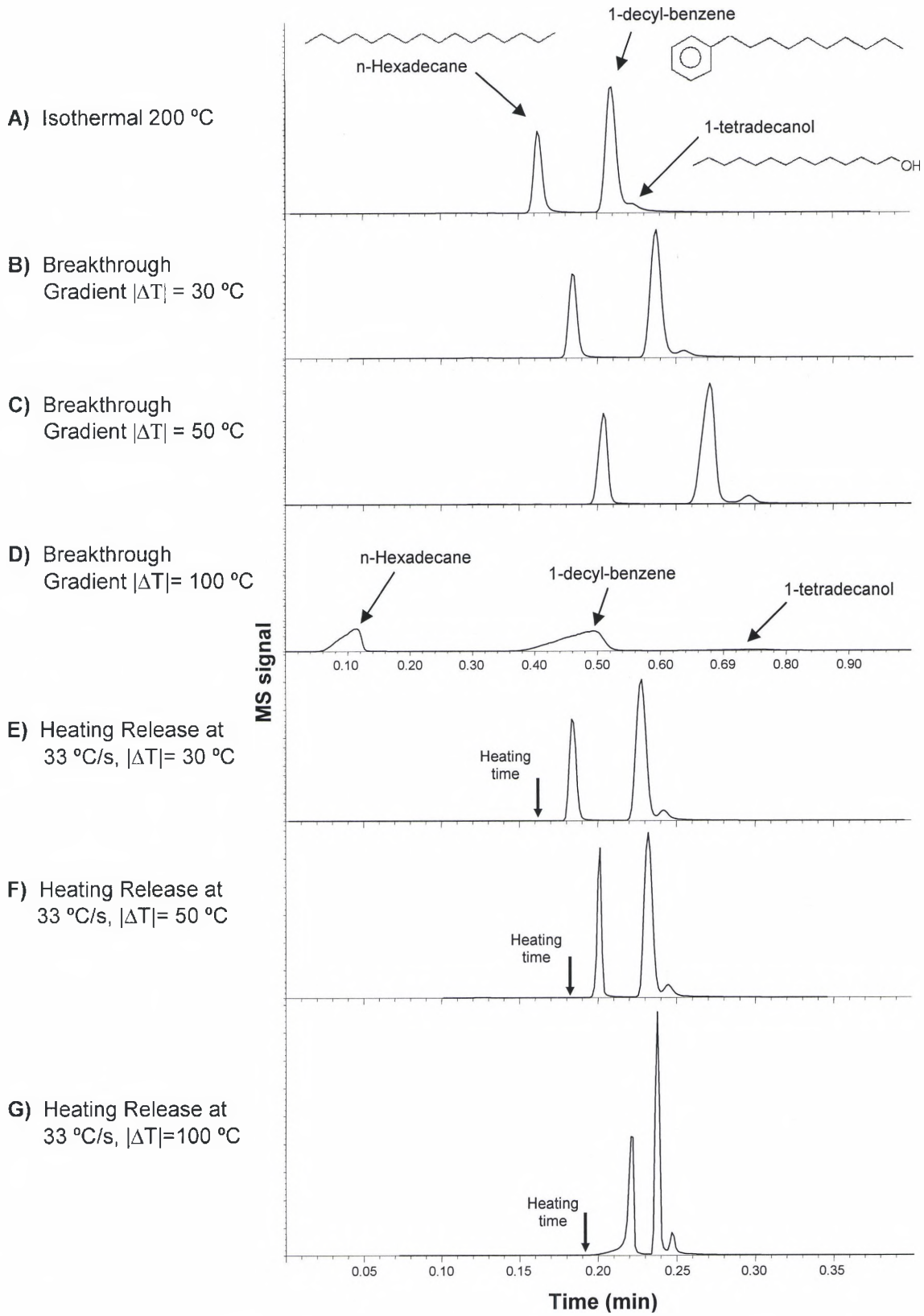

Figure 47. Isothermal, breakthrough, and fast heating release chromatograms of a heartcut mixture at different |ΔT| temperature gradients.

The peaks in the bar plots were represented by letters, A as the n-hexadecane, B as the 1-decyl-benzene and C as the 1-tetradecanol.

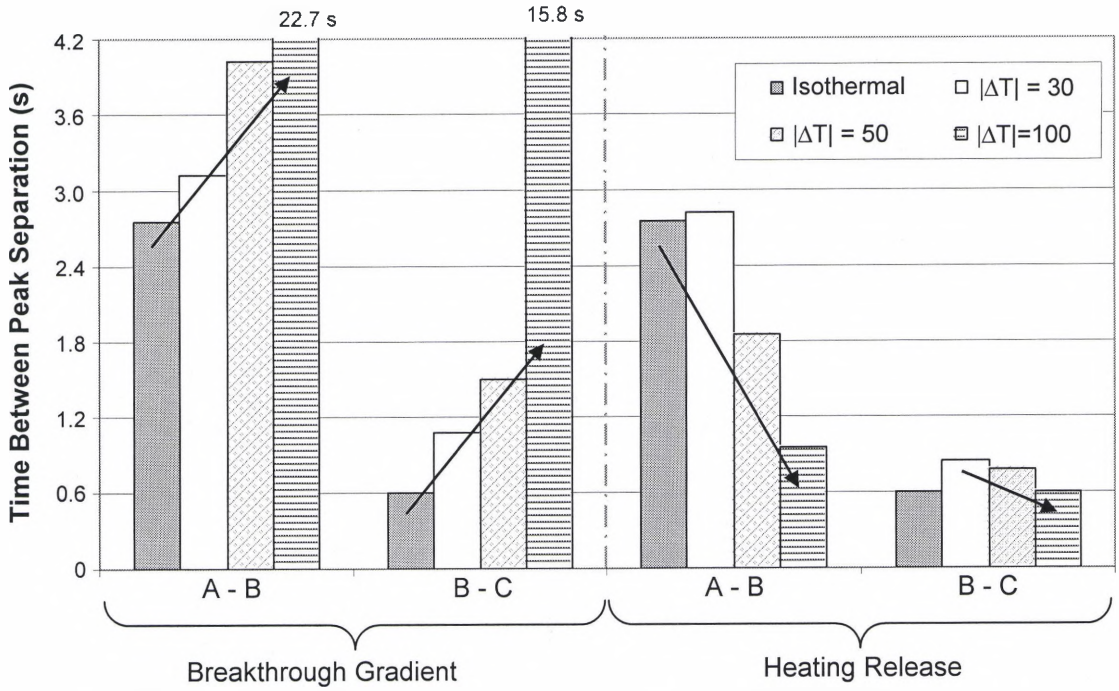

Figure 48. Peak apex separation between peaks A-B and B-C of the chromatograms of Figure 47.

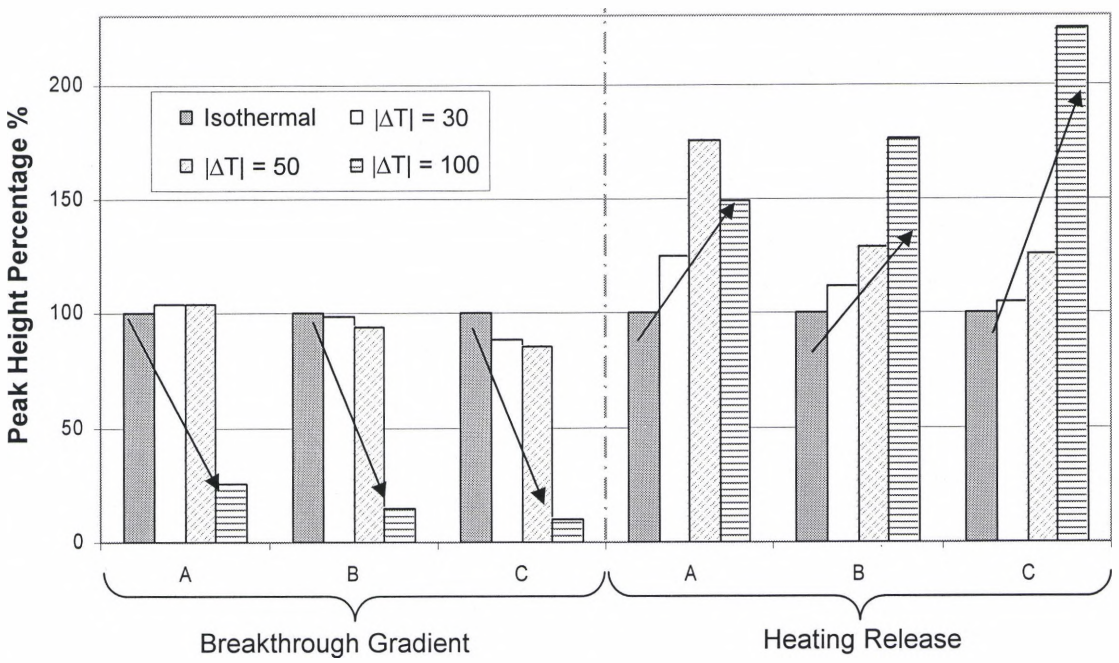

Figure 49. Peak height percentage of the chromatograms of Figure 47.

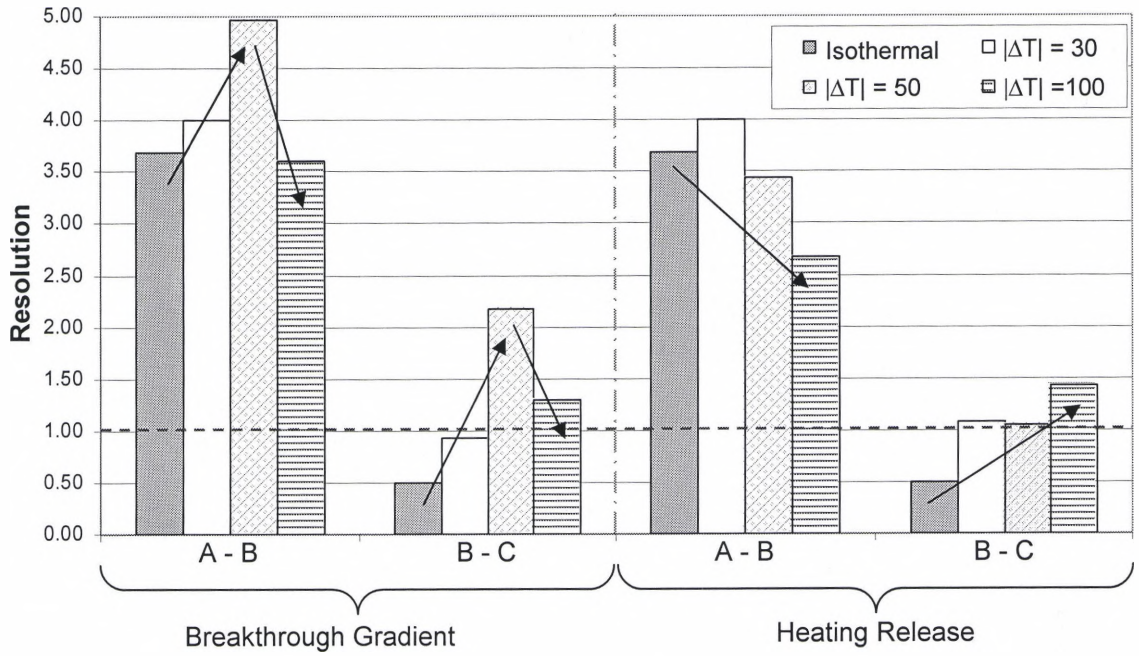

Figure 51. Resolutions of peaks A-B and B-C of the chromatograms of Figure 47.

For the situation where the peaks broke through the gradient (Figure 47-B to D) the compounds were more separated and broader than the isothermal separation, see Figure 48-left side. As can be seen in Figure 47-B to D and Figure 48-left side, the separation and broadening of the peaks increased as the temperature gradient increased, which is noticeable in Figure 47-D, where the peaks are very broad and separated.

For the case where the peaks were released before they broke through the gradient (Figure 47-E to G), the peaks got narrower and taller than the isothermal separation (Figure 49-right side). Although the apexes of the peaks were closer than the isothermal run (Figure 49-right side), the narrow peaks and increased signal provided an enhanced chromatographic separation (increased in resolution Figure 49-right side) that permitted a better identification of the peaks. The peaks got narrower and taller as the temperature gradient $|\Delta T|$ was higher, which is seen in Figure 47-G for the release of the compounds at a $|\Delta T|$ of 100 °C, and Figure 48-right side.

A schematic of the entire second dimension profile (Figure 52) would be helpful to understand what happens when the compounds breakthrough the negative gradient or when they are released by heating before they breakthrough. However it is important to understand first how the compounds move through the column.

The movement of the compounds through the column is determined by the interaction with the stationary phase, the higher the interaction the slower the compounds will move, and the higher the axial diffusion will be. Therefore, in a polar stationary phase, polar compounds that have more affinity to the stationary phase will be broader and move slower than a non-polar compound. Temperature plays a big role in the interaction strength of the compounds with the stationary phase. Generally, the lower the temperature the higher the interaction strength will be.

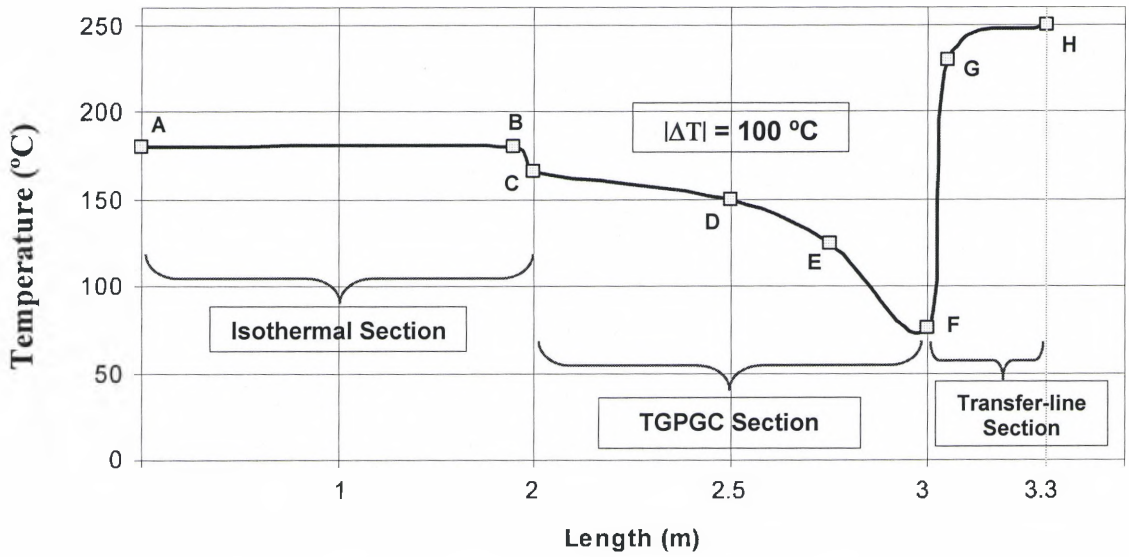

Figure 52. Second dimension column temperature profile.

When the compounds exit the negative gradient they encounter a steep positive temperature gradient, which goes from the colder CSA temperature to the oven temperature and eventually to the MS transfer-line temperature, segment F-G of Figure 52. Now as the opposite effect of a negative gradient, the peaks, will be broadening instead of narrowing. The velocity at the beginning of the peak increases when it

encounters the step positive temperature gradient, leaving the back part of the peak inside the negative gradient at a lower temperature, and thus, lower velocity. This velocity difference is what makes the peak broaden. The bigger the velocity difference between the beginning and end of the migrating zone, the broader the peak becomes. Figure 53 shows what happens to a migrating zone or peak when it encounters a positive gradient.

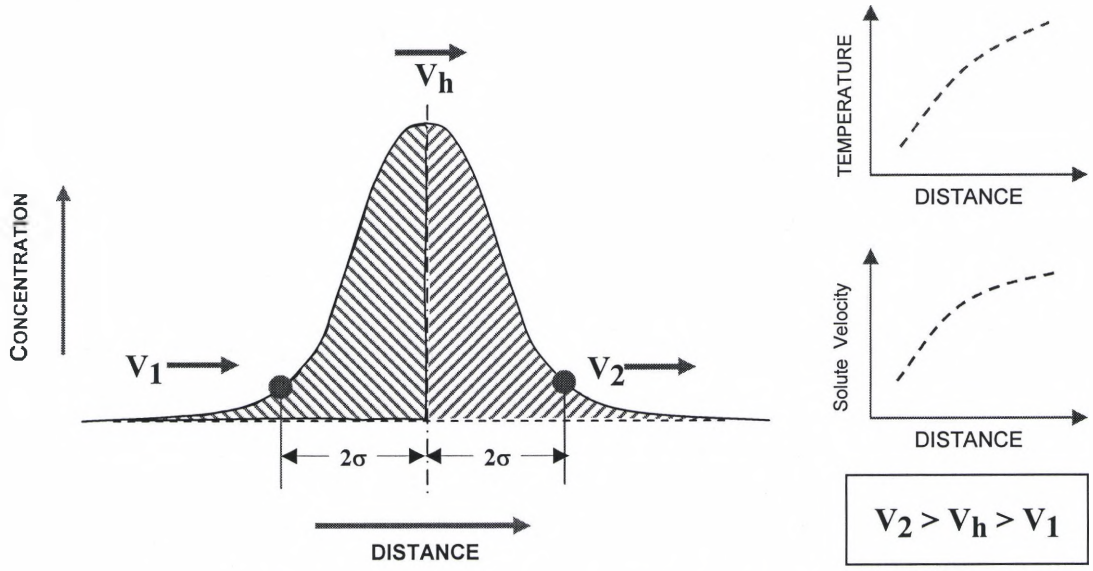

Figure 53. Migration zones velocity aspects.

This is the reason why the peaks shown in Figure 47-B to D become broader and more separated as the $|\Delta T|$ of the gradient profile increased. When the first peak breaks through the gradient, the second is still in the gradient and thus traveling slower, allowing the separation between the peaks. As the $|\Delta T|$ of the negative gradient increases the slower the second peak will be traveling and thus the bigger the separation between the peaks, as shown in the left side of Figure 48, where the separation of the compounds for a $|\Delta T|$ of 100 °C is very large.

However, the peak height, and therefore its signal, is inversely proportional to its width, and for this reason the heights of the peaks obtained in Figure 47-B to D

decreased, due to an increase in their peak widths (Figure 49). The variation of the peak height with respect to its base width is shown in Figure 54, where it is noticeable that decreases in width of an order of magnitude produce a gain of an order of magnitude in height and thus in signal.

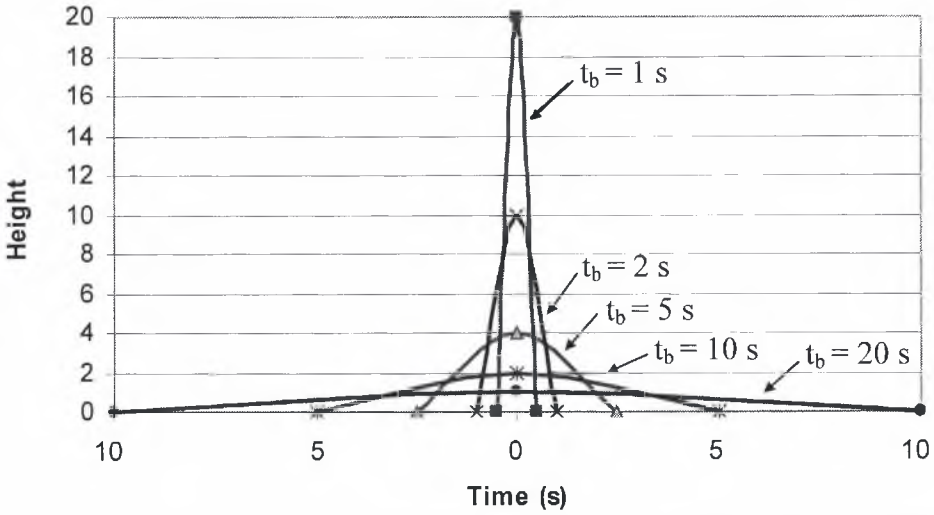

Figure 54. Effect of the peaks narrowing on their height detection.

(t_b = Base time length)

Therefore the decrease in signal or height of the peaks shown in Figure 47-B to D and Figure 49 (left side), is a sign that the peaks were becoming broad. This observation is obvious in Figure 47-D where the last peak is so broad that it can barely be seen.

As can be seen in Figure 49 (left side), the resolution increased when the peaks breakthrough a negative gradient with a low $|\Delta T|$, and decreased for higher $|\Delta T|$ gradients. The increase in resolution obtained with lower $|\Delta T|$ gradients is due to the increase in separation of the peaks. However, higher $|\Delta T|$ gradients make the broadening effect bigger, overcoming the separation effect and hence decreasing the resolution.

The release process consisted of rapidly heating the temperature gradient to isothermal oven temperature, eliminating the temperature gradient. This implied the

application of a positive temperature gradient to the peaks. However the heating method used allowed reducing the broadening effect of the positive gradient by keeping a negative gradient during the heating process (see Figure 55). This negative gradient permitted a reduction of the broadening effect by continuously focusing the peaks during the heating process.

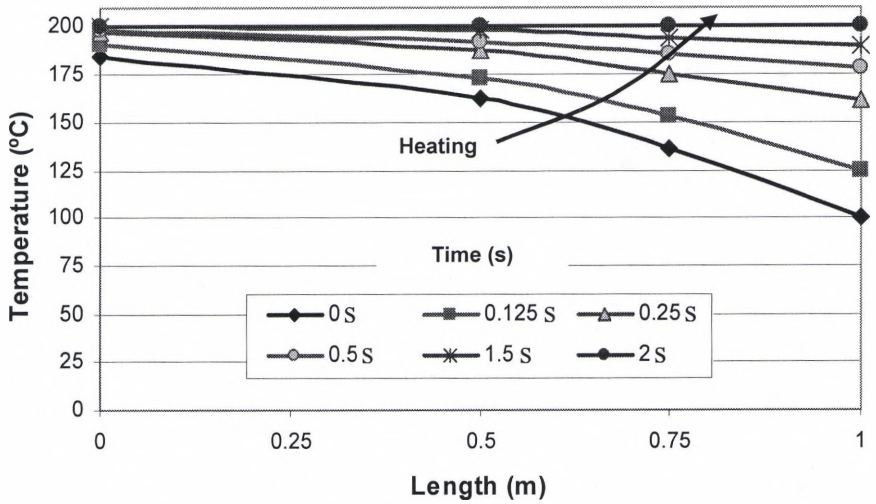

Figure 55. Temperature gradient profile during the heating release process.

Narrow peaks are achieved in the release process of the TGPGC mode, since the beginning and end of the migrating zone is being heated almost at the same time. This heating scheme keeps the velocities of the migrating zone constant, hence, releasing the peak as focused as they were in the negative gradient. Although some resolution is lost due to the heating process, the peaks are kept very narrow and tall, as observed in Figure 47-E to G and the right side of Figure 49.

Narrower and hence taller peaks were obtained at bigger $|\Delta T|$ gradients (see Figure 49). Peaks as narrow as 120 ms were obtained. The reason for this was the colder temperatures and steeper negative gradients caused larger velocity differences in the migrating zone, thus producing narrower peaks (see Figure 47-G).

In the release process of the TGPGC mode the peaks were closer to each other than the isothermal separation as seen in Figure 48 (right side). The peaks get closer to each other since they slow down, due to the lower temperatures encountered in the negative temperature gradient. Even though the peaks are closer to each other compared to the isothermal separation, good chromatographic separations were obtained due to the narrow peaks, as seen in Figure 47-E to G.

The right side of Figure 51 shows the resolution obtained using the release situation of the TGPGC mode. Even though the resolution of peaks A-B was reduced compared to the isothermal separation, it was still over 1.0, which is considered the minimum for a measurable separation to occur and to allow good quantitation[39]. Nevertheless, the resolution of peaks B-C increased more than 100% (Figure 51), even though the peaks where closer, they were narrower (and higher) allowing a good chromatographic separation.

High resolution in the release process of the TGPGC mode is created by the production of narrow peaks. The release process not only improved the chromatographic separation of the peaks, but also increased the signal of the peaks. This increase made the MS more sensitive for lower compound concentrations, reducing its detection limit and improving its quantitation capacity.

As can be seen in Figure 47, the situation where the peaks broke through the gradient in the TGPGC method increased the resolution, though it also reduced the signal of the peaks as can be seen in Figure 49. For the situation where the peaks were released, even though the resolution of the first pair of peaks (A-B) was reduced, the resolution of the second pair and its signal was increased, as can be noticed in Figure 51 and Figure 49 for all the compounds.

The two TGPGC situations can be observed in Figure 56, where the 1-tetradecanol peak at a $|\Delta T|$ gradient of 100 °C, was allowed to breakthrough the gradient

and was then released before the whole peak went through the gradient. In the chromatogram of Figure 56 we can observe the broadening effect at the beginning of the peak, due to gradient breakthrough. The narrowing effect of the negative gradient was also appreciated at the end of the peak, as the remaining part of the peak still retained in the gradient was released.

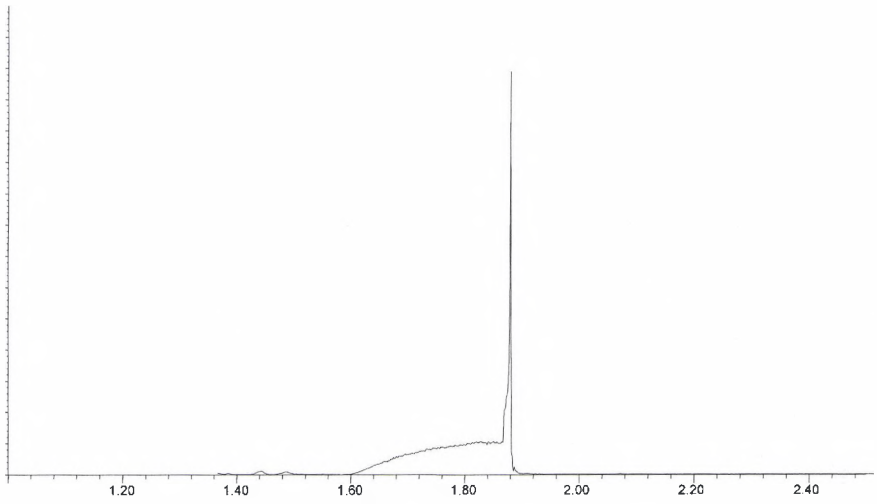

Figure 56. Breakthrough and release of the 1-tetradecanol.

This situation explains the peak shape of 1-hexadecane in Figure 47-G where broadening of the first part of the peak was observed. This means that part of the n-hexadecane broke through the gradient before it was released. The broadening of the peak explains the lower height percentage shown in Figure 49- right side, for the $|\Delta T|$ gradient of 100 ºC. This explains why peak A did not follow the growing height percentage trend observed with peaks B and C as the $|\Delta T|$ gradient increased.

Influence of the heating rate in TGPGC

Different heating rates can be applied for releasing the compounds in TGPGC, however its influence in the separation process is not known. Therefore, experiments were performed to understand the effect of the heating rate on the separation process when the release operation of TGPGC is applied.

The sample and experimental conditions used were the same as the ones used for describing the effect of the negative temperature gradient in the separation process using TGPGC, though, in this experiment only one negative temperature gradient was used, which was the 100 °C $|\Delta T|$ gradient.

The chromatograms generated using TGPGC for the different heating rates are shown in Figure 57-B to G. In these experiments the compounds where released just before they broke through the negative gradient. Figure 57-A shows the isothermal separation of the sample, which was used as the model for comparing the TGPGC separations. As seen before in Figure 46-A, the isothermal separation generated in Figure 57-A shows once more the limitation of the isothermal mode to completely separate the peaks.

As previously mentioned, releasing the peaks before they breakthrough the gradient makes the peaks more closer to each other and become narrower while maintaining good resolution for the first pair of peaks and increasing the resolution of the second pair. The situation depicted in the chromatograms of Figure 57-B to G is the same as the one previously described, even though the heating release process was done at different heating rates.

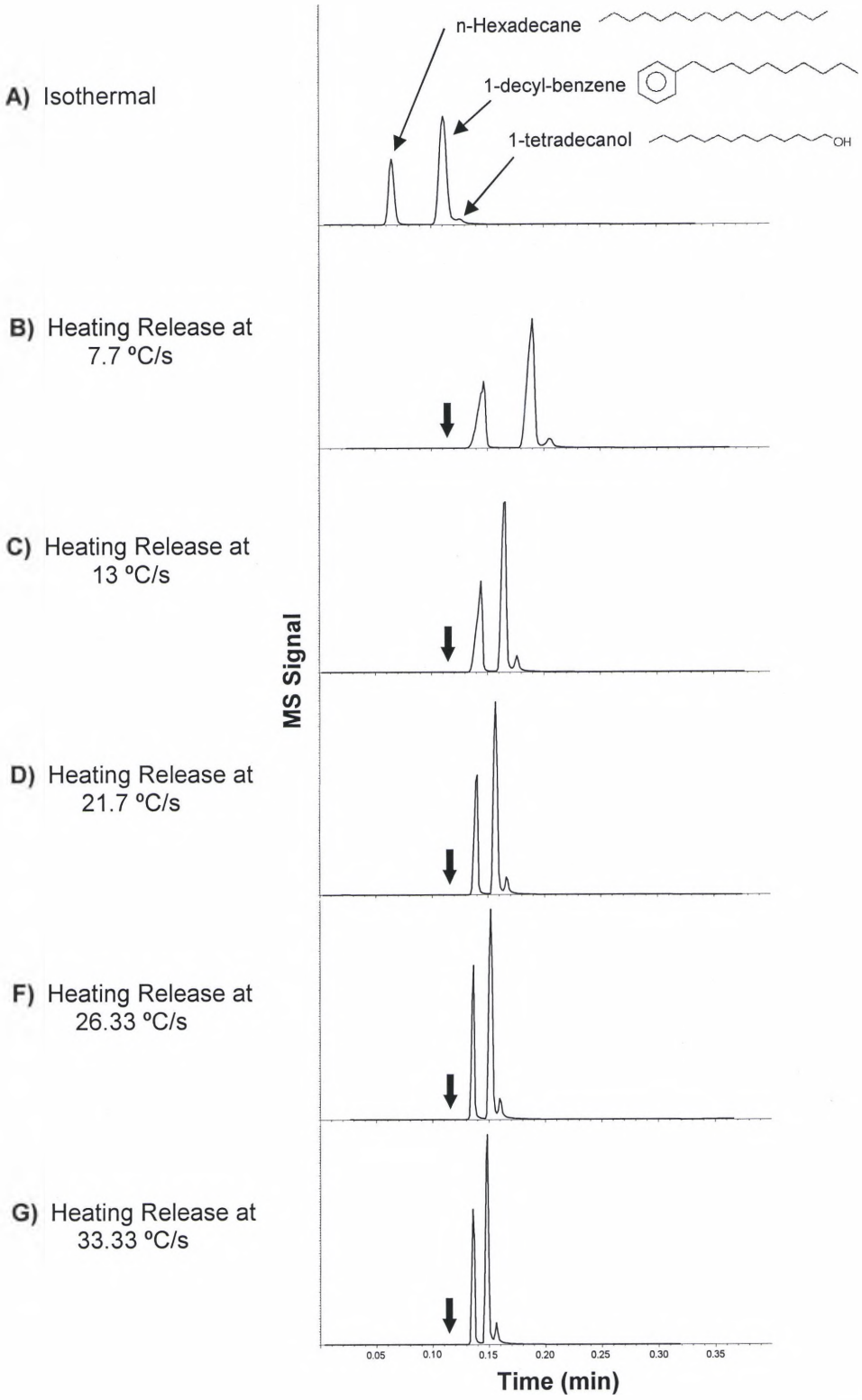

Figure 57. Different heating rates applied in TGPGC separations at a |ΔT| gradient of 100 °C.
(The arrows indicate the initial heating time)

Figure 58 shows the height percentage of the peaks with respect to the isothermal separation, where it is clearly seen that the peak height was higher than the isothermal separation for all the heating rates.

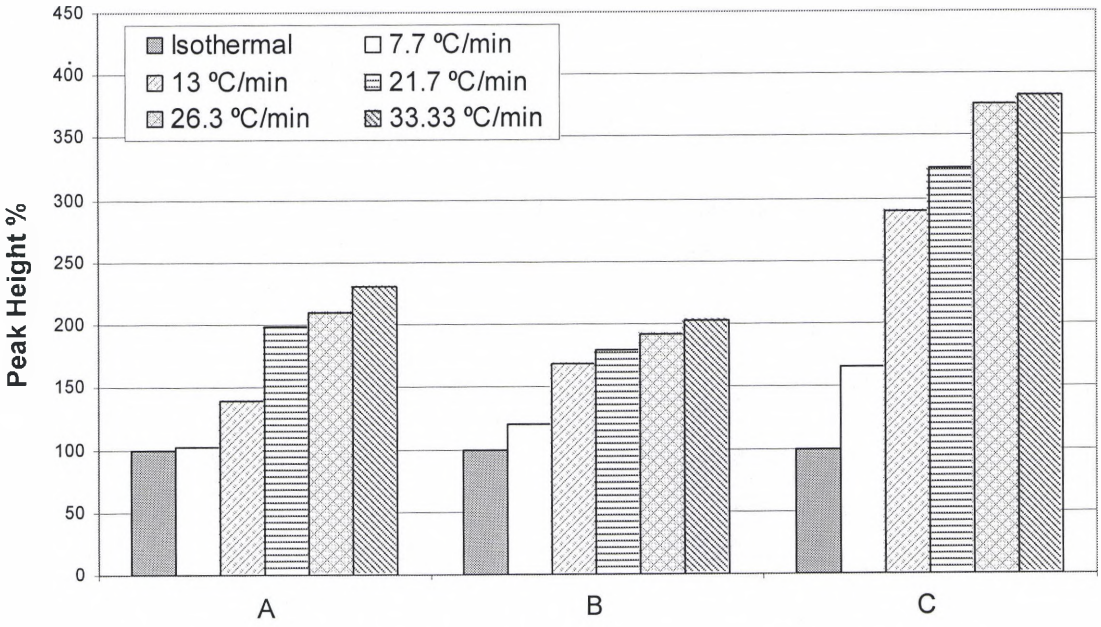

Figure 58. Peak height % of the released peaks shown in Figure 57.

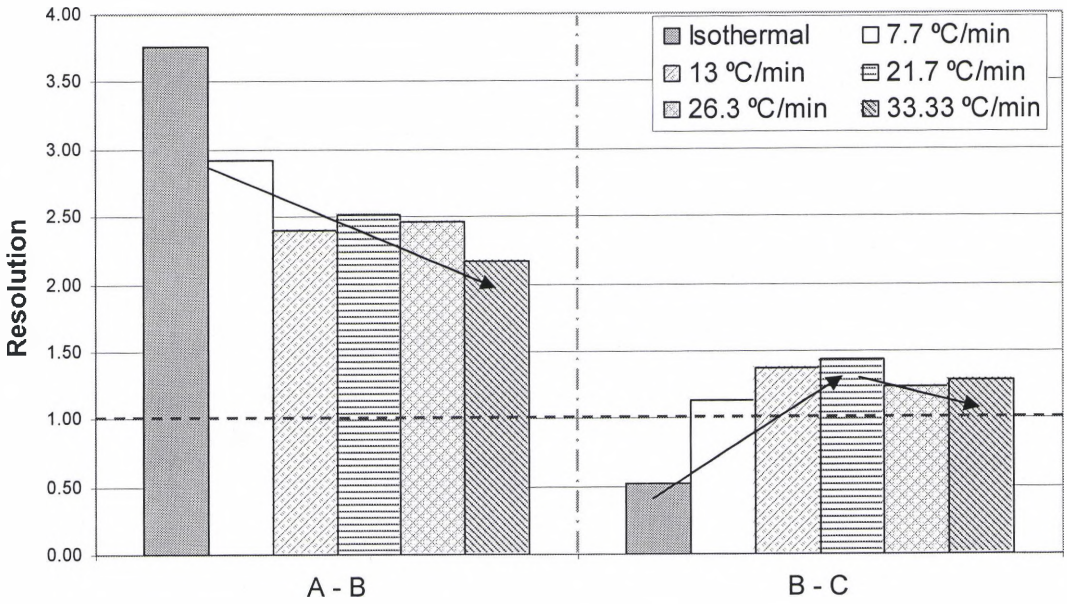

Figure 59. Resolution of the peaks shown in Figure 57.

As seen in Figure 59 higher heating rate does not necessarily mean higher resolution. At lower heating rates the resolution increases due to the narrowing effect obtained from releasing the peaks. It may be that, as the heating rate increases, the peaks get narrower and closer together, possibly reaching a point where the narrowing effect may be overcome by the smaller and smaller distance between the peaks, thus decreasing the resolution.

Nevertheless, the resolution between the peaks of Figure 57-B to G (see Figure 59), followed the trend observed for the peaks that broke through the gradient Figure 48-right, where the first pair of peaks showed lower resolution compared to the isothermal run, and the second pair of peaks showed higher resolution. This implies that for the heating release process in TGPGC, no matter the heating rate, the peaks that are released before they breakthrough the gradient should be nearer to each other, narrower and hence higher, while keeping good resolution.

However, what was notable about releasing the peaks at different heating rates was the fact that the peaks became narrower and closer as the heating rate increased, which was easily observed in Figure 57-B to G.

Thus, an increase in the heating rate implies a decrease in the time it takes to heat the gradient to oven temperature. Then, the variations observed in the chromatograms of Figure 57-B to G must be an effect due to the temperature of the gradient at which the peaks are eluted.

Hence, using the time it takes since the heating release starts to the elution of the last peak (c) 1-tetradecanol, and using the heating rate, we can determine the temperature or the $|\Delta T|$ of the gradient at which the last peak was released. However, since the start of the heating release was not precisely measured, and since peak A immediately comes out after starting the heating release, the releasing time was taken as an average between the elution of peak A and the elution of peak C.

The elution time of peak C with respect to peak A for the different heating rates is shown in Figure 60, where it is seen that the higher the heating rate the less time it takes to elute the peaks. By using the time it takes to elute the peaks of the column (Figure 60) and the heating rate, the $|\Delta T|$ of the gradient at which peak C was released was then calculated (see Figure 61).

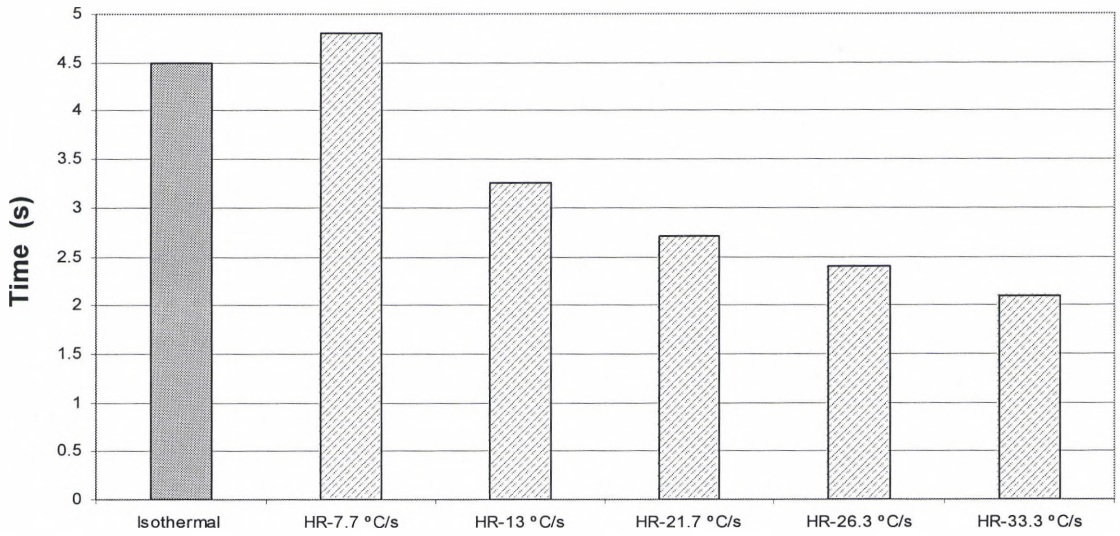

Figure 60. Adjusted retention time of peak C with respect to peak A for the different heating rates.

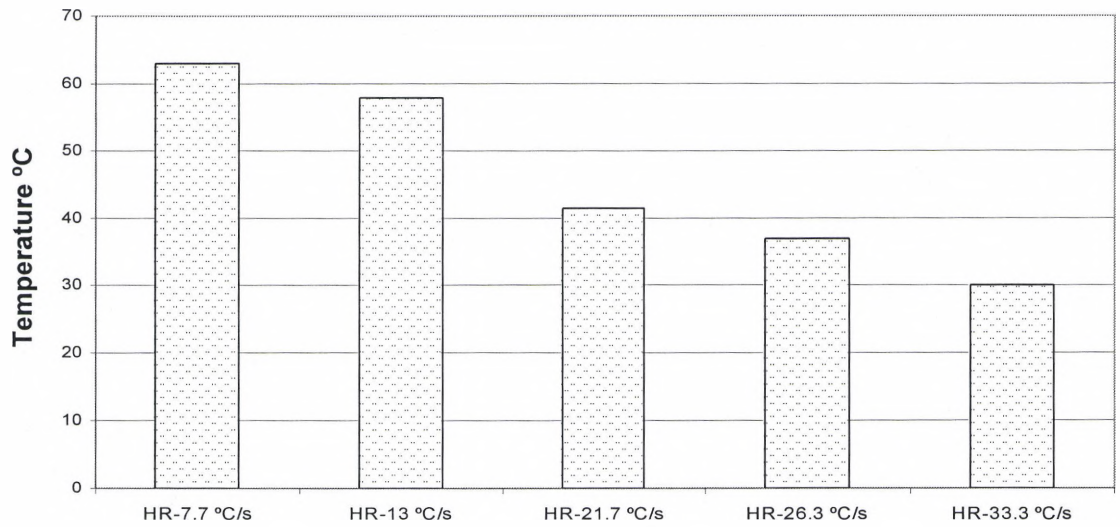

Figure 61. Temperature of the gradient at the elution time of peak C.

As can be seen in Figure 61 the slower the heating rate the bigger the $|\Delta T|$ gradient which peak C, and hence peaks A and B, go through. Slow heating rates do not release the peaks at oven temperature, thus releasing the peaks while still in presence of a gradient. This explains why for lower heating rates, which mean bigger $|\Delta T|$ gradients, the elution time of the peaks was larger (see Figure 60). When the peaks go through a negative temperature gradient they slow down and the bigger the gradient the slower the peaks move, hence the longer the elution time as seen in Figure 60.

The positive gradient that the peaks see once they go through the negative gradient is what makes the peaks broader (Figure 57-B to G), as explained before when the peaks breakthrough a gradient. This situation explains why for lower heating rates, which means bigger $|\Delta T|$ gradients, the peaks where broader and more separated, as can be seen in Figure 62.

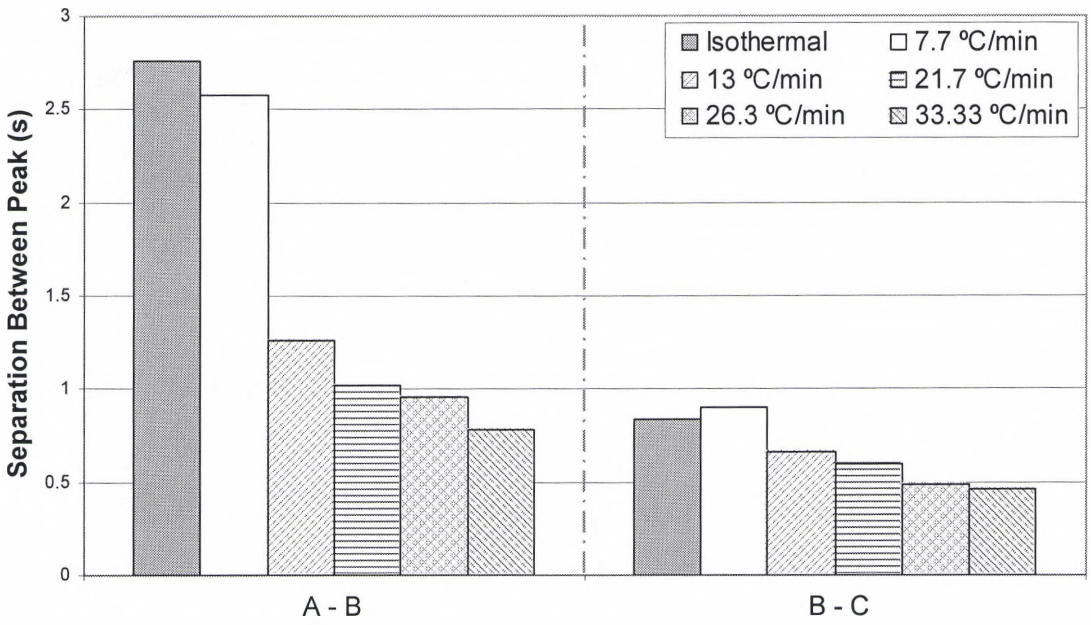

Figure 62. Separation of peaks A-B and B-C of the chromatograms of Figure 25 (s).

As the heating rate increased the peaks got closer and narrower, as seen in Figure 57-B to G, since the $|\Delta T|$ gradient was lower, thus decreasing the effect of breaking through the gradient. Lower heating rates and bigger $|\Delta T|$ gradients made the breakthrough the gradient effect bigger, generating less narrow and more separated peaks, as seen in Figure 57-B to G, Figure 58 and Figure 62.

In all the heating release cases there was some breakthrough effect involved, the effect was not as pronounced as when the gradient was static, which was the case studied in Figure 46-D. In the heating release process the peaks are breaking through a dynamic $|\Delta T|$ gradient that is getting smaller with time, maintaining the velocities of the migrating zone very similar and decreasing the broadening effects observed when a peak broke through a static gradient (Figure 46-D).

In summary, if one wants to take advantage of the narrowing effect of a negative gradient, the heating process must be started before the peaks breakthrough the static gradient. High heating rates must be used, to elute the peaks even though it will not necessarily guarantee the best separation.

The effect of the initial time for heating the gradient in TGPGC

As described earlier, two separation processes can take place in TGPGC. One of them consists in letting the peaks breakthrough the gradient (Figure 63-1), while the other consists in releasing the peaks that are traveling slowly in the gradient by heating the gradient to oven temperature (Figure 63-2 to 4).

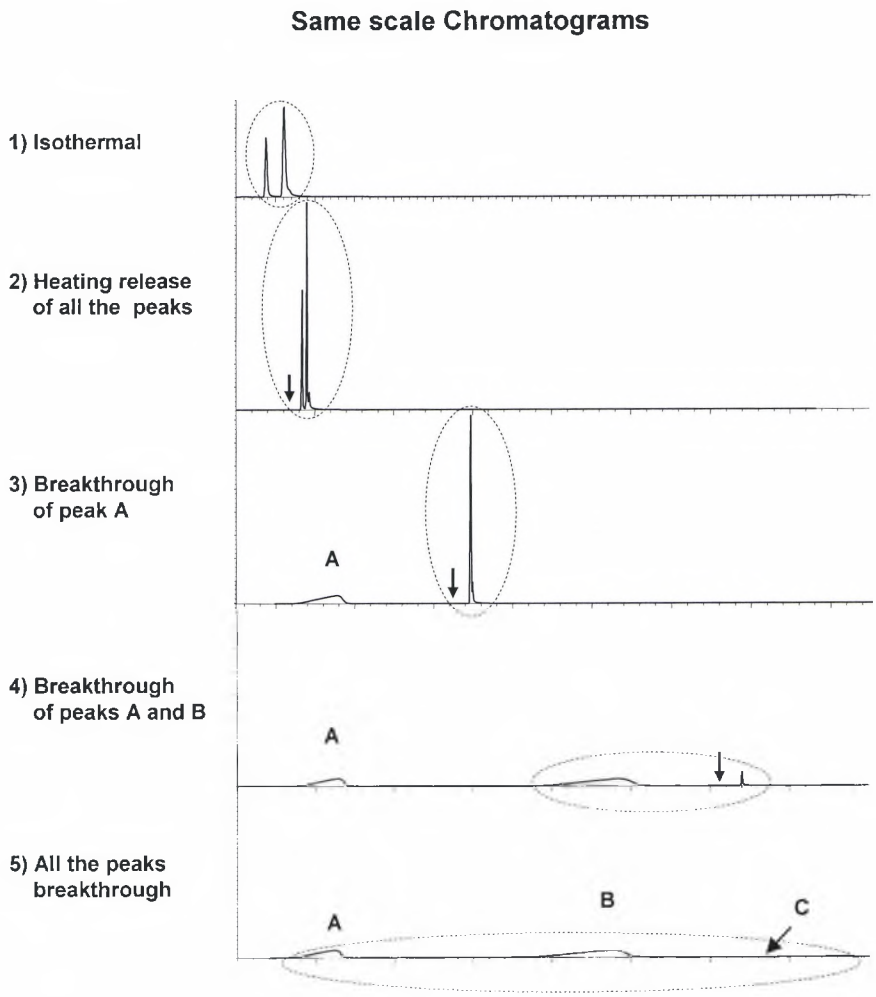

Oven Temp = 200 °C; ΔT gradient = 100 °C; Flow velocity 20 cm/s; column: RTX-200.
The Vertical arrows indicate the initial heating time.

Figure 63. Separations performed at different initial heating times.

In the first process there is an increase in resolution due to the physical separation of the peaks, whereas in the second process, they are chromatographically separated due to the narrow and thus taller peaks obtained (Figure 63-2, 3). Conversely, the first process reduces the signal of the peaks as a result of the broadening effect during the breakthrough, while the second process increases the height of the peaks and consequently the sensitivity of the detector system.

Figure 63 is an example that shows how TGPGC works. Moreover it shows the advantages of using TGPGC, where one can selectively separate the peaks. For instance one can decide to let peak A escape the gradient and then narrow peaks B and C (Figure 63-3), or either decide to just increase the signal of peak C by letting peaks A and B escape from the gradient and then heat the gradient (Figure 63-4).

This feature makes the TGPGC method very attractive for solving the problem encountered in the separation of the second-dimension in MDGC-MS. As previously mentioned, an often encountered difficulty in the second-dimension separations is the presence of zones that are not adequately resolved, representing a form of the general elution problem (GEP). Figure 64 shows a typical GEP chromatogram where, the early eluting peaks are narrow and clustered together, while the later peaks are more separated and broader.

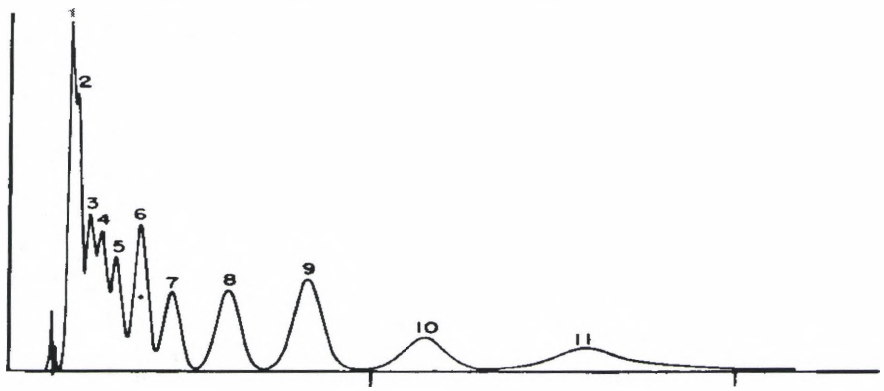

Figure 64. A General Elution Problem example[50].

For this reason the initial heating time of the gradient is very important in solving the GEP, since it determines what section and which separation process would take place in the separation of the heartcut.

To study the effect of the initial heating time in the separation process of the second-dimension, experiments were performed at different heating times. In addition, different heating rates where also tested to further determine the best conditions for increasing the peak capacity in the second-dimension.

The system used for the experiments was the same system used in previous experiments, though, the secondary-column was changed due to the need for faster analysis in the second-dimension. A carbowax column of shorter length (L= 2.3 m) and new GC conditions were used. The higher polar nature of the carbowax column with respect to the RTX-200 increased the separation of polar compounds, compensating the negative separation effect of increasing the carrier gas velocity and decreasing the length of the column. The operational conditions of the GC used were: a column head pressure of 30 psig, a split of 110 ml/min, and a carrier gas velocity of 100 cm/s.

The isothermal oven temperature used in the experiments was determined from a Diesel chromatogram where the n-hexadecane eluted at 180 °C. This temperature allowed us to precisely simulate the heartcut elution of the sample, and hence determine the best conditions for increasing the separation power.

However, due to the new column and GC conditions, a breakthrough test was necessary to establish which $|\Delta T|$ gradient would provide the best separation for the first zone of the heartcut. An unretained compound (n-dodecane) was added to the sample mixture to facilitate the observation of the retention times of the compounds.

Figure 65 shows the four temperature gradient profiles employed in the experiments, while Figure 66 shows the breakthrough of the sample for three different $|\Delta T|$ gradients. The $|\Delta T|$ gradient of 180 °C completely stopped the compounds in the

gradient, hence the peaks never breakthrough the gradient and there is no chromatogram for this experiment.

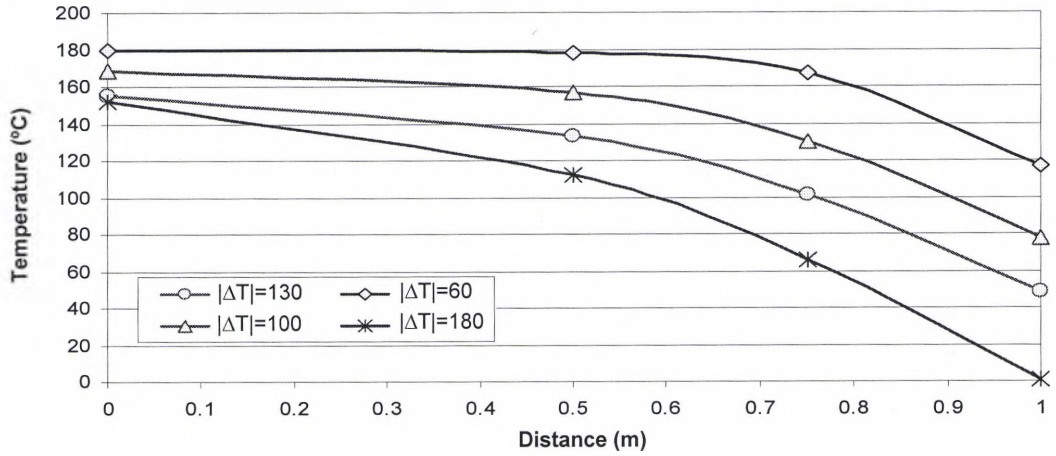

Figure 65. Temperature Gradient Profile used for the Breakthrough experiments.

As seen in Figure 66, an increase in the $|\Delta T|$ gradient increases the retention time of the peaks and also made them broader, which was expected. However, the best $|\Delta T|$ gradient would be the one that allows some retention of the first peaks without broadening the peaks.

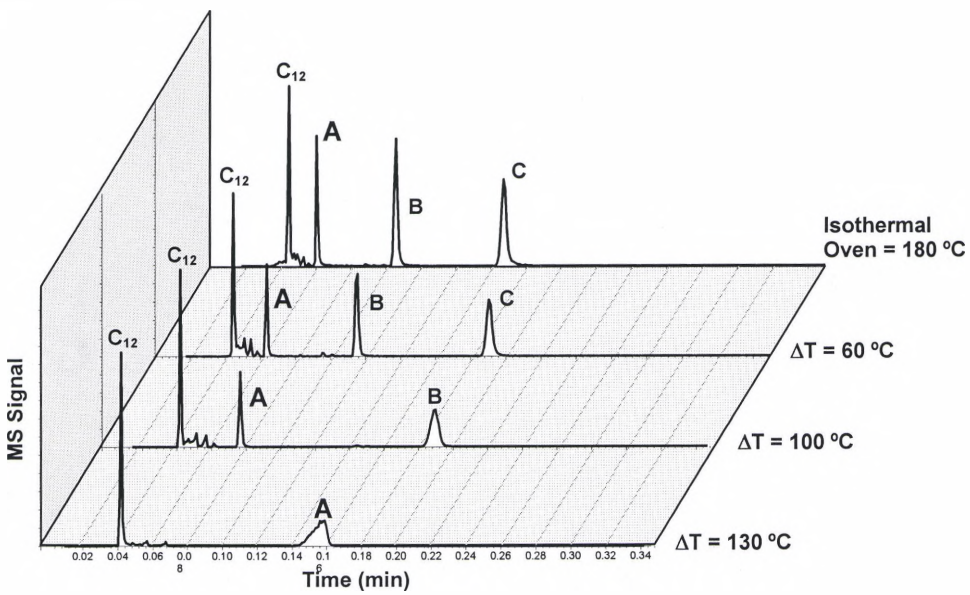

Figure 66. Breakthrough at different ΔT gradient temperatures.

From Figure 66 we can observe that a $|\Delta T|$ of 60 °C barely retains peak A while a $|\Delta T|$ of $\geq$ 130 °C definitely retains peak A, although it also decreases its peak height by 50 %. Higher $|\Delta T|$ gradients of 130 °C would be less likely to be used since it would take a lot of time for the peaks to breakthrough the gradient. Moreover the peaks would be very broad with a low signal. A test was done for a $|\Delta T|$ gradient of 180 °C, and in this case the peaks were stopped. This gives another possibility of using bigger $|\Delta T|$ gradients and stopping all the peaks and then releasing them, though bigger $|\Delta T|$ gradients involve longer times for heating and cooling which in turn would mean longer separation processes that we want to avoid.

A $|\Delta T|$ gradient of 100 °C was then chosen as the best gradient for enhancing the separation of the first peaks of the second-dimension, since as seen in Figure 66 it retained peak A, while keeping a good signal, also maximum resolution.

More compounds were added to the heartcut sample in order to appreciate the effect of the different heating times and heating rates in the separation of the sample. The isothermal run at 180 °C is shown in Figure 66 where all the compounds present in the heartcut can be observed.

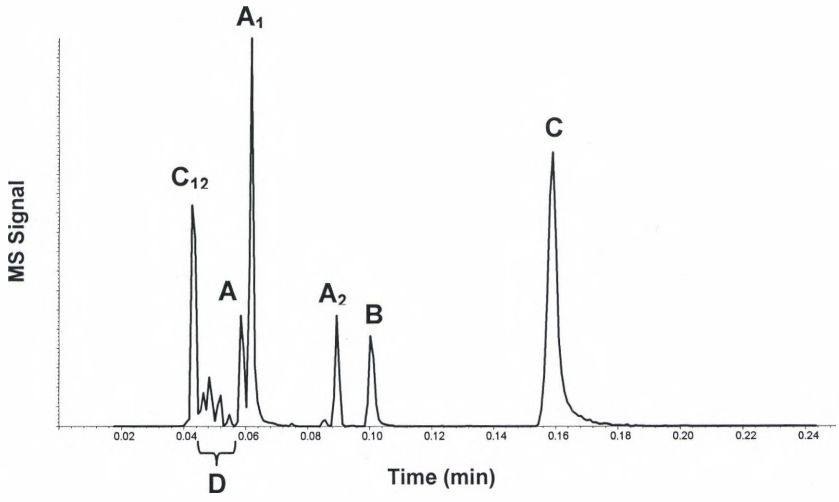

Figure 67. Isothermal run showing all the peaks present in the heartcut sample.

C_{12} is the unretained compound (n-dodecane), the **D** zone is composed by solute and solvent impurities peaks, **A** and **A_1** represents the aliphatic compounds n-hexadecane and n-hexadecene respectively, **B** represents the aromatic compound (1-decyl-benzene), **C** is the 1-tetradecanol and it represents the polar compound. Peak **A_2** is a polar compound 2-methyl-naphthol, and as can be observed, it is eluting before the aromatic compound, which was not expected due to the high polarity of this compound. The reason for this is the fact that peak **A_2** does not belong to the 180 °C heartcut. In a real sample this compound must elute before the n-hexadecane, explaining why peak **A_2** elutes in the middle of the run.

The experiments were performed at three different heating rates and five initial heating times, they are shown in Figure 68 to 69.

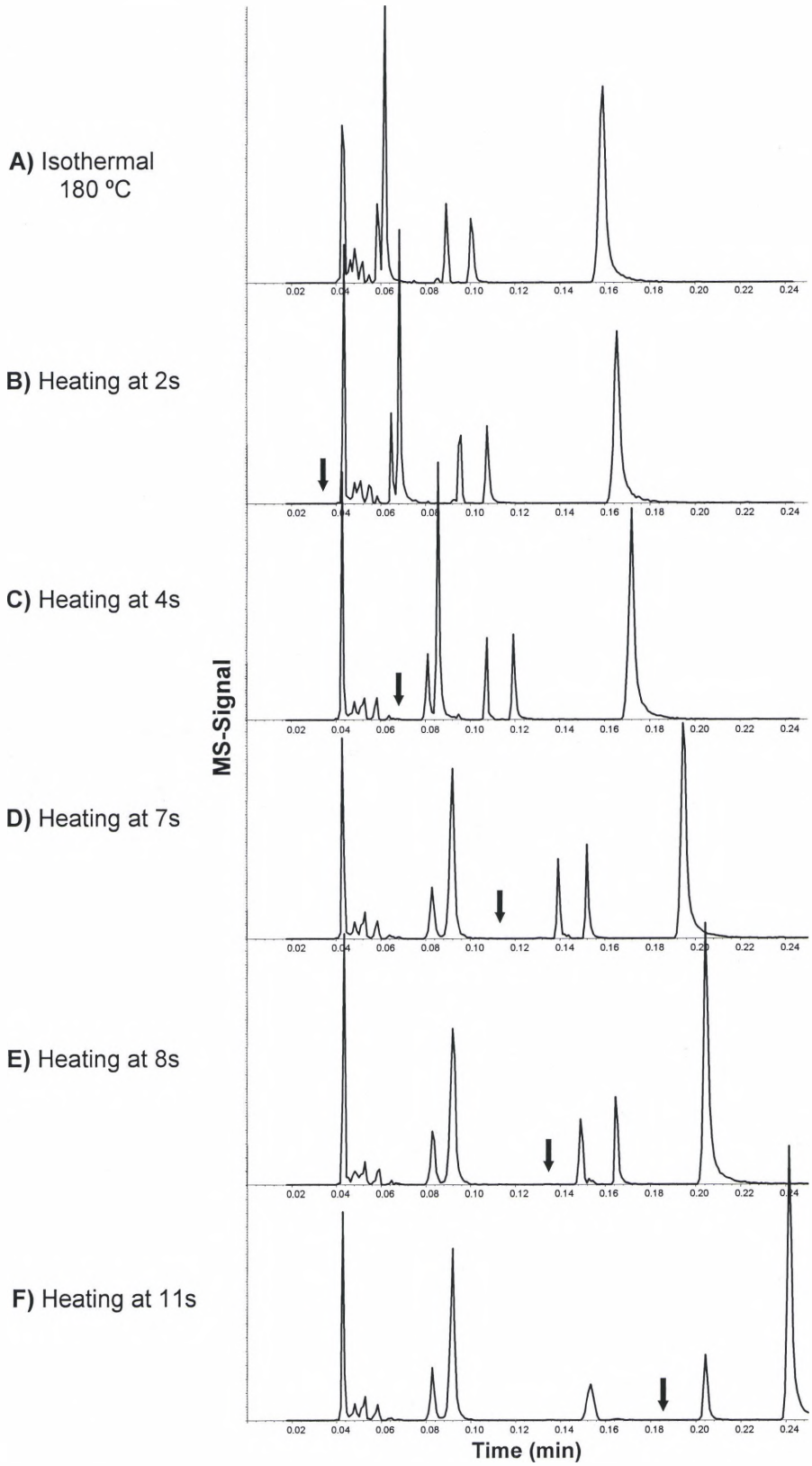

Figure 68. Different initial heating times (IHT) for a heating rate of 9 °C/min and |ΔT| of 100 °C.

(The arrows indicates when the heating started)

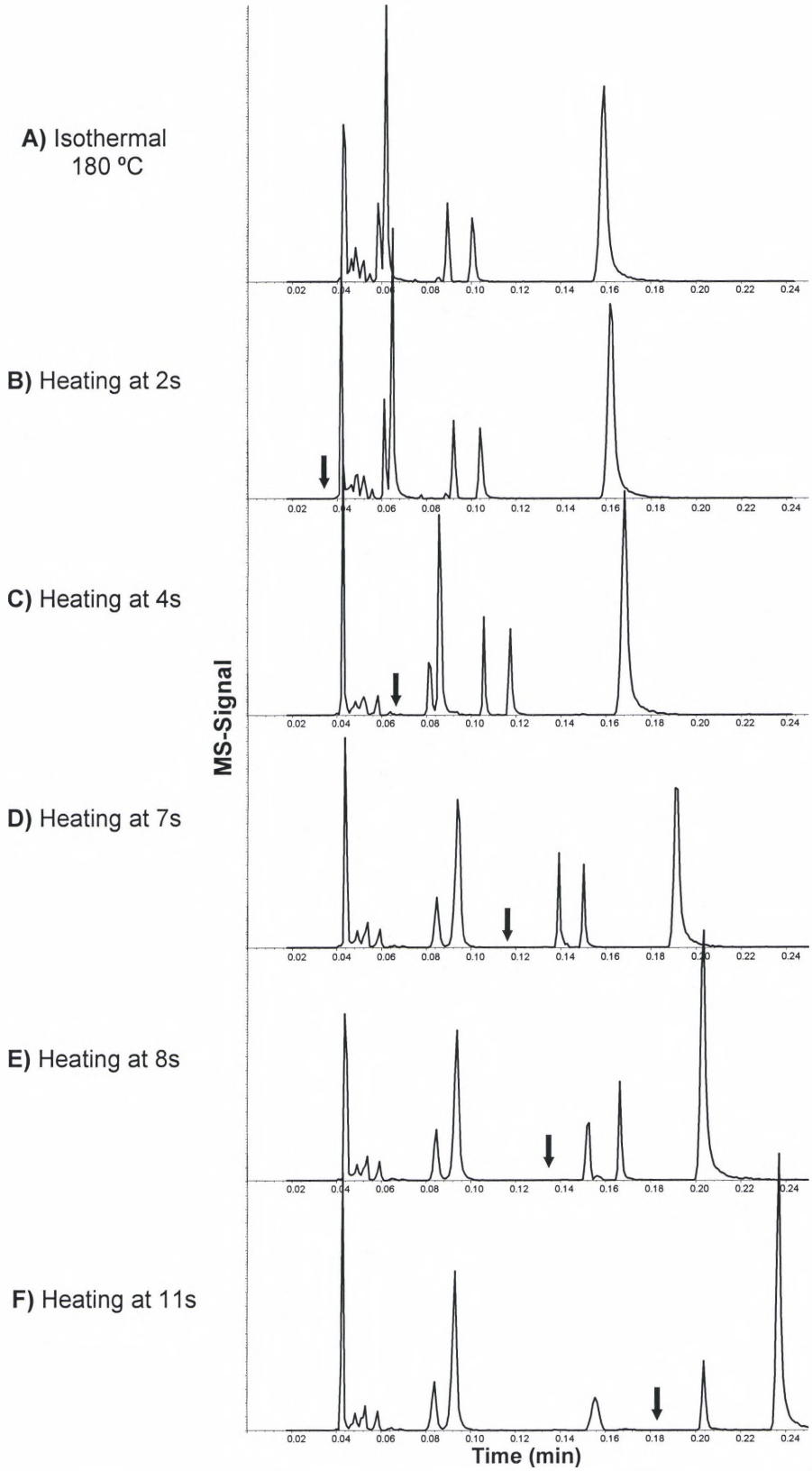

Figure 69. Different initial heating times (IHT) for a heating rate of 18 °C/min and a |ΔT| of 100 °C.
(The arrows indicates when the heating started)

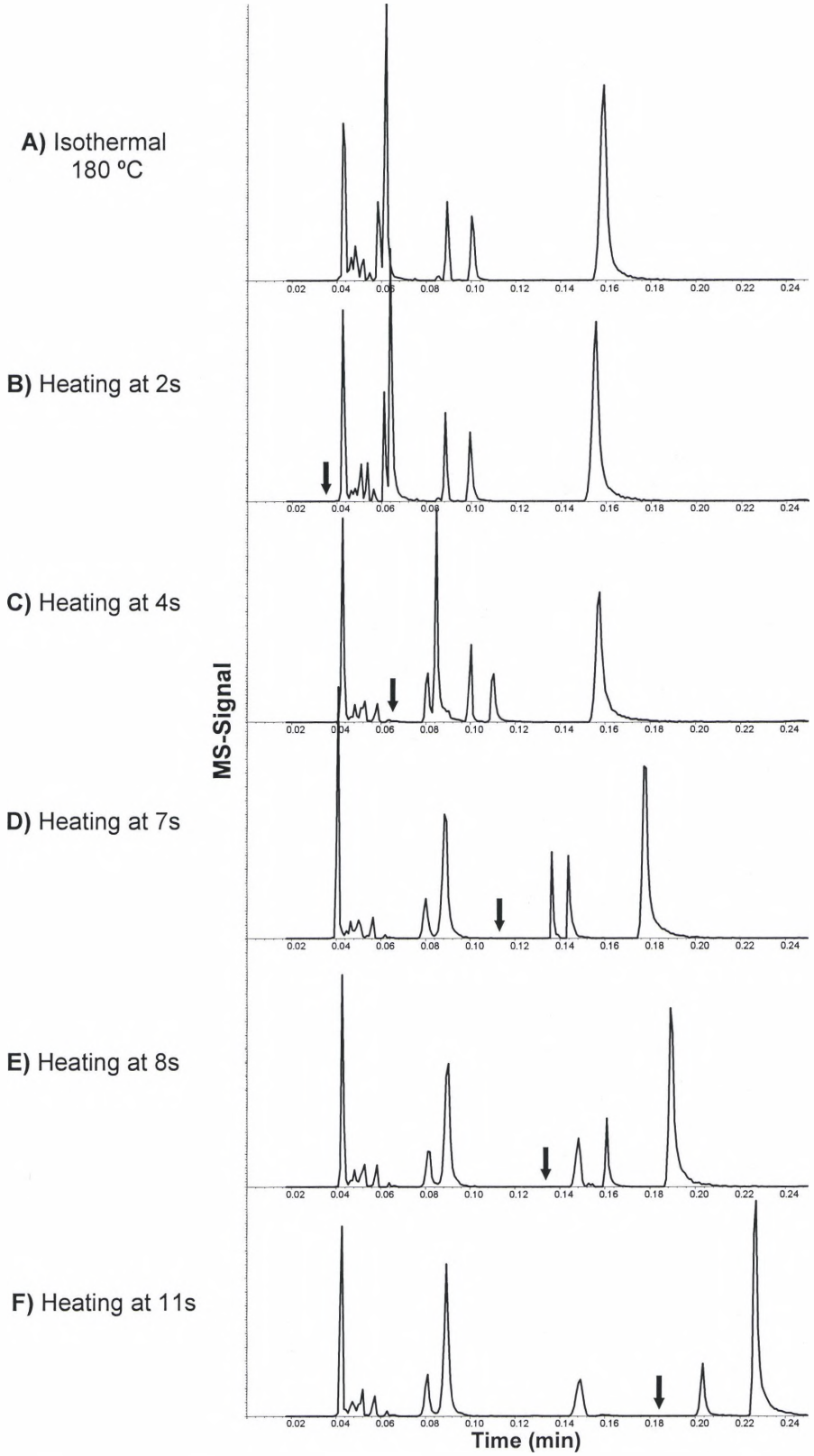

Figure 70. Different initial heating times (IHT) for a heating rate of 33 °C/min and a |ΔT| of 100 °C.

(The arrows indicates when the heating started)

Since it is difficult to visually (qualitatively) evaluate which of the previous runs provides the best conditions for the separation of the heartcut, the peak capacity of each separation was then calculated. The peak capacity (n_p) is the maximum number of peaks that can be resolved side by side into a chromatogram between the holdup time (t_M) and the last peak[39]. The larger the peak capacity the better the overall separation power would be. The following equations are used for the calculation of the peak capacity[33, 39].

$$n_p = 1 + 0.25 \cdot \left(\sqrt{\bar{N}} * Ln\left(1 + \bar{k}\right) \right) \quad (8)$$

$$N = 16\left(t_R / \ w_b\right)^2 \quad (9)$$

$$k = \left(\frac{t_R - t_M}{t_M} \right) \quad (10)$$

$$\bar{N} = \frac{N_1 + N_2 + ...N_n}{n} \quad (11)$$

$$\bar{k} = \frac{k_1 + k_2 + ...k_n}{n} \quad (12)$$

Equation (8) is an approximation for the calculation of the peak capacity, which assumes a resolution of 1.0 for the separations between the peaks. N is the number of theoretical plates, which is a measurement of the efficiency of a column; k is the retention factor or the period of time that the sample component resides in the stationary phase relative to the time it resides in the mobile phase; $\bar{N}$ is the average theoretical plates and $\bar{k}$ is the average retention factor. The other parameters include t_R as the retention time for the sample peak, t_M as the retention time for an unretained peak, and w_b as the base width of the peak.

A bar plot shows (Figure 71) the peak capacity of the chromatograms of Figure 68 to 70, performed at different heating times and heating rates. As can be seen in

Figure 71, the application of the TGPGC method when initially heated at 4s produces an increase in peak capacity for any heating rate. However, for a heating rate of 9 °C/s the peak capacity increases starting from a 2s initial heating time. The reason for the increase in peak capacity at the initial heating time of 4s is a result of the increase in resolution of peaks **A** and $\mathbf{A_1}$, due to the heating release effect, and after 4s the increase in resolution is due to the breakthrough effect as seen in Figure 68 to 70.

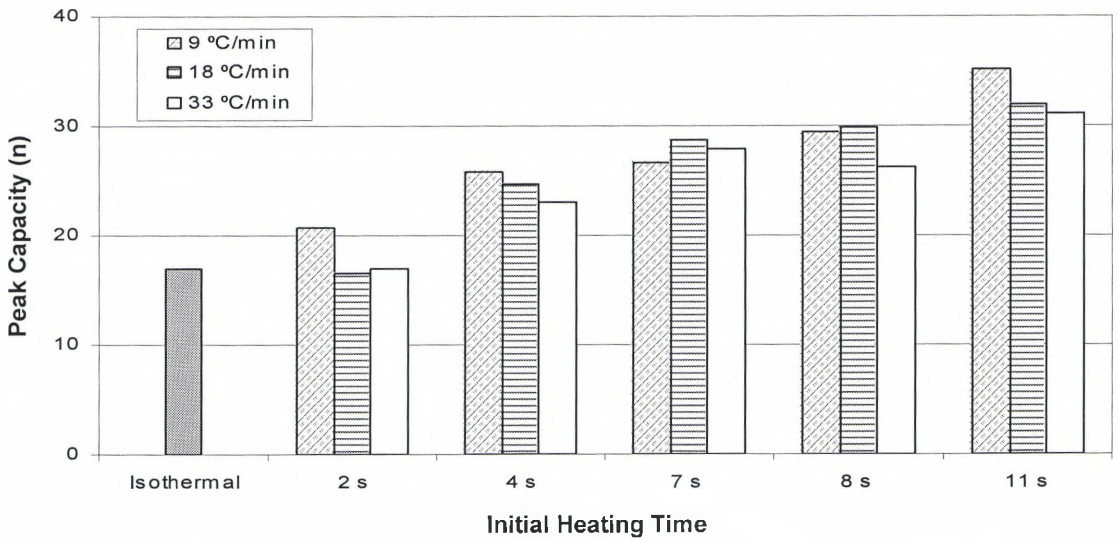

Figure 71. Peak capacity (n) of the chromatograms of Figure 68 to 70.

Lower heating rates make the gradient heat slower. Consequently when the peaks elute, they elute at lower temperatures in presence of a $|\Delta T|$ gradient and not at oven temperatures. This causes separation due to the breakthrough gradient effect, where the peaks get broader and physically separated. This process was explained earlier. This is the reason why for an initial heating time of 2s, only the heating rate of 9 °C/s experienced an increase in the resolution of peaks **A** and $\mathbf{A_1}$ and hence its peak capacity increases. This explains why the peak capacity for higher heating rates does not increase for an initial heating time of 2s.

The peak capacity is a function of the analysis time and the longer the analysis time the larger the peak capacity would be. This is the reason why the peak capacity for

the heating rates of 9 and 18 °C/s were longer compared to 33 °C/s. Slower heating rates means that larger amount of peaks would be affected by the negative gradient during its heating time, and hence would increase the retention time of the peaks and the analysis time. This was not observed for fast heating rates where the effect of the gradient would be limited for those peaks that are on the gradient and during the heating period which is shorter compared to the slow heating rates.

Figure 72 shows the temperature of the gradient at which the last peak (1-tetradecanol) elutes, showing that at lower heating rates (9 °C/s) all the peaks will be eluting through a higher $|\Delta T|$ gradient compared to the fast heating rates.

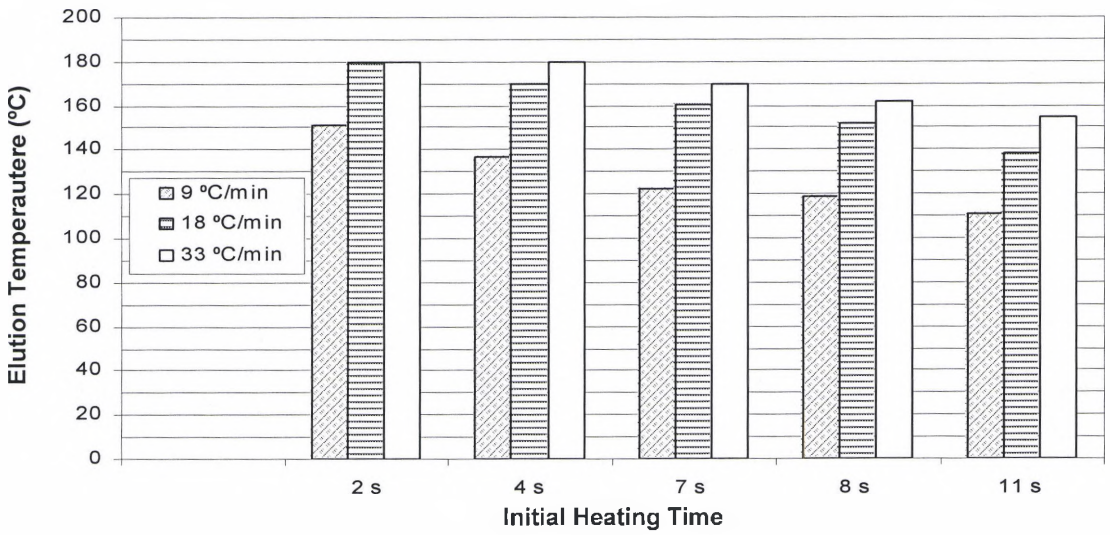

Figure 72. Temperature of elution of the last peak (1-tetradecanol).

Figure 73 shows the total analysis time for the chromatograms shown in Figure 68 to 70. As can be seen, higher peak capacity implies higher separation power; however it also implies higher analysis time.

Figure 73 shows that lower heating rates increase the analysis time due to the increase in retention time of the peaks, since all of the peaks elute at temperatures lower than the oven temperature (see Figure 72). Fast heating rates only have influence over

the peaks that go through the gradient; they do not influence the retention time of the last peak. As a result the analysis can be done faster.

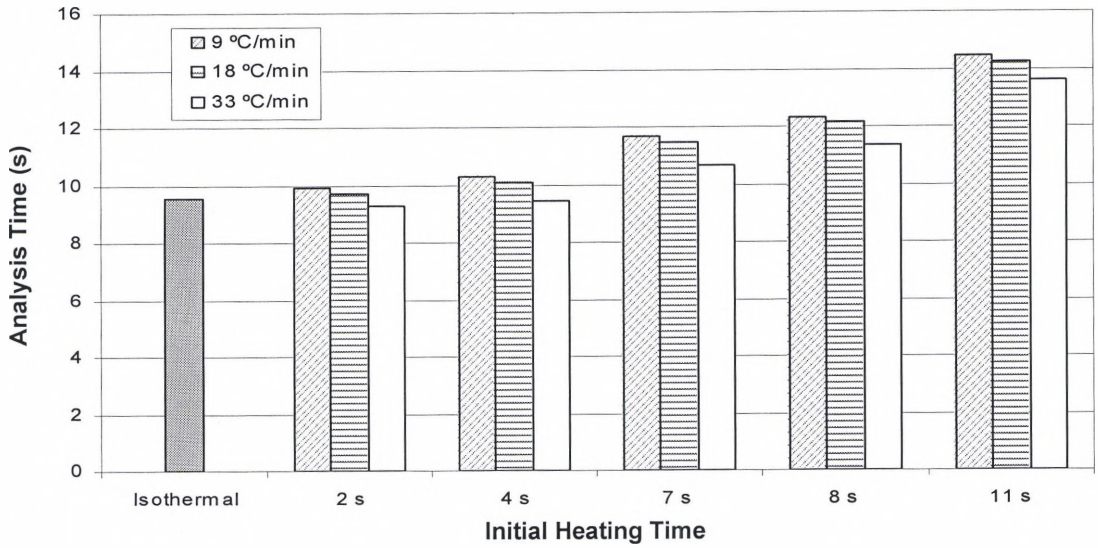

Figure 73. Total analysis time of the chromatogram of Figures 34 to 36.

As discussed before, not only the peak capacity of the second dimension is important, but also it's total analysis time. Therefore a plot of peak capacity divided by analysis time for the chromatograms of Figure 68 to 70 was done to determine the best conditions for the application of the TGPGC in the second-dimension.

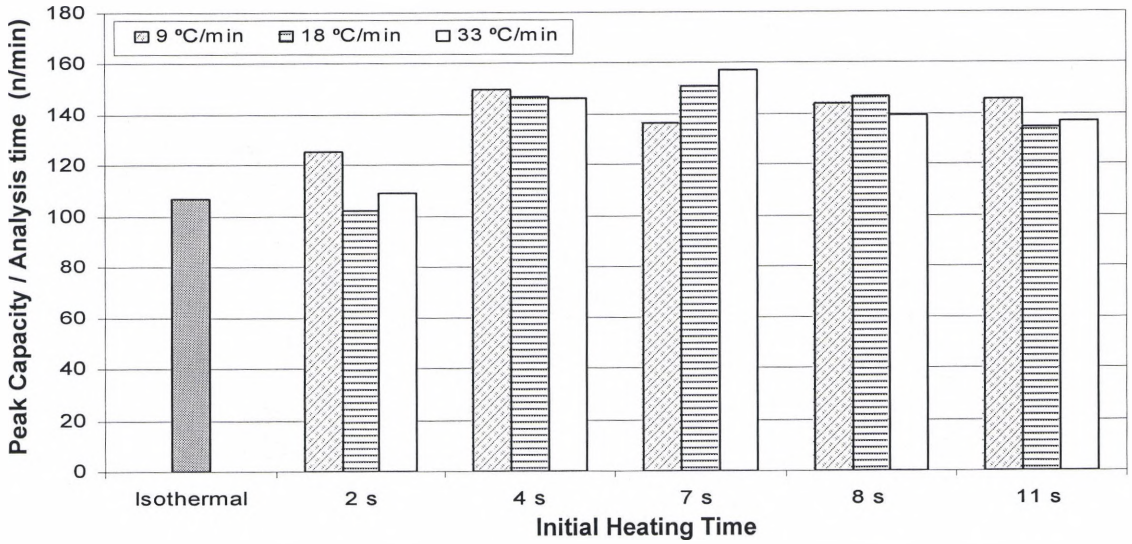

Figure 74. Peak capacity/analysis time of all the different experiments performed.

Figure 74 shows how the peak capacity analysis time ratio increases when it is initially heated at 4s or later, maintaining an average value of 145 peaks/minute or 2.4 peaks/s. Therefore, we can discard the idea of initially heating the gradient at 2s since it produces the lowest value of n/analysis time.

Looking at the GEP chromatogram (Figure 64) and the isothermal separation of the heartcut sample (Figure 67), it can be observed that the separation problem is poor resolution at the beginning of the chromatogram and too much resolution at the end. Therefore, the ideal situation for applying the TGPGC in the second-dimension, would be to let the early peaks breakthrough the gradient and apply the release process to the last zone of the chromatogram where the peaks are spatially broad. This situation was observed at initial heating times of 7s and 8s, where the peaks were physically separated at the beginning, peaks **A, A_1** and the peaks in **D**, while the last peaks were closer, peaks **A_2**, **B** and **C**. This approach allowed the physical separation of the early peaks, while making the last peaks narrower and closer, thus increasing the peak capacity of the whole chromatogram.

The sacrifice in signal due to the broadening effect of breaking through the gradient was not significant for the first peaks, since they are typically narrower and taller. Besides, it is compensated by the increase in separation and thus resolution, as can be seen in Figure 68 to 70 shows that for the initial heating times of 7s, 8s and 11s, there was an increase in resolution of 90% compared to the isothermal separation.

As seen in Figure 74 any heating time after 4s produces a good amount of peak capacity in a given analysis time, however its value starts to decrease for an initial heating time of 11s. This was one of the reasons why the initial time of 11s was discarded. Furthermore, it also had the longest analysis time as seen in Figure 73. An initial heating time of 7s and a heating rate of 33 °C/s were chosen as the best conditions for applying the TGPGC method in the second-dimension of MDGC-MS.

These conditions provided the lowest analysis time among the different initial heating times, while still providing the best peak capacity/analysis time value. The fastest heating rate allowed obtaining the maximum narrowing effect and also the minimum analysis time among the 3 heating rates.

A comparison between the isothermal separation of the heartcut sample and the best TGPGC separation is shown in Figure 75, and a comparison of the quantitative values obtained from the chromatograms are shown in Table 9.

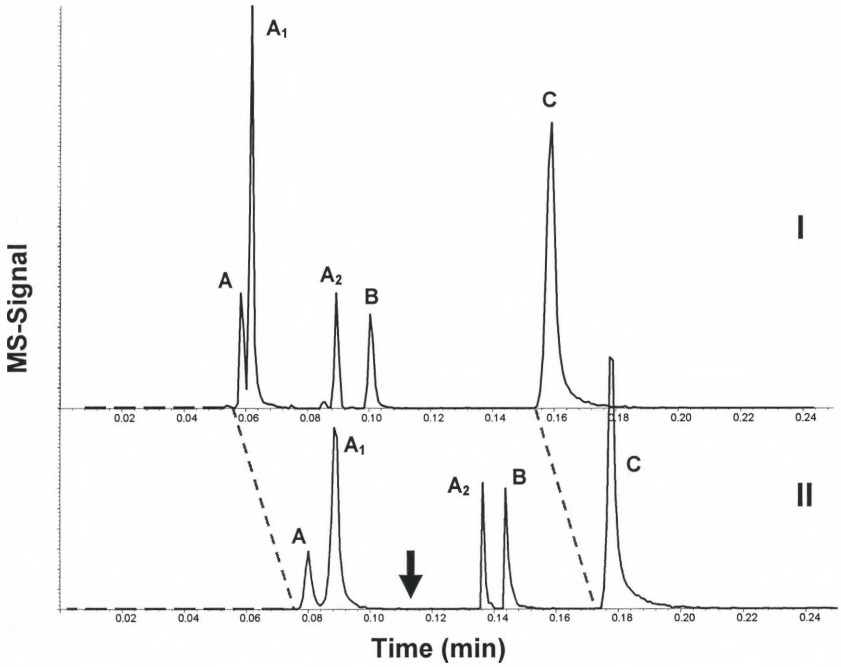

Figure 75. Isothermal and TGPGC separation of the heartcut sample.
I) Isothermal Mode
II) TGPGC mode for an initial heating time (IHT) of 7s (arrow), and at 33 °C/s

Table 9. Quantitative comparison between the Isothermal and TGPGC separation.

	Separation Modes	Isothermal	TGPGC Heating at 7s	% Comparison between the TGPGC vs Isothermal
Resolution	R_{A-A1}	0.86	1.64	91
	R_{A1-A2}	6.75	11.75	74
	R_{A2-B}	3.00	3.20	7
	R_{B-C}	9.67	6.18	-36
	Peak Capacity (n)	16.98	30.21	78
	Analysis time (s)	9.54	10.58	11
	Peak Capacity/Analysis time n/min	1.78	2.86	60

Even though the separation does not appear significantly better an increase of 78% in the peak capacity will definitely improve the resolution of a complex mixture.

From Figure 75 we can observe a notable increase in the resolution of the early peaks **A** and $\mathbf{A_1}$, of 90% (Table 9), the narrowing effect of the later peaks ($\mathbf{A_2}$ and **B**), and the decrease in resolution for the last peaks **B** and **C**.

Overall the peak capacity of the separation of the heartcut sample obtained with the TGPGC mode had showed an increase of 78%. This means a theoretical 78% increase in the total peak capacity of the MDGC-MS system, since the peak capacity of a multidimensional system (Equation 13) is the product of the peak capacity of the individual columns[36, 40].

$$n_{Total} = n_{c1} \cdot n_{c2} \qquad (13)$$

The increase in the peak capacity ensures an improvement in the separation power of the system, though it could only be appreciated by doing a complete separation of a complex sample.

Even though the analysis of the heartcut done by TGPGC increased the analysis time by 11%, the gain in resolution and peak capacity is promising when compared to the approaches used today to improve the resolution and GEP of the secondary separation. These approaches consist of putting the secondary column in a programmable second oven, where the isothermal temperature of the secondary column was changed, either to a higher or lower temperature with respect to the primary column. Therefore, isothermal separations of the heartcut sample were performed at different oven temperatures, to compare the TGPGC separation with these methods. Figure 76 shows the isothermal separations of the heartcut at different oven temperatures.

As can be seen in Figure 76, temperatures lower than the oven temperatures were used to increase the resolution of the early peaks, while higher temperatures were

used to improve the resolution and detection limit of the last peaks, as well as to reduce the analysis time and wraparound problems.

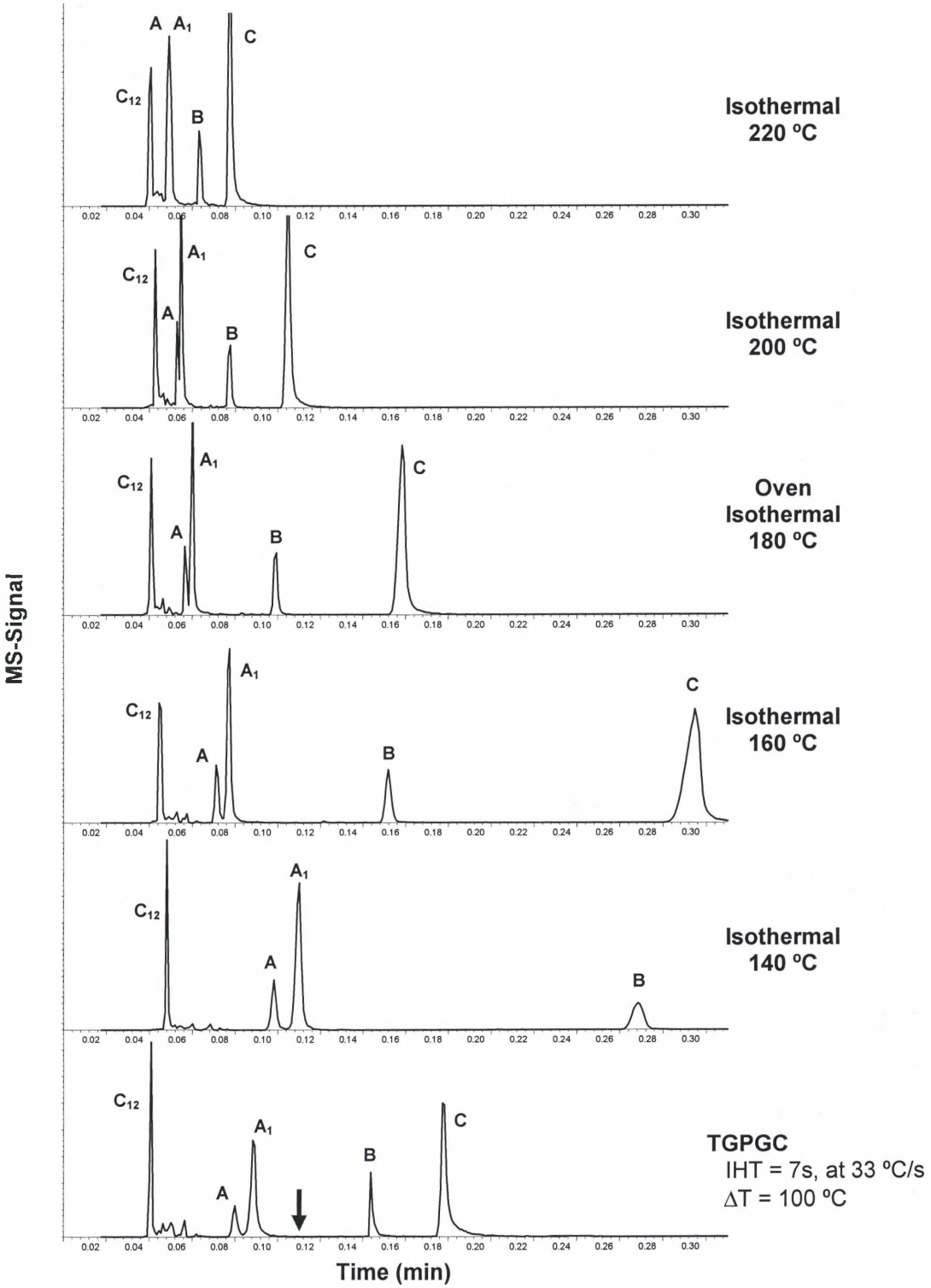

Figure 76. Comparison between the isothermal and TGPGC separations of the heartcut sample. (IHT = Initial Heating Time)

Conversely, higher temperatures make the early peaks merge together (220 °C) and lower temperatures make the late peaks so broad that they were hardly detected (140 °C), and it also produced wraparound problems. Wraparound may be the most significant shortcoming in MDGC as it is practice today. These approaches were not a complete solution for the GEP encountered in MDGC-MS.

Figure 76 shows how temperatures higher than the oven temperatures (220 °C) make peaks **A** and $\mathbf{A_1}$ merge together, while lower oven temperatures (140 °C) increase the separation of these peaks, though it decreases the signal of the later eluted peaks like **B**, and it increases the analysis time.

Figure 76 also allows us to appreciate the advantages of using the TGPGC mode in the second-dimension of the MDGC-MS system. The separation done by TGPGC shows how this powerful method can allow a separation enhancement of the early peaks similar to the one obtained in the isothermal mode at 140 °C; however, the TGPGC separation was performed 3.7 times faster than the isothermal separation at 140 °C. Furthermore, the late peaks in the heartcut where kept as narrow as the 180 °C isothermal separation, showing that the TGPGC is a good solution for the GEP in the second-dimension of MDGC-MS.

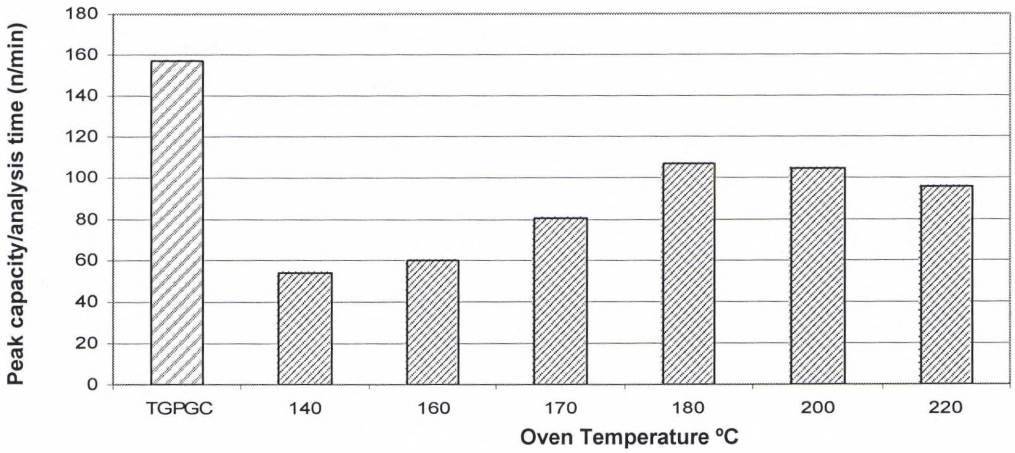

Figure 77. Comparison of the peak capacity/analysis time for the isothermal oven temperatures and TGPGC separations.

Regarding the peak capacity, Figure 77 shows the peak capacity divided by the analysis time for the different isothermal separations and also the TGPGC separation. Figure 77 shows that the ratio of peak capacity and analysis time has a maximum value for the isothermal separation of 180 °C, or the heartcut elution temperature, which means that the best separation with respect to analysis time is performed at this temperature.

It also explains why the use of higher or lower temperatures with respect to the elution temperature does not yield a good separation with respect to time. Lower temperatures increase the analysis time, while higher temperatures decrease the peak capacity. It is for these reasons that the actual methods used in MDGC-MS are not efficient.

TGPGC is an alternative for increasing the separation power, by obtaining higher peak capacities in a short analysis time, as seen in Figure 75 and Figure 76. The increase in n/analysis time is proportionally related with the separation power as seen in Figure 75 and 76 when the TGPGC separation was compared with the isothermal runs.

Application of TGPGC in the second dimension of the MDGC-TOFMS system

The TGPGC method produces peaks as narrow as 120 ms, although the system that was being used for the detection of these peaks was not adequate. A HP5969 mass spectrometer has a maximum scanning rate, for a limited amount of ions (60 ions), of 15 Hz, or a full scan every 66.66 ms. This translates to 2 or 3 full scans per peak; however the average peak widths were on the order of 180 ms for the peaks that where released from the gradient, allowing 4 to 5 points as seen in Figure 78 for peak **C**.

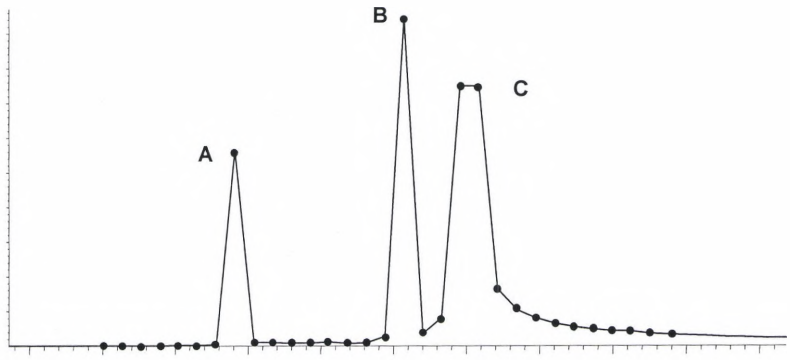

Figure 78. Narrow peaks detected with a scanning rate of 15 Hz.

As can be seen in Figure 78, the low scanning rates do not allow the obtaining of Gaussian peaks, and also identification of the peaks by the use of the MS libraries is limited by the nunber of ions employed. Peaks **A** and **B** were 120 ms base width, which was the minimum peak width that could be measured, since a 60.66 ms/scan was the lowest available, hence it is likely that the peak widths could be less than 120ms wide. Moreover peak **C** was truncated, showing that the real height of the peak is not properly seen (i.e., the area of the peak is inaccurate).

With all these limitations of the detection, the implementation of the TGPGC in the second-dimension of an MDGC-MS would be useless, since the identification and analysis of the peaks would not be possible.

A higher scanning rate detector was necessary to apply the TGPGC method in the MDGC-MS system. The Time of Flight Mass Spectrometer (TOFMS) detector (LECO PEGASUS III) was capable of solving this situation, since it had a scanning capability of 500 Hz. This was ideal for the narrow peaks produced by the TGPGC method. Therefore, the MDGC system was reassembled into a GC-TOFMS system.

In order to demonstrate the complete separation capability of TGPGC, a complex mixture was analyzed using this technique. The detector used in this analysis was the TOFMS, and the scan use was of 100 Hz. The MDGC-TOFMS with the TGPGC system was assembled (shown in Figure 24 and 25), and its separation power was demonstrated through experimentation.

The complex mixture used was a solid phase extraction (SPE) sample from an aviation turbine fuel (SPE 3686). This sample contained polar and non-polar compounds, thereby it was ideal for demonstrating the TGPGC separation capability. The conditions of the MDGC-TOFMS system used to analyze the SPE aviation turbine fuel sample are listed in Table 10. A ramped pressure was required to maintain the optimal helium gas velocity in both columns. The ramped pressure was calculated by applying a mass balance at the split tee that connected the two columns as previously explained.

Table 10. Oven conditions used to analyze the SPE aviation jet fuel sample using

	Multidimensional GC-TOFMS
Injector (°C)	250 isothermal
Initial T (°C)	40 (15 min hold)
Temperature Ramp Rate (°C/min)	4
Final T (°C)	250 (15 min hold)
Injector Mode	splitless, (3ul)
MS Scan Range	40-300 amu
MS Scan Rate	100 (Hz)
Initial Preassure (psi)	38 (15 min hold)
Pressure Ramp (psi)	0.32 (psi/min)
Final Pressure (psi)	55 (15 min hold)
Heartcut Time (s)	20

For the TGPGC mode, the thermal field employed had a temperature gradient of 100 °C/m, and the heating was performed at 7s after the injection of each heartcut. The heating rate employed was 30 °C/min. Figure 79-A shows the conventional MDGC-TOFMS chromatogram for the SPE aviation turbine fuel sample, where each line (or cluster) observed represents a second-dimension separation, as seen in Figure 79-B.

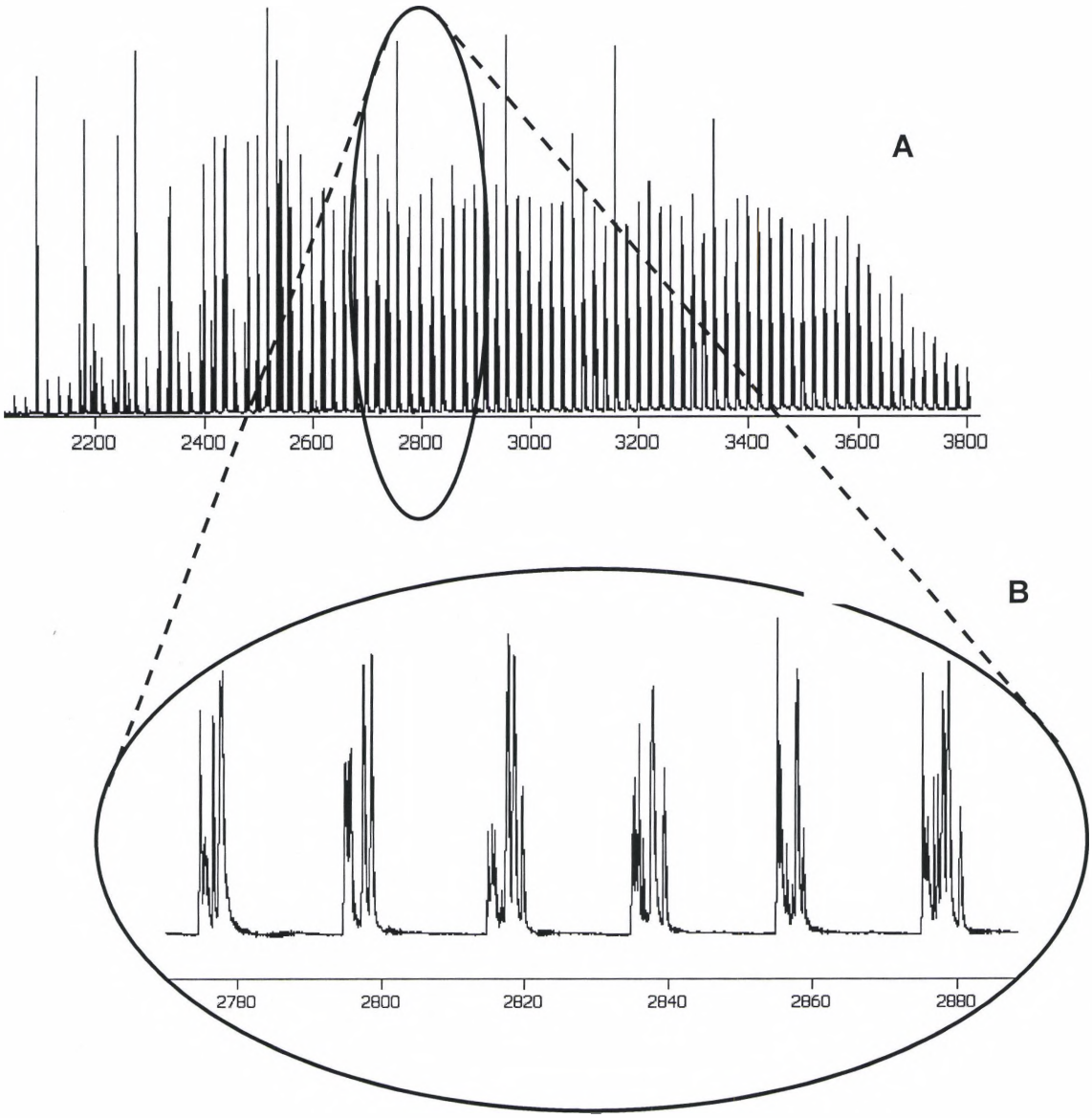

Figure 79. MDGC chromatogram of the SPE aviation turbine fuel.

Both of the separation modes (TGPGC and ITGC) employed in the second-dimension of the MDGC-TOFMS system were applied to the SPE aviation turbine fuel sample. Within the analysis of this solution were numerous examples of where the conventional multidimensional separation was improved by the TGPGC mode. Figure 80 shows a single heartcut of each separation mode to compare both separation methods.

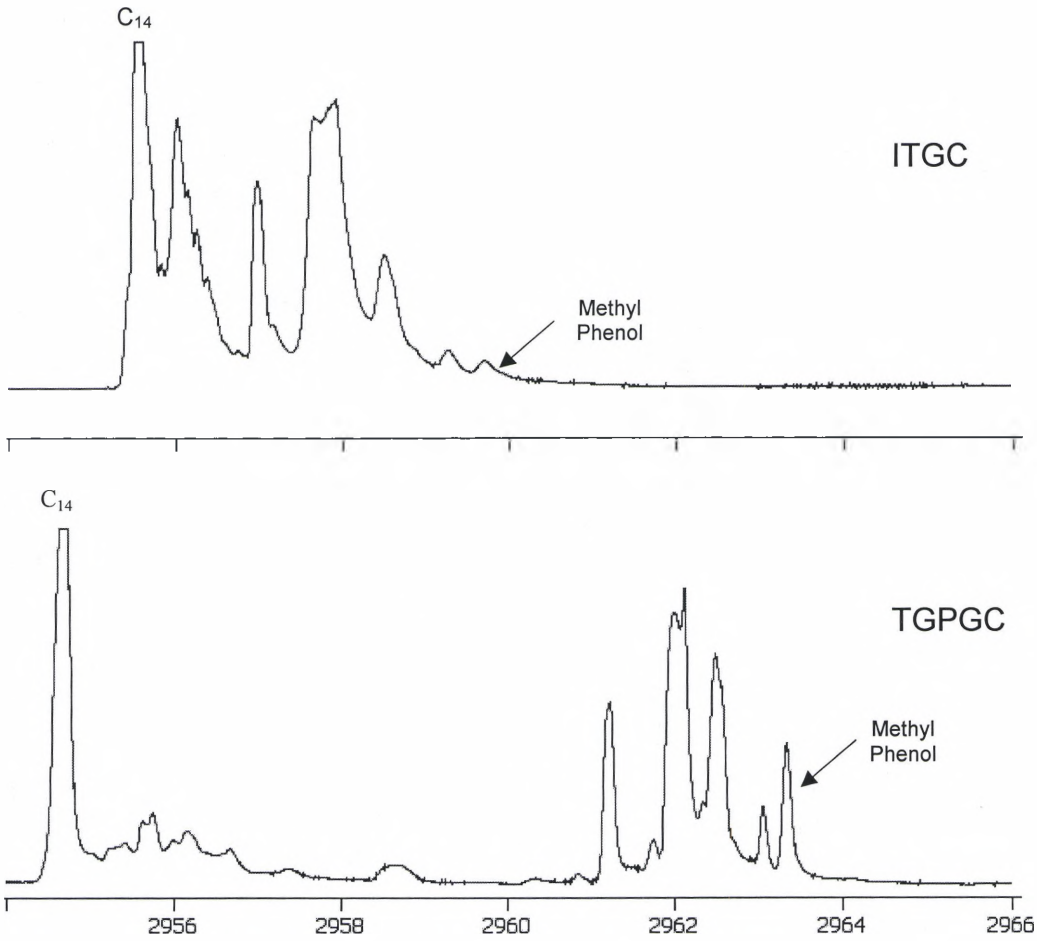

Figure 80. Comparison of the TGPGC and ITGC mode in the second-dimension separation of an MDGC-TOFMS system.

Figure 81 is a good example of the separation improvement that the TGPGC method provides. The compounds marked in these chromatograms show the start and

end of the heartcut, and also help to verify that the selected chromatograms belong to the same heartcut of the sample.

In the TGPGC chromatogram of the two separation processes, the breakthrough and the heating release of the compounds are well distinguished (Figure 81). For the breakthrough process, the compounds became more separated, broader and had a lower signal (see zone A Figure 81). For the heating release process, the compounds became focused, which caused the peak height to increase, improvement in the MDGC sensitivity, and a lower minimum detection limit. (zone B Figure 81).

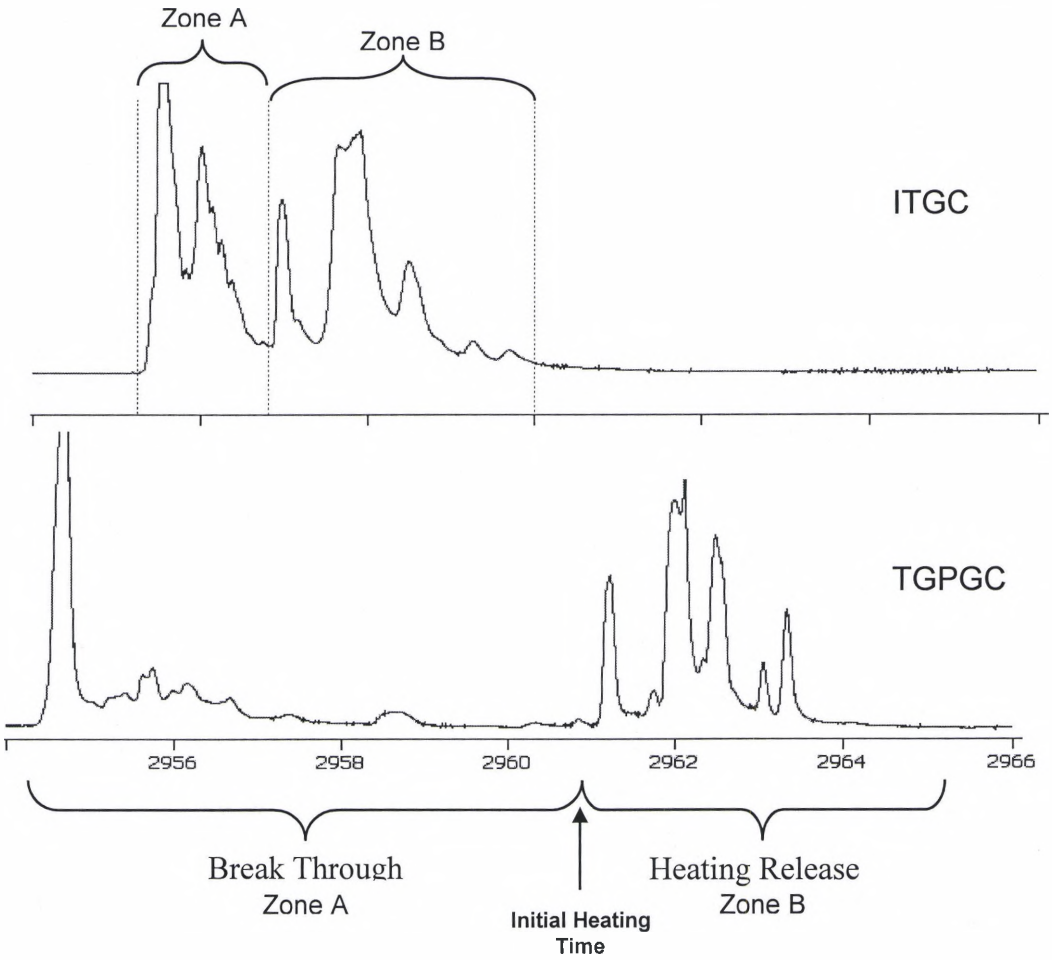

Figure 81. Separation processes of the TGPGC mode, in the heartcut sample.

Even though the signal decreased for zone A, the gain in separation overcame this decrease, since the use of an automatic library search gave an excellent match quality. Furthermore, more peaks were found in the TGPGC separation than in the conventional MDGC-TOFMS output.

As an example of the separation enhancement of the TGPGC mode, Figure 82 shows how the Quinoline-2,7-dimethyl and the Octanoic acid, along with other compounds, were not able to be separated by conventional MDGC, but the separation was achieved by the application of the TGPGC mode.

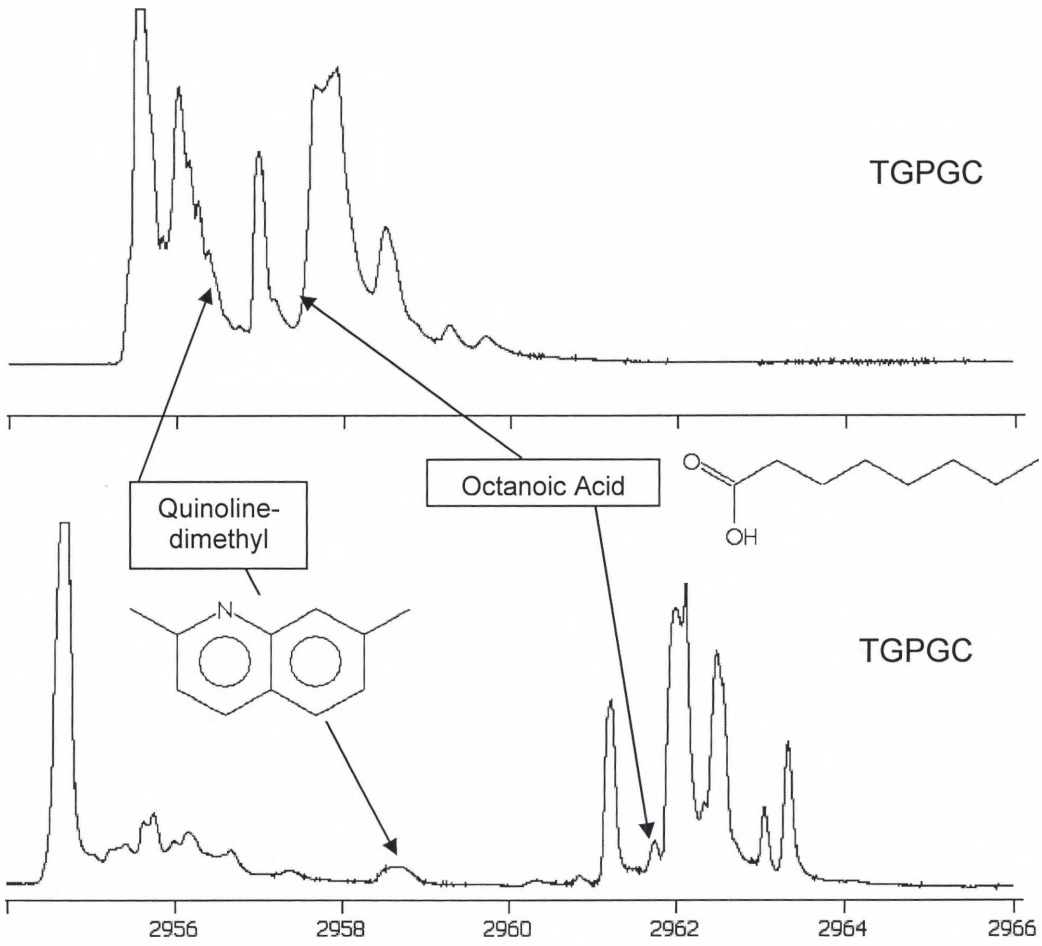

Figure 82. Identification of compounds in the TGPGC separation mode.

A particular heartcut has been studied however in order to appreciate more generally the separation enhancement of the application of the TGPGC. A 2D plot is used.

By stacking side by side the second-dimension chromatograms, the multidimensional chromatogram can be transformed to a two-dimensional chromatogram. In this case one dimension will represent the retention time on the first column, and on the second dimension, the retention time on the second column. The signal intensity is represented by contour lines and shadings. The transformation into a 2D matrix array was performed by laboratory-written software (Basic).

Figure 83 shows the 2D chromatogram of the conventional MDGC separation. It can be observed from the empty space at the top of the plot in Figure 83 that only 50 % of the separation space is being used. Most of the peaks elute at the beginning of the second-dimension.

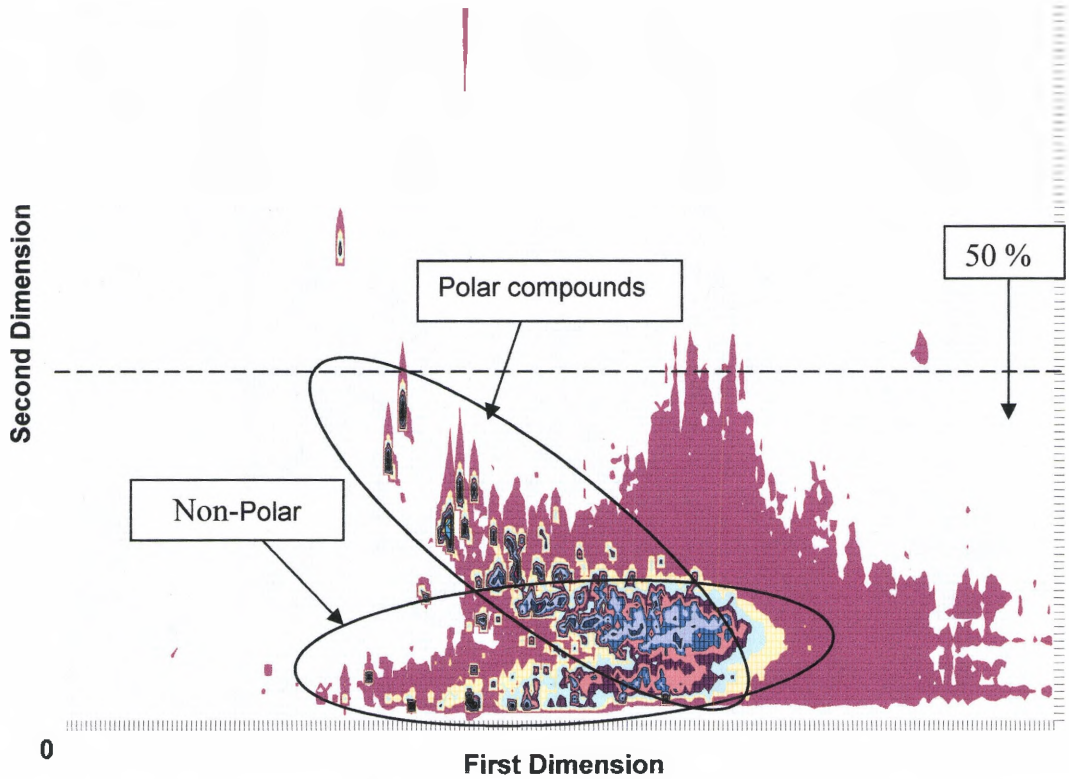

Figure 83. 2D chromatogram of the conventional MDGC-TOFMS separation of the aviation turbine fuel.

Figure 84 shows the 2D chromatogram of the TGPGC MDGC-TOFMS separation, which shows how the TGPGC mode takes advantage of the whole separation space and the time of the second dimension. Two groups of compounds are clearly seen. The first group, near to the starting time of the second dimension, represent non-polar compounds, while the ones at the end of the second dimension are polar compounds.

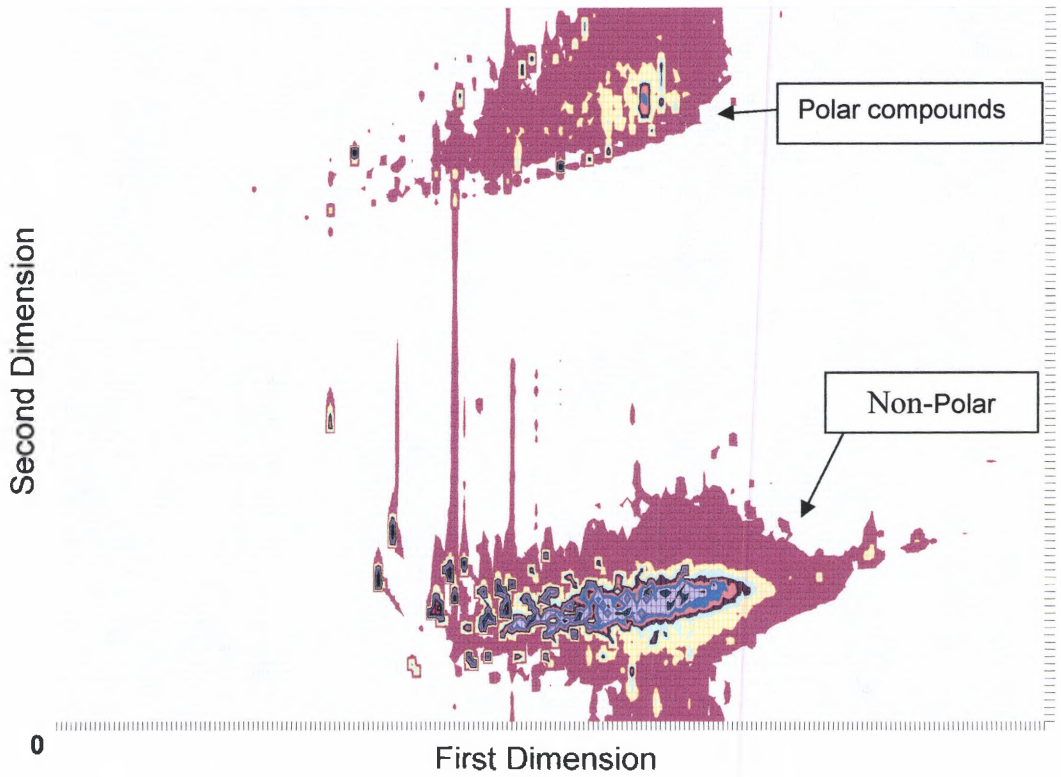

Figure 84. 2D chromatogram of the conventional MDGC-TOFMS separation of the aviation turbine fuel.

These two groups of polar and non-polar compounds were also seen in Figure 83. However, in this case the two groups appear overlapped and the conventional MDGC does not separate them. Showing that the separation between the peaks

diminishes as the temperature of the oven increases. This situation does not occur when the TGPGC method was applied as seen in Figure 84.

The use of the TGPGC separation offers the advantage of easily distinguishing the polar from the non-polar compounds. It also keeps the polar and non-polar groups separated, maintaining a good resolution even at high oven temperatures. The TGPGC mode was demonstrated to be a good solution for the GEP in the second dimension of the MDGC system, due to its fast turn around cycles and the enhance in separation produced. However, further applications need to be performed to take advantages of its maximum separation power.

Complex samples need to be analyzed to adjust and improve TGPGC separation power to take advantage of its best performance TGPGC does significantly enhance separation in the second dimension of MDGC-MS.

Quality Assurance

In general, the experiments carried out for this research were conducted with Good Laboratory practices in mind. Thermocouple measurements were an important part of the research conducted. While the thermocouple measurements were not calibrated to NIST traceable standards, they were validated by accurate temperature measurements made inside the gas chromatographs, which are accurately calibrated. For example, the use of thermocouples to measure temperature of the column sheath assembly should result in a temperature curve which approached the oven temperature which, in all cases was measured using a separate temperature measurement system. Because these thermocouples all recorded the same temperatures, to within one degree C, we were comfortable with the accuracy of the temperature measurement.

In the case of the chromatographic analyses regarding retention time or peak heights, these measurements were carried out in duplicate, typically. Retention times were generally accurate to one one-hundredth of a minute. Peak heights were generally accurate to 10 percent and were also analyzed in duplicate, in most cases.

Because of the design and construction nature of this project, the great majority of work was not subject to typical quality assurance methods. Since no direct quantitation was required in this project, standards, replicates, blanks and the like were not considered in the protocol of the experiments.

CHAPTER V

CONCLUSIONS

A multidimensional gas chromatography time of flight mass spectrometer with second-dimension thermal gradient programmed gas chromatography was developed (MDGC-TOFMS with TGPGC).

The application of the TGPGC in the second-dimension of the MDGC system has been accomplished through the use of a column sheath assembly (CSA). A convective heat exchanger design was used, which consisted of a coiled tube placed inside an air-bath GC oven where the capillary column was placed coaxially inside of the CSA, allowing the formation of an axial temperature gradient and radial temperature uniformity. A hand-made, thin walled ¼" OD polyimide tubing was the tube that performed the best among the tubes tested. The polyimide tube was structurally strong and supported the wide and rapid changes in temperature and pressure, sustaining up to 30 psig at 260 °C. Furthermore, the low thermal mass of the CSA allowed it to be highly compliant, achieving heating and cooling rates of 33 °C/s and 200 °C/s, respectively, which are much higher than any other heating device currently available. These heating and cooling rates allowed the generation of thermal fields as required for the application of TGPGC in the second-dimension of the MDGC system.

The tuning of the TGPGC technique consisted of adjusting values for the operational variables that enhanced the separation of the heartcut sample in the second-dimension column of the MDGC-MS system. The studies performed showed that two

separation processes can take place when the TGPGC separation technique is applied. The first separation process takes place when the compounds are allowed to breakthrough the negative gradient, making the peaks physically separated and broader. The second separation process happens when the compounds are released before they get through the gradient, by heating the gradient to the oven temperature. In this case the peaks get narrower and closer together, though chromatographically separated and with an increase in signal.

The influence of the $|\Delta T|$ gradient in the TGPGC separation process showed that for the breakthrough situation, as the $|\Delta T|$ gradient increased, the broader and physically more separated the peaks became. The resolution increased up to a point where the broadening effect overcame the separation effect. While for the release situation, the peaks got closer and narrower as the $|\Delta T|$ gradient increased. The distance decreased for the later peaks, due to the heating release effect and resolution increased for those peaks at the beginning due to the breakthrough effect.

The influence of the heating rate in the TGPGC releasing situation showed that the higher the heating rate the narrower and closer the peaks were eluted. In this case the resolution increased reaching a point where the narrowing effect may have been overcome by the smaller distance between the peaks, thus decreasing the resolution.

From these studies, we concluded that the ideal situation for applying the TGPGC in the second-dimension and solving the GEP would be to let the early sharp and coeluted peaks breakthrough the gradient, and apply the release process to the last zones of the chromatogram where the peaks are spatially broad.

Different heating rates and initial heating times where investigated. The best conditions for improving the separation in the shortest time for a 15s heartcut sample applying the TGPGC method were: a 100 °C $|\Delta T|$ gradient, heating at 7s with a heating

rate of 33 °C/s. A notable increase in the resolution (90%) of the early peaks was obtained. In addition an increase in peak capacity of more than 69% was achieved, which means a theoretical 69% increase in the total peak capacity of the MDGC-MS system.

The separation obtained in the first peaks was comparable to an isothermal separation of the same sample at 140 °C. However it was done 3.7 times faster, while maintaining the latest peaks close together and narrow, which was the intention.

We have successfully demonstrated TGPGC as an important technique for the second dimension of the MDGC-MS system. In contrast with conventional MDGC-MS, the application of TGPGC in MDGC-TOFMS showed a more complete analysis of complex organic samples, in less time (50%), while better addressing the non-linear distribution or spread of generated solutes, i.e., the general elution problem. Moreover, the enhanced analytical performance of the experimental system resulted in well-defined mass spectral patterns, which enabled more accurate peak identification using MS with higher library matches.

Despite the cumbersome nature of the system and its implementation, these results showed that the TGPGC mode not only enhances the peak capacity of the chromatogram, but also is a very good option for solving the GEP encountered in the second-dimension of MDGC-MS.

CHAPTER VI

FUTURE WORK AND RECOMMENDATIONS

This work showed that in contrast with conventional MDGC-MS, the application of TGPGC in MDGC-MS showed a more complete analysis of complex organic samples, in less time, while better addressing the non-linear distribution or spread of generated solutes, i.e., the general elution problem. However, further work is still required to optimize and evaluate the effects of different rapidly generated thermal fields in the performance of TGPGC for the second-dimension separations.

The employment of a faster scanning rate MS, like the recently acquired Time-of-Flight Mass Spectrometer (TOFMS), will provide improved peak definition and more accurate peak areas and heights. This will permit a more detailed study of the effects of the main variables of TGPGC in the separation process, and moreover, it will allow performing faster separations than the ones considered in this thesis.

To further study the separation capabilities of the TGPGC method, the generation of different temperature gradient profiles and thus thermal fields would be required. To achieve this, previous simulations suggested that placing the CSA in a separate thermal environment rather than the GC oven would have the possibility of having different inlet temperatures and thereby permit the CSA to be capable of generating a wide variety of thermal fields.

A limitation that the actual system has that should definitely be addressed is the maximum analysis temperature, which is limited by to the hand-made polyimide tube and the stationary phase of the secondary column. These restrictions would be

overcome by finding a source that could provide a coiled polyimide tube using the specifications recommended in this thesis, and by using a higher temperature polar column (many are currently under development). Some less-polar columns will support higher temperatures. The loss of retention and resolution with the less polar column could be compensated by the application of the TGPGC method, and therefore allowing the complete analysis of complex mixtures.

Another major problem in MDGC-MS, which TGPGC has not completely addressed, is the presence of wraparound. This occurs when compounds do not elute during their required modulation time. The use of TGPGC technology could help to overcome this difficulty, by placing a CSA in the isothermal zone of the secondary separation. Heating this zone to higher oven temperatures, before the next heartcut is injected, would help to cleanse the secondary column and hence ensure that all the compounds have eluted, thus eliminating wraparound. It is important to mention that before the next heartcut is transferred to the secondary-column, the column would be at oven temperature again, ready for the next separation. This approach will not only eliminate wraparound but also allow the use of longer secondary columns (increasing resolution), while still maintaining short analysis times. Currently this approach is under investigation and has shown promising results.

To further improve the TGPGC method, the application of a flow gradient in conjunction with temperature will definitely increase the separation power and efficiency of the TGPGC method. The use of lower flows at the beginning of the thermal field with increase in flow at the end would allow for maximum resolution in the whole separation. However, the application of this new variable will certainly make the system instrumentation and development quite complicated.

Another suggestion would be to change the cryogenic trap design. The current trap mechanically moves the capillary chromatography column in and out the cryogenic

zone. Although one of the principle concerns with this design was the breakage of the column, this has never happened. However, the column has separated from the septa that connects it to the moving rod, thus stopping the heartcut sampling. Recently cryogenic jet systems have been used as a modulator[82]. These systems consist of using pulses of cold nitrogen or CO_2 directly onto the chromatographic column, trapping the sample, and then releasing it by using hot pulses of air. Due to its instantaneous heating and cooling of the column, it would enable more rapid heartcutting and smaller heartcut time-spans. Furthermore, there are no moving parts in this system, making it more robust and reliable.

Of course, as we investigate the different parameters of TGPGC we will be generating different applications to evaluate the capability of the TGPGC method in real complex samples.

BIBLIOGRAPHY

1. Internet. **2004**, Pioule : A health giving water. http://www.pioule.com/us/bien.htm.
2. Internet. **2004**, Detailed Composition of Seawater. http://www.seafriends.org.nz/oceano/seawater.htm.
3. Rubey, W.A. *Journal High Resol. Chromatogr.*, **1992**: p. 795-799.
4. Bartle, K.D. and P. Myers. *Trends in Analytical Chemistry*, **2002**. 21(9+10): p. 547-557.
5. Dalluge, J., et al. *Journal of Chromatography A*, **2002**. 974: p. 169-184.
6. Edward B. Ledford, J., C.A. Billesbach, and Q. Zhu. *Journal High Resol. Chromatogr.*, **2000**. 23(3): p. 205-207.
7. Grob, R.L., Modern Practice of Gas Chromatography. **1977**, New York: Wiley-Interscience.
8. Ettre, L.S. *LC-GC*, **2001**. 19(2): p. 120-123.
9. Bertsch, W. *Journal High Resol. Chromatogr.*, **1999**. 22(12): p. 647-665.
10. Bertsch, W. *Journal High Resol. Chromatogr.*, **2000**. 23(3): p. 167-181.
11. Blumberg, L.M. and M.S. Klee. *Journal of Chromatography A*, **2001**. 933: p. 13-26.
12. John V. Seeley, Frederick Kramp, and C.J. Hicks. *Anal. Chem.*, **2000**. 72(18): p. 4346-4352.
13. Dimandja, J.-M., et al. *Journal High Resol. Chromatogr.*, **2000**. 23(3): p. 208-214.
14. Phillips, J.B. and J. Xu. *Journal of Chromatography A*, **1995**. 693: p. 327-334.
15. Marriott, P.J., Multidimensional Chromatography. **2002**: Jonh Wiley & Sons Ltd.
16. Dalluge, J., et al. *Journal of Chromatography A*, **2002**. 965(2002): p. 207-217.
17. Handley, A.J. and E.R. Adlard, Gas Chromatographic Techniques and Applications, ed. J.M.C.a.A.J. Handley. **2001**: CRC Press.
18. Giddings, J.C. *Journal of Chromatography A*, **1995**. 693: p. 3-15.
19. Glenn S. Frysinger and R.B. Gaines. *Journal High Resol. Chromatogr.*, **1999**. 22(5): p. 251-255.
20. Geus, H.-J.d., et al. *Journal High Resol. Chromatogr.*, **2000**. 23(3): p. 189-196.
21. Dalluge, J., J. Beens, and U.A.T. Brinkman. *Journal of Chromatography A*, **2003**. 1000: p. 69-108.
22. Glenn S. Frysinger and R.B. Gaines. *Journal High Resol. Chromatogr.*, **2000**. 23(3): p. 197-201.
23. Beens, J., J. Blomberg, and P.J. Schoenmakers. *Journal High Resol. Chromatogr.*, **2000**. 23(3): p. 182-188.

24. Striebich, R.C., W.A. Rubey, and J.R. Klosterman. *Waste Management*, **2002**. 22: p. 413-420.
25. Mohamed Adahchour, et al. *Journal Sep. Sci.*, **2003**. 26: p. 753-760.
26. Rubey, W.A. *Rev. Sci. Instrum.*, **1994**. 65(9): p. 2802-2807.
27. Carlos G. Fraga, Bryan J. Prazen, and R.E. Synovec. *Journal High Resol. Chromatogr.*, **2000**. 23(3): p. 215-224.
28. Striebich, R.C. and W.A. Rubey.*14th International Symposium on Capillary Chromatography*. **1992**. Baltimore.
29. Rubey, W.A. *Journal High Resol. Chromatogr.*, **1991**. 14: p. 542-548.
30. Heftmann, E., Chromatography. Third Edition ed. **1975**, New Yoek: Van Nostrand Reinhold Company. 969.
31. Grant, D.W., Capillary Gas Chromatography. **1996**, New York: Jhon Wiley & Sons. 925.
32. Ettre, L.S., Introduction to Open Tubular Columns. **1978**, Connecticut: The Perkin-Elmer Corporation.
33. Ettre, L.S. and J.V. Hinshaw, Basic Relationships of Gas Chromatography. **1993**, Dayton: Advanstar Communications. 177.
34. Deans, D.R. *Journal of Chromatography*, **1981**. 203: p. 19-28.
35. Berezkin, V.G. *Journal Analytical Chemistry*, **2001**. 56(6): p. 587-592.
36. Phillips, J.B. and J. Beens. *Journal of Chromatography A*, **1999**. 856: p. 331-347.
37. Hirschfeld, T. *Analytical Chemistry*, **1980**. 52(2): p. 298A-312A.
38. Giddings, J.C. *Anal. Chem.*, **1984**. 56(12): p. 1258A-1269A.
39. Majors, R.E. and P.W. Carr. *LCGC*, **2001**. 12(2): p. 1-19.
40. Mondello, L., A.C. Lewis, and K.D. Bartle, Multidimensional Chromatography. **2002**: John Wiley & Sons, LTD.
41. Kinghorn, R.M. and P.J. Marriott. *Journal High Resol. Chromatogr.*, **1998**. 21(11): p. 620-622.
42. Schomburg, G. *Journal of Chromatography A*, **1995**. 693: p. 309-325.
43. Schomburg, G., H. Husmann, and F. Weeke. *Journal Chromatography*, **1975**. 112: p. 205-217.
44. Rubey, W.A. and S.L. Mazer.*Pittsburgh Conference*. **1986**. Atlantic CIty.
45. Klosterman, J.R., *Master Degree Thesis*. **2002**, University of Dayton: Dayton. p. 75.
46. Dalluge, J., et al. *Journal of Separation Science*, **2002**. 25: p. 201-214.
47. Marriott, P. and R. Shellie. *Trends in Analytical Chemistry*, **2002**. 21(9-10): p. 573-583.
48. Marriott, P.J., et al. *Journal High Resol. Chromatogr.*, **2000**. 23(3): p. 253-258.
49. Kinghorn, R.M., P.J. Marriott, and P.A. Dawes. *Journal High Resol. Chromatogr.*, **2000**. 23(3): p. 245-252.
50. Kirkland, J.J., Modern Practice of Liquid Chromatography. **1971**, New York: Jhon Wiley & Sons, Inc.
51. Hinshaw, J.V. *LC-GC*, **2001**. 19(2): p. 169-177.
52. Lieshourt, M.v., et al. *Journal High Resol. Chromatogr.*, **1998**. 21(11): p. 583-586.
53. Dalluge, J., et al. *Journal High Resol. Chromatogr.*, **1999**. 22(8): p. 459-464.

54. Es, A.v., et al. *Journal High Resolution Chromatography & Chromatography Communications*, **1988**. 11(12): p. 852-857.
55. Russell M. Kinghorn and P.J. Marriott. *Journal High Resol. Chromatogr.*, **1999**. 22(4): p. 235-238.
56. Eiceman, G.A., et al. *Anal. Chem.*, **2002**. 74: p. 2771-2780.
57. Cramers, C.A., et al. *Journal of Chromatography A*, **1999**. 856: p. 315-329.
58. Mastovska, K. and S.J. Lehotay. *Journal of Chromatography A*, **2003**. 1000: p. 153-180.
59. Mustacich, R., J. Everson, and J. Richards. *American Laboratory*, **2003**. 35(3): p. 38-41.
60. Grall, A., C. Leonard, and R. Sacks. *Analytical Chemistry*, **2000**. 72: p. 591-598.
61. Deursen, M.v., J. Beens, and C.A. Cramers. *Journal High Resol. Chromatogr.*, **1999**. 22(9): p. 509-513.
62. Sacks, R., et al. *Journal High Resol. Chromatogr.*, **2000**. 23(3): p. 225-234.
63. Sloan, K.M., R.V. Mustacich, and B.A. Eckenrode. *Field Analytical Chemistry and Technology*, **2001**. 5(6): p. 288-301.
64. McNair, H.M. and G.L. Reed. *J. Microcolumns Separation*, **2000**. 12(6): p. 351-355.
65. Rubey, W.A.*23rd International Simposium on Capillary Chromatography*. **2000**. Riva del Garda, Italy.
66. Rubey, W.A.*Annual Pittsburg Conference*. **1993**. Atlanta.
67. Rubey, W.A. *32nd Annual Rocky Mountain Conference on Analytical Chemistry in Denver*, **1990**.
68. Rubey, W.A., *U.S. Patent 4,923,486*. **1990**.
69. Internet. **2004**, Dispersion in Chromatography Columns. http://www.laboratorytalk.com/books/chem/chrom/rs_9/contents.html.
69. Ehrmann, E.U., et al. *Journal of Chromatographic Science*, **1996**. 34(December): p. 533-539.
71. Gaisford, S. *American Laboratory*, **2002**. 34(10): p. 10.
72. Deursen, M.v., et al. *J. Microcolumns Separation*, **2001**. 13(8): p. 337-345.
73. Hinshaw, J.V. *LC-GC*, **2000**. 18(11): p. 1142-1147.
74. Perry, J.A., Introduction to Analytical Gas Chromatography. **1981**, New York: Marcel Dekker, INC. 426.
75. Internet. **2004**, Restec Web Page http://www.restekcorp.com/.
76. Internet. **2004**, SGE Web Page http://www.sge.com/.
77. Internet. **2004**, Agilent Web Page http://we.home.agilent.com.
78. Internet. **2004**, Parallax Web Page http://www.parallaxinc.com/.
79. Internet. **2004**, Zeus Web Page http://www.zeusinc.com/.
80. Internet. **2004**, DuPont Web Page http://www.DuPont.com/.
81. Internet. **2004**, Cole-Parmer Web Page http://www.Cole-Parmer.com/.
82. Jacqueline F. Hamilton, Alastair C. Lewis, and K.D. Bartle. *Journal Sep. Sci.*, **2003**. 26: p. 578-584.

VITA

Agoust 15, 1977	Born---Merida, Merida, Venezuela.
2001	B.S. in Chemical Engineering, University of Los Andes Merida, Merida, Venezuela
2002-2004	Research Assistant Energy and Environmental Engineering, UDRI Dayton, OH
2003	M.S. in Chemical Engineering, University of Dayton Dayton, OH

Conference Proceedings

J. Contreras and R.C. Striebich, "Determinations of Polar Components in Aviation Fuels Using MDGC-MS," Poster Presentation at the AIAA 100th Anniversary of Flight Symposium, Dayton, Ohio, July, 2003.

Richard C. Striebich, Jesse Contreras, Karin Straley, Brian Gullett, Sukh Sidhu, "Analysis of Diesel Engine Exhaust for Non-Target Compounds Using MDGC-MS". Proceedings of Dioxin 2003, Boston, MA, August 2003.

Richard C. Striebich, Joy R. Klosterman, Wayne A. Rubey, Jesse Contreras, Philip H. Taylor. "MDGC-MS to Analyze Trace Emissions from Efficient Combustion Systems". A&WMA's 96th Annual Conference and Exhibition, San Diego, CA, June, 2003

Richard C. Striebich, Joy R. Klosterman, Wayne A. Rubey, Jesse Contreras, Philip H. "MDGC-MS to Analyze Trace Emissions from Efficient Combustion Systems". Combustion Emissions Workshop RTP, December 2003.